INTER-INDIVIDUAL DIFFERENCES IN TRICHLOROETHYLENE TOXICOKINETICS AND TOXICODYNAMICS IN GENETICALLY-DIVERSE MICE

Abhishek Venkatratnam

A dissertation submitted to the faculty at the University of North Carolina at Chapel Hill in partial fulfillment of the requirements for the degree of Doctor of Philosophy in the Department of Environmental Sciences and Engineering in the Gillings School of Global Public Health.

Chapel Hill
2018

Approved by:

Ivan Rusyn

Avram Gold

Wanda M. Bodnar

Weihsueh Chiu

Terry Wade

ABSTRACT

Abhishek Venkatratnam: Inter-individual differences in trichloroethylene toxicokinetics and toxicodynamics in genetically-diverse mice.
(Under the direction of Ivan Rusyn)

One of the many challenging issues in toxicology is addressing human variability in chemical risk assessment. Among several intrinsic and extrinsic factors that contribute towards inter-individual differences in toxic responses, genetic differences are well known to drive variability in xenobiotic metabolism and adverse effects. Traditional toxicity studies in rodents often rely on single genotype-based models that fail to capture diverse responses similar to those observed in humans. Recent advances in mouse genetics have led to the development of large panels of recombinant lines collectively known as population-based mouse models. Although their utility in biomedical research has been sufficiently demonstrated, their application in toxicity studies needs to be investigated. My doctoral dissertation focuses on investigating inter-individual differences in toxicokinetics (TK) and toxicodynamics (TD) in population-based mouse models with trichloroethylene (TCE) as case study toxicant. The central hypothesis of my dissertation is that *genetic differences in the mouse population will drive inter-individual differences in TCE metabolism and related effects*. **Aim 1** demonstrated sufficient statistical power and precision in the mouse population to identify genetic loci driving variability in TCE metabolism and TD. Next, extent of quantitative variability in some toxicokinetic parameters were comparable to those observed in humans suggesting the appropriateness of such model in addressing human variability in adverse outcomes. **Aim 2** characterized transcriptional responses that were strongly influenced by genetic background, dose, or a combination of genetic background and dose to better

understand individual- versus population-level responses. **Aim 3** assessed the utility of different population-based models in capturing diverse responses in a standard 90-day oral toxicity study that is often conducted for safety assessments. Collectively, this doctoral dissertation serves as a comprehensive guide in incorporating population-based mouse models in toxicity studies.

ACKNOWLEDGEMENTS

I would like to thank my doctoral advisor Dr. Ivan Rusyn for the opportunity to conduct my doctoral research in his lab and for providing an environment to interact with other trainees in the lab with diverse academic backgrounds. I would like to express my sincere appreciation to my doctoral committee members Drs. Avram Gold, Wanda M. Bodnar, Weihsueh Chiu, and Terry Wade for their support and comments on my dissertation research. As an international graduate student, conducting my graduate work off-campus is a unique experience that cannot be described by words. My interaction within the lab has led to an everlasting bond of friendship with both past and current members of the Rusyn lab. I am thankful to Ms. Grace A. Chappell and Ms. Lauren Lewis for spending time with me over occasional drinks at stressful times. Scintillating conversations ranging from coffee to toxicology with Drs. Fabian A. Grimm and William (Bill) D. Klaren are indeed cherish able memories that I would carry with me after my departure from the lab. I would also like to thank both of them for their support and timely advises over the course of my doctoral research. As my doctoral work involves working with rodents, I would like to acknowledge Mrs. Oksana Kosyk (former manager of the Rusyn lab) and Dr. Shinji Furuya for training me with mouse handling and administration procedures. In a similar vein, I also recognize Dr. Joseph A. Cichocki Mr. Yu-Syuan Luo and Dr. Hisataka Fukushima for their help with experiments.

My dissertation research is a collaborative effort of several individuals and labs in Texas and North Carolina. I would like to express my gratitude to Mr. Leonard Collins and Dr. Wanda

M. Bodnar for their initial support with method development for quantifying trichloroethylene metabolites. I am very grateful to Drs. Rachel Lynch and David Threadgill for their support with logistics and operations involved with the 90-day oral toxicity study. I would also like to thank Dr. Amie Perry for her histopathological observations.

As one aspect of my work heavily relied on bioinformatics analysis, I acknowledge Mr. Kranti Kongati and Dr. John House for their collaborative support with differential gene expression analysis. I am very grateful to Dr. Fred Wright for making frequent visits to Texas A & M University and engaging in meetings with me to discuss the progress and scope of one of the projects in my dissertation. Similarly, I would also like to thank Dr. David Aylor and his staff for designing R-based scripts for conducting quantitative trait loci (QTL) analysis.

Lastly, I thank my parents, immediate family-relatives, and friends for being supportive over the last several years. I would like to thank my significant half for providing emotional support in the midst of failures and excruciating circumstances during my dissertation and will fulfill the promises I have made to her over the coming years. Nonetheless, it has been an incredible journey and I hope to move on with my life towards a prosperous future.

TABLE OF CONTENTS

LIST OF TABLES

LIST OF FIGURES

CHAPTER 1: INTRODUCTION

I. Risk assessment of chemicals

Regulation of human exposure to toxic substances has been in existence for more than a century. The Pure Food and Drug Act of 1906 (enacted by the 59th US Congress) included consumer protection laws and established the Food and Drug Administration. It was replaced/amended by the US. Federal Food Drug and Cosmetic Act in 1938 (75th US Congress) (Barkan, 1985). In 1970s, a key initiative by the U.S. Food and Drug Administration was the establishment of the National Center for Toxicological Research that serves as a hub of studying health effects with chemicals. Since then, exposure to chemicals, toxicants, or pharmaceuticals has raised concerns of adverse health effects in humans, thereby, prompting the need for a regulatory framework to address risk associated with such exposures. Human health risk assessment involves systematic processes that aim to characterize the association of health effects with chemical exposures to aid with regulatory decisions regarding public health. Risk assessment models predict and create awareness of risk associated with particular chemical exposures and helps prioritize control measures in case of accidental release into the environment (Leeuwen & Hermens, 1995). Four components of risk assessment are hazard identification, dose-response assessment, exposure assessment, and risk characterization. For the purposes of this dissertation work hazard identification and dose-response components of risk assessment will be discussed below.

I.A. Hazard identification

Hazard identification is the qualitative assessment that aims to understand the nature of adverse health effect caused by chemicals. The cause-effect relationship is established based on epidemiological data, *in vitro* models or rodent carcinogenicity bioassay data. Epidemiological studies may aid in deriving associations between a chemical and an adverse health outcome (cancer, reproductive, or developmental toxicity) and play a crucial role in risk assessments (Adami et al., 2011). As epidemiological data are often unavailable for most chemicals due to challenges with assessing exposures, rodent bioassays are the most common method to identify hazards associated with chemical exposures. In these bioassays, mice and rats of both sexes are exposed to repeated doses of the chemical of interest and signs of both cancer and non-cancer toxicities are examined (Bucher, 2002). The findings from these studies are based on the general assumption that rodent assays are good models of humans (King-Herbert & Thayer, 2006). Across different regulatory agencies including the U.S. EPA, there is a general need to prioritize toxicity testing of chemicals (Dix et al., 2007). With the advancement in high throughput screening (HTS), the U.S. EPA initiated a research program titled "Toxicity Forecaster" or ToxCast™ that focuses in the development of a rapid and inexpensive platform to predict toxicity in chemicals based on bio-activity profiling (Knight et al., 2009). Previous studies have demonstrated the usefulness of ToxCast™ data to prioritize chemicals for hazard identification (Reif et al., 2010; Sipes et al., 2011).

Underlying biochemical events that are perturbed to cause an adverse effect with exposures are called mechanisms of action. Understanding the mechanism of action (MOA) helps to characterize a hazard because the relevance of such mechanisms across species can be considered when extrapolating findings from rodents to humans. Currently, evidence for mechanisms of

action for chemicals are often gathered using mechanistic models that rely on knock-out, knock-in, or humanized rodent models thereby identifying critical pathways of toxicity (Boverhof et al., 2011).

I. B. Dose-response assessment

Dose-response assessment in environmental toxicology often aims identify a point of departures (PoD) which is a point on the dose-response curve that is often used to derive an estimate of the low dose at which adverse health effects are expected to occur. With the use of epidemiological data, the dose can be established based on direct observations of health effects in humans. In the absence of human data, lowest doses are extrapolated based on data from rodents to humans. A persistent challenge in this approach is that the shape of the dose-response curve is vastly influenced by the degree of variability and uncertainty associated with the available data, often leading to inaccurate dose estimates (National Research Council, 2009).

II. Variability and uncertainty in components of risk assessment

Uncertainty in risk assessment arises due to lack of data or incomplete information (National Research Council, 2009). Uncertainty exists in all components of risk assessment (WHO, 1995). In theory, uncertainty will always exist due to gaps in knowledge and can only be minimized based on the quality, quantity, relevance of data, and the inferences applied towards risk assessment (2009). For example, appropriateness of the animal model and reliability of assays may significantly contribute to uncertainty in hazard identification. Differences in the mathematical models applied in capturing shapes of dose-response curves can result in large uncertainty associated with dose-response assessments. . Uncertainty in estimating tissue-specific internal doses of chemicals also poses a challenge in exposure assessments.

Variability refers to differences in responses due to heterogeneity within a species or population. Unlike uncertainty, variability cannot be minimized but can only be better characterized (National Research Council, 2009). Biological variability in responses arises from both intrinsic and extrinsic factors. These include hereditary factors (genetics or epigenetics), sex, age, pre-existing conditions, co-exposures, diet etc. (Zeise et al., 2013). Several studies have reported that exposures to pharmaceuticals in humans show inter-individual differences in responses leading to variable susceptibility to toxicity and adverse effects (Harrill, Watkins, et al., 2009; Hattis, Erdreich, & Ballew, 1987; Kwara et al., 2009). Further, as these responses can be qualitatively or quantitatively different in a population, addressing variability is critical in properly characterizing risk in human health risk assessments.

II.A. Traditional methods to address variability and uncertainty in risk assessment

Two approaches have been widely used to address uncertainty in risk assessment (Richardson, 1996).

Deterministic approach – In this approach each parameter or variable used in risk assessment processes is considered as a point estimate and uncertainty is addressed by using conservative assumptions. A common approach used by regulators to address uncertainty is to rely on defaults. In simple terms, defaults are inference guidelines that aid in the completion of risk assessment in the absence of chemical- or endpoint-specific data. Defaults are applied in cases when insufficient or lacking data lead to critical data gaps, in a manner to facilitate the risk assessment process (National Research Council, 2009). Use of safety factors is an example of applying defaults to address uncertainty due to data gaps in assessment. Traditionally, an uncertainty or safety factor of 100-fold is applied to establish no observed adverse health effect level (NOAEL) data from chronic rodent studies to humans (Dourson, Felter, & Robinson, 1996;

Lehman, 1954). A 10-fold factor is applied to account for intra-species variability in toxicokinetics (TK) and toxicodynamics (TD) ($10^{0.5}$=3.16 for each of these parameters). Another 10-fold factor accounts for variable response in human population. The use of defaults have always been a subject of debate as to whether it underestimates or overestimates risk estimates derived from rodent data. Depending on availability of data, the uncertainty with toxicity values can been reduced. Although efforts to address uncertainty using defaults have long existed, there is a need to develop better approaches to minimize uncertainty in risk assessments.

Probabilistic and statistical approach – Probabilistic and statistical approaches are perceived to be more realistic in deriving risk estimates and so have gained popularity in recent years. Benchmark dose (BMD) analysis is a useful metric to determine safe chemical exposure levels and deals with deriving NOAEL (Geter, Bhat, Gollapudi, Sura, & Hester, 2014). Traditionally, this analysis aims to establish dose-response relationships based on data on apical endpoints from sub-chronic or chronic rodent toxicity studies. In a statistical approach, uncertainty factors are implemented to derive safe estimates. In a probabilistic approach, each parameter from the rodent data is derived as a probability density function to provide a range of risk estimates. Although no clear guidelines are available in identifying the right numerical techniques to provide a risk distribution, use of computational approaches such as Monte Carlo Simulations, are more commonly implemented to assist with such applications.

Monte Carlo Simulation (MCS) – MCS is a numerical approach that involves repeated random sampling to generate results. It has been primarily implemented in risk assessment processes to address and minimize uncertainties in toxicokinetic responses with chemical exposures. Physiologically-based-pharmacokinetic (PBPK) models are mathematical models that are used to predict dose-time relationships of chemicals. These models are conceptually driven by

mass balance equations and can be multi-compartmental in nature to address complex TK profiles in different tissues. MCS is applied in PBPK models by randomly selecting values for each parameter in a mass-balance equation while keeping other parameters in the equation fixed. This process is repeated several times, until a probability distribution for each parameter is acquired, leading to range of estimates.

Although these approaches to address uncertainty in assessments have evolved over time, efforts to address variability still remains in infancy. It is evident that biological variability in toxic responses arise from several sources. Although it is difficult to identify the specific factor/s driving variability, the need to develop models to address variability is important and relevant to human health assessments. Several cases from the pharmaceutical industry have shown over the last decade that genetic variants or single nucleotide polymorphisms (SNPs) result in large variability in xenobiotic metabolism and drug-induced toxic effects (R. B. Kim, O'Shea, & Wilkinson, 1994; Krueger & Williams, 2005; Lanfear & McLeod, 2007). As classical rodent models are based on single strains or genotypes of rats and mice, the heterogeneous responses as observed in humans are often poorly captured in such models. Further, extrapolation of data from these rodent models to humans often raises questions as to whether data acquired in single strains of rodents are indeed reflective of sensitive individuals in the human population.

II. B. Individual- versus population-based risk assessment

Variability in human susceptibility to chemicals is a persistent challenge in risk assessments. As toxicity data in single-strain rodent models have been historically extrapolated to humans, variability in these responses due to genetic differences within the rodent species needs to be assessed to understand the divergence of derived toxicity values from their true values. One

critical concern with these extrapolations is that whether the rodent strain used in toxicity testing is a good model in mimicking qualitative and quantitative responses as observed in the susceptible groups or individuals in humans. Figure 1.1 shows an illustration depicting the relevance of incorporating susceptible individuals in toxicity testing. This figure demonstrates that within any population in a species there will be individuals or sub-groups that demonstrate higher risk to adverse health effects with exposures. Thus, use of susceptible individuals from one population may serve as good models to enhance hazard identification with chemical exposures.

Some environmental chemicals are known to interact with several biological targets suggesting the possibility of multiple mechanisms of action underlying elicited adverse outcomes. As toxicological assessments of these chemicals are often conducted in single rodent strains whether a particular mechanism of action for a chemical is predominant in the population or susceptible groups or individuals remains unaddressed (Figure 1.2**)**. This figure shows that two individuals in a population may demonstrate different dose-response relationships for identical exposure suggesting that population-level differences in the underlying mechanisms of responses needs to better understood. This information would then be useful in understanding inter-individual differences in toxic outcomes and also help build confidence in addressing human variability in risk assessments. Figure 1.3 shows a graph that demonstrates the significance of understanding population average responses. Herein, we observe that individuals in a population showing different degrees of effects. It is perceived that data from epidemiological and rodent studies provide risk estimates of population median; but information on whether population median and average differ significantly may be relevant in risk assessments. Despite understanding the limitations in existing models to assess risk with exposures, efforts to improve existing models to address variability is critical.

III. Implementation of emerging sciences and technologies to improve risk assessment

The objective of toxicity testing is to assess risk posed to humans by chemical exposures. Current approaches of toxicity testing originate nearly half a century ago at a time when knowledge on the biological hierarchy of signaling was in its infancy (Bhattacharya, Zhang, Carmichael, Boekelheide, & Andersen, 2011). In the last decade, numerous reports have highlighted the persistent challenges with current approaches of toxicity testing (National Research Council, 2007, 2009). For instance, in 2007 the National Research Council (NRC) outlined a far-reaching vision to incorporate emerging sciences and technologies in toxicity testing to better aid with characterization and identification of hazard. In 2009, NRC also published a book titled "Science and Decisions" emphasizing better approaches to address uncertainty and variability in scientific data to improve public health assessments. Additional reports have supported incorporating advances in molecular and systems biology into risk assessment practices (Andersen & Krewski, 2009; Cote et al., 2012).

III.A. Advances in mouse genetics that aid in the characterization of population-level health assessment

Rodent models have been widely implemented in biomedical research due to their supposed physiological similarities with humans (Roberts & Threadgill, 2005). These models are relatively inexpensive and can be generated in large quantities in a short period of time. Rodents are easily housed and handled during agent administration and sample collection procedures. Among different rodents, mice and rats are most common species for toxicity testing.

Laboratory mice have been historically used to study cancer, genetics, chronic diseases, infectious diseases, biomarker discovery, and other biomedical applications. In toxicology, mice

have been used to identify hazards and characterize dose-response relationships (OECD, 1996). Early advances in genetics enabled knock-out of specific genes thereby facilitating the development of mechanistic mouse models (Donehower, 1996). Later developments in genetics led to the creation of 'humanized' mice where functionally-active genes, cells or tissues from humans have been inserted into mice to characterize inter-species differences in dose-response relationships (Dorner et al., 2011). Despite significant progress in mouse genetics, efforts to develop mouse populations to characterize human genetic variability in adverse reactions remained unestablished through the early 2000s. For instance, although use of mouse diversity panels since 2000s involve the use of multiple strains, they are genetically close to each other due to historical breeding strategies from common stocks. Further, the use of population-based mouse models in biomedical research have demonstrated their utility in identifying genetic markers for complex traits but are yet to be adopted in the risk assessment processes.

In 2004, mouse geneticists developed a community resource to establish a reference panel of mice for integrating complex analysis to address human variability in adverse outcomes and diseases (Churchill et al., 2004). The Collaborative Cross (CC) is large panel of recombinant inbred lines derived from a genetically-diverse set of founder strains. Due to the breeding strategy the genomic structure of each CC line is a mosaic representation of genetic variants from the founder strains. Further, each CC line offers abundant genetic diversity by retaining a single nucleotide polymorphism (SNP) for every 100-200 bp thereby representing genomic structure as observed in humans (Churchill et al., 2004). Thus, the CC is a genetically-diverse and a reproducible model that may be useful in characterizing inter-individual differences in toxicokinetic and toxicodynamic responses with exposures.

In 2012, another population-based rodent model was developed from the CC model (Churchill, Gatti, Munger, & Svenson, 2012). The Diversity Outbred (DO) are F2 generation of randomly selected CC strains. Consequently, each DO mouse is heterozygous in its genotype and unique, and more similar to humans. Several studies have utilized DO populations to identify genetic drivers of variability in responses (Church et al., 2015; French et al., 2015; Smallwood et al., 2014). One major concern with DO is that the model is not reproducible and data produced from these models may be highly variable due to batch-to-batch differences in their genetic diversity.

Few studies have utilized the F1 intercrosses of CCs also known as CC recombinant intercrosses (RIXs) as a mouse population model for humans (Green et al., 2016a; Green et al., 2016b). CC RIXs are heterozygous in their genotypes and unlike the DO are reproducible. Although the different mouse populations described above have been used in several biomedical applications, their usefulness in toxicity testing is just starting to be evaluated.

III.B. Incorporation of genetic data to improve health assessment

Population geneticists have often employed scientific and technological advances relevant to the central dogma of molecular biology to draw connections between variability in a phenotype and genotype (Doerge, 2002). As many phenotypes or traits are often complex or driven by multifactorial elements, it is often required to identify all the regions in the DNA responsible to characterize total phenotypic variability in a population. Quantitative trait loci (QTL) is the region of DNA identified by a statistical analysis that is associated with the variability of a phenotype in a population.

Advances in next-generation DNA sequencing technologies have led to the rapid collection of genomic sequence information from individuals in a population to facilitate genotype-phenotype association analysis (Lappalainen et al., 2013). Human genome-wide association studies (GWAS) have enabled identification of genetic factors associated with metabolic diseases, drug metabolism and efficacy, and biomarkers of toxicity (Duerr et al., 2006). The underlying basis of GWAS is that SNPs can exert influence on a trait either due to a functional change in the protein sequence or in the rate of transcription. Although human GWAS is a powerful approach in identifying common genetic variants with risk of adverse effects, poor characterization of environmental exposures can lead to issues identifying risk-specific genetic factors. As rodent studies are always conducted in controlled environments, implementing population-based rodent models will help in accurately characterizing gene-environment interactions.

III.C. Pathway-based approaches to understand variability in mechanisms of action

In the last decade, transcriptomic approaches have been frequently applied in the field of toxicology to advance risk assessment by providing molecular insights on the mode of action of pharmaceuticals or chemicals (Burczynski et al., 2000; Harrill & Rusyn, 2008; E. Y. Xu et al., 2008). Traditional transcriptomic-based studies often aim to identify genes perturbed with treatment and provide little or no information on dose-expression relationships (Heijne, Stierum, Slijper, van Bladeren, & van Ommen, 2003; Robinson et al., 2010). Recent studies have provided strong evidences to support the incorporation of transcriptomic-dose response data for hazard identification or dose-response assessment (Andersen, Clewell, Bermudez, Willson, & Thomas, 2008; Thomas, Philbert, et al., 2013b). Combining pathway analysis with dose-expression responses can help identify sensitive cellular pathways and establish reference doses at which pathways are perturbed by treatment (Thomas et al., 2007a). Due to the high cost associated with

conducting two-year cancer bioassays, studies have shown that PoDs from gene expression data from acute toxicity studies may be used as an alternative to apical endpoints to establish dose-response relationships (Bercu et al., 2010; Thomas et al., 2007a; Thomas et al., 2012).

IV. Critical problem in human health risk assessments

Chemical risk assessments aid in informing the public on hazard associated with exposures. Addressing human variability in susceptibility to toxic effects is a persistent unmet need in risk assessments. Evidences suggests that use of uncertainty factors to address inter-individual responses in toxicokinetics and toxicodynamics may not cover human variability that arise from genetic polymorphisms (Dalen, Dahl, Bernal Ruiz, Nordin, & Bertilsson, 1998; Dorne, Walton, & Renwick, 2003, 2005; Harrill, Watkins, et al., 2009). Due to limited genetic diversity, current mouse panels have limited precision in identifying genetic factors that aid in the characterization of variability in mechanisms of toxicity in a population. Current approaches in evaluating variability in responses often are poorly rationalized in terms of selection of strains, study designs, and end points investigated to establish dose-response relationships. Existing models lack the power to implement systems genetic approaches in drawing connections between variability in toxic responses and molecular events. Further, toxicity testing for regulatory purposes employs single strains of rodents to identify and characterize chemical-specific effects. Such practices in toxicological studies highlight the *critical need in evaluating and characterizing variability in toxicodynamic and toxicokinetic responses using population-based rodent models*.

Population-based rodent studies are often expensive, tedious, and labor intensive. Although previous studies using population-based rodent models exist, their relevance to regulatory

toxicology is difficult to establish. Thus, the overall objective of this doctoral dissertation is to serve as a systematic guide in conducting population-based rodent studies and provide relevant information to improve human health assessments. Several toxicokinetic and toxicodynamic studies were conducted to fully characterize variability in responses driven by a case-study toxicant trichloroethylene.

V. Trichloroethylene (TCE) as a case study toxicant

Despite toxicological information gathered over several decades, TCE is still one of the ten chemicals that will be evaluated for potential risks to human health under The Toxic Substances Control Act (TSCA), amended by the Frank R. Lautenberg Chemical Safety for the 21st Century Act in 2016. TCE is a chlorinated solvent that is colorless, odorless, volatile, and insoluble in water. It was initially produced in large quantities in the 1920s in Germany and United States with the primary application as a degreasing agent in industrial operations (Cotter, 1950). Due to poor waste disposal practices of TCE it is recognized as a ubiquitous environmental contaminant and found in elevated levels in soil and ground water. Its high volatility poses chronic human health risk with exposures in residential and public spaces.

V.A. Health hazard with TCE

TCE is associated with both cancer and non-cancer adverse health effects (Rusyn et al., 2014). Previous occupational studies have shown strong positive associations between TCE exposure and kidney cancer in humans (McGregor, Heseltine, & Moller, 1995). Studies in rats have shown increased incidences of kidney tumors with TCE exposures across both sexes (National Toxicology Program, 1988). Epidemiological Studies have also shown positive association between TCE exposure and non-Hodgkin lymphomas (Guha et al., 2012). In mice,

exposure to TCE has led to statistical increases in the formation of liver tumors (Bull et al., 2002). The International Agency for Research on Cancer (IARC) classifies TCE as Group 1 chemical, *carcinogenic to humans*, based on strong epidemiological evidence for kidney cancer and mechanistic evidence from animal studies (Guha et al., 2012; IARC, 2014).

V.B. Metabolism of TCE

The majority of adverse effects from TCE exposures are associated with its metabolites. TCE is primarily metabolized by two major pathways (Figure 2.1) in both rodents and humans – the Cytochrome P450 (CYP) dependent oxidation and glutathione (GSH) conjugation. Although oxidative metabolism of TCE takes place primarily in the liver, it can also occur in lung, kidney and other organs (Cummings & Lash, 2000; Forkert, Lash, Nadeau, Tardif, & Simmonds, 2002; Odum, Foster, & Green, 1992). Among many metabolites generated in the oxidative pathway, trichloroacetic acid (TCA) and dichloroacetic acid (DCA) are associated with formation of liver tumors in mice (Bull, Sanchez, Nelson, Larson, & Lansing, 1990). Glutathione-dependent metabolites of TCE are further biotransformed to reactive intermediates that are associated with kidney toxicity (Lash, Fisher, Lipscomb, & Parker, 2000). Quantitative differences in levels of TCE metabolites are known to exist between species and may contribute to inter-species differences in TCE adverse effects (Rusyn et al., 2014). PBPK modeling has shown that the quantitative extent of variability in oxidative metabolites are similar in target tissues among both humans and mice (Chiu et al., 2014a).

Previous reports suggest that specific metabolites of TCE can act by either genotoxic or non-genotoxic mechanisms of toxicity on target tissues (Chang, Daniel, & DeAngelo, 1992; Dekant et al., 1986; Giller, Le Curieux, Gauthier, Erb, & Marzin, 1995; Vamvakas, Elfarra,

Dekant, Henschler, & Anders, 1988; Y. C. Zhou & Waxman, 1998). For instance, it is well known that TCA and DCA are peroxisome proliferator-activated receptor α (PPARα) activators that induce peroxisome proliferation and hepatocellular proliferation in rodents. The glutathione-dependent metabolite S-(1, 2-dichlorovinyl) glutathione (DCVG) is known to exhibit genotoxic mechanism of action in the kidney (Vamvakas et al., 1988).

Inter-individual differences in TCE toxicokinetics and toxicodynamics have been previously investigated in both rodents and humans. Studies in humans have shown inter-individual differences in TCE toxicokinetics suggesting the existence of susceptibility to TCE toxicity (Ertle, Henschler, Muller, & Spassowski, 1972; Muller, Spassovski, & Henschler, 1974; Muller, Spassowski, & Henschler, 1975). Rodent studies have demonstrated inter-strain differences in oxidative and GSH-dependent metabolite levels suggesting dominance of different mechanisms of action for each strain with repeated TCE exposures (Bradford et al., 2011). This evidences suggest that inter-individual variability in adverse responses exists in both rodents and humans. However, there is a need to better characterize variability by identifying genetic drivers underlying these responses.

VI. Rationale and Specific Aims

VI.A. Choice of population-based rodent resource

Among different population-based rodent models available, we selected the CC model for most of our studies for several reasons. First, the CC is a large panel of recombinant inbred lines that provides sufficient statistical power to perform systems genetic analysis. Second, the model is reproducible and so the findings from our studies can be repeated to establish data reproducibility. Third, the genetic data of the CC population is well curated to perform genetic and

genomic analyses. In order to evaluate variability between different models one of our studies involved using CC, DO, and CC-RIX strains to assess models with large variability in toxic effects.

VI.B. Choice of case-study toxicant

Trichloroethylene was selected as the case study toxicant for our studies. First, TCE is a known carcinogen in both humans and mice. Evidences of inter-individual differences in TCE metabolism and toxicity has been reported in both humans and mice (Muller & Spassows.M, 1973; Yoo, Bradford, Kosyk, et al., 2015b). Exposure to TCE generates metabolites that are associated with organ-specific cancer toxicities, and PBPK modeling has shown that the quantitative extent of variability in these metabolites is similar in target tissues among both humans and mice (Chiu et al., 2014b).

VI.C. Choice of study designs

We conducted single-dose acute toxicity studies to characterize toxicodynamic and toxicokinetic responses. We also conducted a 90-day oral toxicity study in close accordance to the OECD guidelines to evaluate variability in toxic responses within and between different population mouse models in reference to B6C3F1.

VI.D. Specific Aims

Aim 1: To evaluate and characterize inter-individual differences of TCE metabolism in CC

Hypothesis: Inter-individual differences in TCE metabolism are driven by genetic diversity in the CC model

Aim 2: To evaluate and characterize inter-individual variability in liver gene-expression responses in CC

Hypothesis: TCE exposure causes differential expression of genes in the liver in a dose-, strain-, and dose*strain- dependent manner

Aim 3: To evaluate inter-individual differences in TCE metabolism and toxicity in a 90-day oral toxicity study using genetically-diverse mouse populations.

Hypothesis: We hypothesize that inter-strain differences in responses within different mouse populations will be highly variable compared to intra-strain variability in B6C3F1 mice, and will exhibit wide variability in TCE toxicity from sub-chronic exposures will be observed.

VII. Figures and Tables

Figure 1.1. An illustration depicting susceptible individuals from two species to risk with exposures.

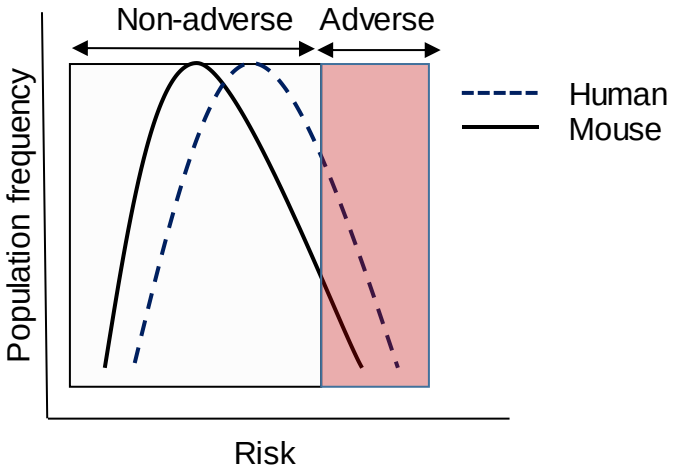

Figure 1.2. A sketch depicting two individuals showing different dose-response relationships with identical exposure.

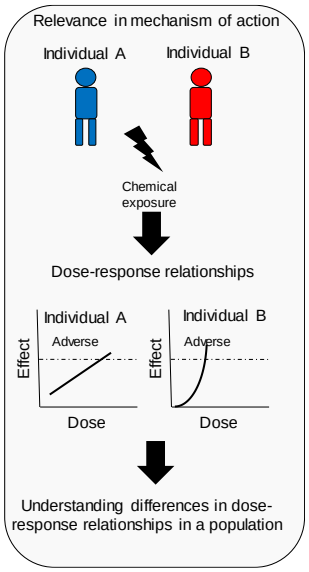

Figure 1.3. An illustration depicting individual versus population dose-response relationships.

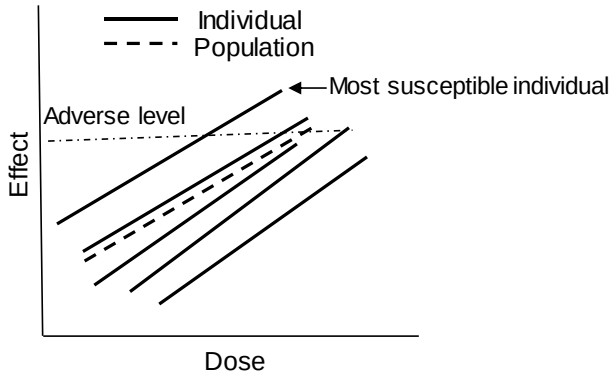

CHAPTER 2: EVALUATION AND CHARACTERIZATION OF INTER-INDIVIDUAL DIFFERENCES IN TCE METABOLISM[1]

I. Introduction

Addressing population-level variability in susceptibility to toxic effects of environmental exposures is a persistent unmet need in human health assessments (Zeise et al., 2013). Traditional toxicity testing is conducted in a single isogenic strain of laboratory rodents (Festing, 1986), which complicates the extrapolation to the heterogeneous human population. Recent studies demonstrated the utility of the mouse population-based approach for quantitative evaluation of the variability in metabolism and toxicity (Bradford et al., 2011; Chiu et al., 2014a; French et al., 2015), characterization of the susceptibility mechanisms (Harrill, Watkins, et al., 2009; Koturbash et al., 2011; Yoo, Bradford, Kosyk, et al., 2015a; Yoo, Bradford, Kosyk, Uehara, et al., 2015), and mapping of the loci that may confer susceptibility to toxicants (Church et al., 2015; French et al., 2015; Harrill, Watkins, et al., 2009).

The use of population-based mouse models in experimental biomedical research have flourished with the recent advancements in mouse genetics and the availability of the Diversity Outbred (DO) and Collaborative Cross (CC) populations (Aylor et al., 2011; Bogue, Churchill, & Chesler, 2015). These mouse populations were designed to randomize genetic variation so that all components of systems can be interrogated as allele frequencies are ideal for quantitative trait

[1] The text from this chapter is reproduced with permission from Toxicological Sciences 158(1): 48-62 (2017).

locus (QTL) mapping; they are also sufficiently large to power analyses of modest interactions (Threadgill & Churchill, 2012). The genome of each CC and DO line represents a mosaic of eight parental inbred strains distributed randomly across the genome; however, because CC lines have been inbred they carry an advantage of infinitely reproducible model to support data integration and reproduction across laboratories, chemicals and study designs (Threadgill & Churchill, 2012). The CC mouse model has been highly efficient in identifying candidate genetic markers responsible for several pathophysiological conditions, genetic analysis of complex traits, identification of novel gene functions, and modeling emergent diseases (Aylor et al., 2011; Durrant et al., 2011; Ferris et al., 2013; Kovacs et al., 2011; Rasmussen et al., 2014; Rogala et al., 2014).

Experimental toxicology is poised to make use of the CC population for investigations of the genetic and molecular determinants of inter-individual variability in toxicokinetics and toxicodynamics. For example, quantitative assessment of inter-individual variability in metabolism of several environmental contaminants of major public health relevance, such as chlorinated solvent trichloroethylene (TCE), is among the critical needs for human health assessments (Cichocki et al., 2016). TCE is a ubiquitous environmental chemical and is a carcinogen in humans (Rusyn et al., 2014). It is primarily metabolized (Figure 1) by the cytochrome P450 (CYP) system and glutathione conjugation generating qualitatively similar metabolites in both humans and rodents (Lash, Chiu, Guyton, & Rusyn, 2014). Among the metabolites of TCE, trichloroacetic acid (TCA) is the prevalent oxidative metabolite and a known peroxisome proliferator-activated receptor alpha (PPARα) agonist that is thought to be one of the key drivers of TCE toxicity (Bull et al., 1990; Chiu et al., 2013; Corton, 2008). Previous studies have demonstrated inter-individual differences in oxidative TCE metabolism and toxicity in humans (Muller et al., 1974; Muller et al., 1975) and multi-strain studies in mice (Bradford et al.,

2011; Yoo, Bradford, Kosyk, et al., 2015a; Yoo, Bradford, Kosyk, Uehara, et al., 2015). Interestingly, PPARα-mediated pathways, including the metabolism genes induced by TCE, are among the most distinct effects that are dependent on genetic background (Bradford et al., 2011).

The objective of this study was to evaluate the extent of inter-strain variability in the oxidative metabolism of TCE, and to identify loci that may be driving these differences. We hypothesized that genetic diversity affects inter-strain differences in TCE metabolism and toxicity. We conducted a dose– response (0, 24, 80, 240, or 800 mg/kg of TCE) study in 50 CC strains. Inter-strain variability in TCA levels, as well as protein or activity levels of several TCE-metabolizing enzymes, was examined in the CC mouse population at 24 h after dosing. We identified several QTLs associated with variability in TCE metabolism that provide genetic evidence for the role of PPAR pathway in the oxidative metabolism of TCE.

II. Materials and methods

Animals and treatments. Adult male mice (8–12 weeks old) from 50 CC strains were acquired from the University of North Carolina Systems Genetics Core (Chapel Hill, NC). Animals were fed an NTP 2000 wafer diet (Zeigler Brothers, Inc., Gardners, PA) and water ad libitum. The housing room was maintained on a 12-h light–dark cycle. Animals were allowed to acclimate to the room for at least 10 days prior to beginning experimentation. The experimental design sought to maximize the number of strains relative to within-strain replications based on the power analysis for QTL mapping in mouse populations (Kaeppler, 1997); therefore, one mouse was used per strain/dose group. Male animals were used because maximal rates of TCE oxidative metabolism in rodents differ between males and females, higher concentrations of CYP-derived metabolites of TCE were found in livers of males than in females (Lash, Putt, & Parker, 2006). Mice were orally

administered a single dose of 0, 24, 80, 240, or 800 mg/kg TCE (Sigma Aldrich, St. Louis, MO) in 5% Alkamuls EL620 vehicle (Solvay, Deptford, NJ). The highest dose was selected based on the studies of sub-chronic toxicity and carcinogenicity of TCE in mice (National Toxicology Program, 1990). Mice were sacrificed 24 h after treatment, tissues were flash frozen in liquid nitrogen and stored at 80 C until analysis. In the highest dose group, mice from 5 CC strains died before sacrifice; therefore, all further analyses were conducted on 45 CC strains with complete dose–response data. All treatments were conducted between 8 and 11 am to limit potential diurnal variation in TCE metabolism. In life portion of the study was conducted over a 6-week time-frame to limit seasonal variations. These studies were approved by the Institutional Animal Care and Use Committees at Texas A&M University and the University of North Carolina.

TCA levels in tissues. Analyses were performed by a modification of US EPA method 552.2 (Domino, Pepich, Munch, Fair, & Xie, 2003).(Domino, Pepich, Munch, Fair, & Xie, 2003) In brief, 50 mg of kidney, 100 mg of liver, 50 mg of brain, or 100 µL of serum was homogenized in 1 mL chloroform: methanol (1:1) containing 20 µL of 2-bromobutyric acid (550 nmol/mL). Distilled deionized water (300 µL) was added to the homogenate followed by vortexing and centrifugation at 15 000 rpm for 10 min. The supernatant was transferred to a new vial containing 1.5 mL of 10% sulfuric acid in methanol and incubated in a water bath at 50 C for 2 h. Methyl esters were extracted in 2 mL methyl tert-butyl ether followed by addition of 3 mL sodium sulfate (100 g/L). . The organic layer was neutralized by addition of 3 mL saturated sodium bicarbonate solution and concentrated under a stream of nitrogen gas to a volume <50 µL. A calibration curve from 0 to 1000 nmol/g consisting of TCA spiked into tissues before extraction was run with each batch for quantitative analysis. The extracts were analyzed using a HP 6890 gas chromatography system coupled with a HP 5973 mass selective detector (Agilent Technologies, Santa Clara, CA).

A 2 µL sample was introduced into gas chromatograph by splitless injection on to a 30 m x 0.25 mm, 0.25 mm HP5-ms column (Agilent Technologies). The carrier gas flow was set at a constant flow rate of 1 mL/min. The oven was held isothermally at 40 C for 10 min and then ramped to 65 C over the next 10 min, then to 85 C for the next 2 min, and finally to 205 C over 6 min. The injector and transfer line temperatures were maintained at 210 C and 280 C, respectively. The mass selective detector operated in the electron impact mode with the ion source set at 230 C and electron energy at 70 eV. Methyl esters of TCA and 2-bromobutyric acid were quantified by monitoring the ion at 59 m/z. Ions at m/z 117, 119, 151, and 153 were used to identify the analytes.

Extraction of hepatic microsomes and cytosolic fractions. A published protocol was adapted for the extraction of microsomal and cytosolic fractions (Yan and Caldwell, 2004). In brief, 100 mg of liver tissue was homogenized in 1 mL ice-cold 50 mM tris base solution containing 15 mM potassium chloride and centrifuged at 9000 g for 20 min. The supernatant was transferred to a new vial and ultra-centrifuged at 100,000 g for 1 h at 4C. The supernatant was aliquoted and the microsomal pellet was re-suspended in 200 µL 50 mM tris-HCl (with 20% glycerol, pH 7.4) and stored at 80 C. Total protein concentration was measured using a Pierce BCA Protein Assay Kit (ThermoFisher Scientific, Waltham, MA).

Alcohol dehydrogenase (ADH) and aldehyde dehydrogenase (ALDH) activity assays. ADH and ALDH activity assay kits were purchased from Sigma-Aldrich. Activity assays were performed on cytosolic extracts according to the manufacturer's protocol.

CYP1A1 activity assay. Magnesium chloride, glucose-6-phosphate, glucose-6-phosphate dehydrogenase, resorufin, resorufin ethyl ether, and b-nicotinamide adenine dinucleotide phosphate hydrate reduced tetra sodium salt hydrate (NADPH) were purchased from Sigma-

Aldrich. Microsomal incubations were setup according to a published protocol (Yan and Caldwell, 2004). In brief, 100 µL of chilled tris base buffer, 50 µL of 5 mM MgCl2, 50 µL of 5 mM glucose-6-phosphate, 50 µL of 0.5 mM NADPH, 250 mg of microsomal protein, and 10 µL of 3.3 mM resorufin ethyl ether were incubated in a 96-well plate. Formation of resorufin was monitored at excitation and emission wavelengths of 530 nm and 585 nm, respectively. A standard curve from 0 to 1 mM for resorufin was generated using heat-inactivated microsomes.

CYP2E1 protein expression. About 20–30 mg pulverized liver tissue was homogenized in 400 µL tissue protein extraction reagent (T-PER, ThermoFisher Scientific) containing HALT protease inhibitor cocktail (ThermoFisher Scientific). The homogenate was centrifuged at 10,000 g for 5 min and the proteins in the supernatant were transferred to a new vial. The isolated proteins were quantified using Pierce BCA Protein Assay Kit (ThermoFisher Scientific). Protein aliquots (20 mg) were loaded on to an SDS-PAGE containing of Mini-Protean TGX precast gels (Bio-Rad, Richmond, CA). Western blotting was performed using Trans-blot Turbo Transfer System (Bio-Rad), and Immuno-Blot PVDF membranes (Bio-Rad). Membranes were blocked using Odyssey blocking buffer (Li-Cor, Lincoln, NE) and were incubated overnight at 4 C with 1:5000 anti-CYP2E1 antibody (Abcam, Cambridge, MA). The membranes were then washed and incubated with 1:2500 goat anti-rabbit antibody conjugated with peroxidase (Millipore, Bedford, MA). Protein bands were developed by chemiluminescent staining with WesternSure ECL Substrate visualized by C-Digit Blot-Scanner (Li-Cor). Anti-b-actin antibody (1:2500, Abcam) staining was used as a loading control.

Gene expression analysis by RT-PCR. Total RNA was isolated from 20 to 30 mg of pulverized left liver lobes in liquid nitrogen using MiRNeasy mini kit (Qiagen, Valencia, CA). RNA concentrations were measured using Nanodrop ND-1000 (Thermo Fisher Scientific). cDNA

was synthesized from 2 µg RNA using High Capacity cDNA Achieve kit (Thermo Fisher Scientific). Quantitative real-time PCR was performed using Taqman probes for genes Acox1, Acot8, Cyp4a10, Cd40, Fitm2, and Top1 (Abcam) on Light Cycler 96 (Roche, Indianapolis, IN).

Genome-wide quantitative trait locus (QTL) mapping. High-density sequences of CC genomes for strains used in this study were downloaded from the UNC Systems Genetic Core (http: //csbio. unc.edu/CCstatus/index.py?run¼Pseudo; last accessed March 31, 2017). Information on reference SNPs for genes were acquired from the Mouse Genome Informatics database (http:// www.informatics.jax.org/; last accessed March 31, 2017). Flanking DNA sequences for each SNP in each CC strain was performed using a custom R script. QTL mapping was performed using DOQTL package (D. M. Gatti et al., 2014) using a model that considered each of the eight founder alleles separately. Only seven founder alleles were present in the mapping population at the location Acox1 QTL, resulting in overfitting of DOQTL's eight-allele model. In order to better estimate the QTL effects, we simulated CC mapping populations that consisted of our actual CC lines plus an additional three simulated lines that harbored the PWK allele missing form our mapping population. We assigned each simulated line a phenotype randomly sampled the observed phenotype distribution (such that the simulated lines would not affect the QTL) and remapped in the QTL region. These simulations yielded a properly fitted model and improved estimates of the effects of the other seven alleles.

Statistical analysis. Graph Pad Prism (La Jolla, CA) was used to perform statistical tests. R (v.3.1.2) was used to generate line graphs and boxplots (ggplot2). For all tests, a $P < .05$ was required for statistical significance. In analyses that involved multiple comparisons, a false discover-corrected q values were derived. Data availability. All raw data are publically-available through the Mouse Phenome Database (http://phenome.jax.org/; ID: Rusyn8).

III. Results

Mouse Population Variability in Metabolism of TCE to TCA. Metabolism is critical for the toxicity, mutagenicity, and carcinogenicity of TCE; TCA is the most abundant metabolite that is formed through cytochrome P450 (CYP)-dependent oxidation [Figure 2.1, reviewed in (Cichocki et al., 2016; Lash et al., 2014). Because of the focus on the dose–response effects of TCE and toxicodynamic responses among multi-tissues, a single time point of 24 h was selected. At this time point, only TCA is detectable in mouse tissues at comparable highest doses (S. Kim et al., 2009). We observed extensive strain-dependent variability in TCA levels in mouse tissues (liver, kidney, brain, and serum) 24 h after oral dosing with TCE (Figure 2.2, Supplementary Figures 1.1A–1.1C). At each dose (24–800 mg/kg), the capacity to metabolize TCE via the oxidative pathway varied by an order of magnitude or more among strains. Appreciable consistency exists among strains with high, intermediate, or low TCA levels across all dose groups (Supplementary Figure 2.1). For example, strains CC028/GeniUnc, CC059/TauUNC, and CC010/GeniUnc showed relatively high levels of TCA in liver across different dose groups (Figure 2.2). Similarly, strains CC042/GeniUnc, CC017/Unc, and CC055/TauUnc are low responders, and strains CC006/TauUnc, CC030/GeniUnc, and CC003/Unc show intermediate levels of TCA at 24 h after dosing. We observed similar trends in kidney, brain and serum (Supplementary Figures 2.1–2.3).

Next, we compared the population-level (using data from 45 CC strains) variability in TCA amounts at 24 h in liver, kidney, brain, and serum with that predicted by a population-wide physiologically based pharmacokinetic (PBPK) model (Chiu et al., 2014a) that was calibrated with data from 15 classical inbred strains (Bradford et al., 2011). Figure 2.3 shows data from each strain (circles) compared with the PBPK model predictions (boxes). Liver TCA levels at doses of 24, 80, and 240 mg/kg for more than 85% of CC strains fall within the 95% confidence interval of the

PBPK model predictions (Figure 2.3A). Interestingly, liver TCA levels in the 800 mg/kg dose group are higher than the predicted 95% confidence interval for more than half of CC strains (Figure 2.3A). Kidney TCA levels at 24 mg/kg and 80 mg/kg doses were below the limit of detection for most of the CC strains; at the 240 mg/kg dose, TCA levels fall within the 95% confidence interval for more than 85% of CC strains (Figure 2.3B). In 800 mg/kg dose group, about one third of the strains fall outside of the 95% confidence interval for model-predicted kidney TCA levels (Figure 2.3B). Similarly, while serum TCA levels at 24 and 80 mg/kg were generally within the 95% confidence limit of the model, close to half of the strains are greater than this confidence interval in 240 and 800 mg/kg dose groups (Figure 2.3C). The most striking feature is the difference in predicted and observed medians, nearly every CC animal is above the median value predicted by the model. Overall, these results from a much larger population-based study of TCE toxicokinetics show that the PBPK model is under-predicting the levels of TCA in different tissues, especially at the highest doses.

Induction of Enzyme Levels/Activity in Response to TCE Treatment.

Oxidative metabolism of TCE to TCA is thought to involve a number of cytochrome P450 and other enzymes (Lash et al., 2014); therefore, we sought to examine effects of TCE exposure on several key enzymes. Specifically, because of the observed wide range of liver TCA levels among strains, we sought to examine whether basal or TCE-induced levels of major microsomal and cytosolic enzymes involved in TCE metabolism might explain the inter-strain variability in liver TCA levels. Liver Cyp2e1 protein levels (Figs. 2.4A-2.4B) and liver Cyp1a1 activity (Figs. 2.4C–2.4D) varied extensively among strains in both vehicle- and TCE (800 mg/kg) treated

animals. No difference of the group means was observed in response to TCE for either of these enzymes, albeit the variance in these parameters increased in TCE-treated group. This observation is concordant with a previous report that treatment with TCE was without effect on protein levels of liver Cyp2e1 across seven inbred strains (Yoo, Bradford, Kosyk, Uehara, et al., 2015).

Alcohol dehydrogenases (ADH) and aldehyde dehydrogenases (ALDH) also play a key role in determining the metabolic flux of chloral hydrate, an intermediate metabolite that yields TCA (Figure 2.1). We examined activity of ADH and ALDH in livers of both vehicle- and TCE (800 mg/kg)-treated animals. A statistically significant increase ($P < .05$) in activity of both ADH and ALDH was observed with TCE exposure (Figure 2.5).

Because we observed large differences in liver levels of TCA among strains, we also examined whether TCE-induced peroxisomal proliferation varied. While TCE and TCA are PPARα ligands (Maloney & Waxman, 1999; Y. C. Zhou & Waxman, 1998), it is well known that expression and protein levels of PPARα are not affected by TCE (Fang et al., 2013; Ramdhan et al., 2008) and other peroxisome proliferators (Ito et al., 2007) but its transcription factor activity is affected. Therefore, we examined transcript levels of two PPARα-responsive genes, cytochrome P450 subfamily 4 polypeptide 10 (Cyp4a10) and acyl-CoA oxidase 1 (Acox1) in livers of vehicle and TCE (800 mg/kg) treated animals. Both Acox1 and Cyp4a10 transcript levels were induced ($P < .05$) by TCE (Figure 2.6). Similar to our observation in a smaller population of inbred strains (Bradford et al., 2011) strain-specific effects were prominent. The expression of both transcripts was either not affected or increased in TCE-treated animals in all strains (with the exception of Cyp4a10 levels in strain CC037/TauUnc). The magnitude of the effects on PPARα-mediated gene expression was much more robust than effects on Cyp2e1, Cyp1a1, ADH, or Aldh (Figs. 2.4 and 2.5).

Correlation of Enzyme Levels/Activity with TCA Liver Concentrations.

To further examine the relationships between TCA levels in different tissues and other phenotypes evaluated in this population-based mouse study, we performed correlation (Spearman rank) analysis using data on CC mice from the 800 mg/kg dose group (Supplementary Table 2.1). We observed that TCA levels correlate positively among all tissues examined, with the highest correlation among liver, brain and kidney (Figure 2.7A). In addition, we found that liver TCA levels positively correlated with induction of Acox1 transcript levels in the liver, and the transcriptional effects of TCE on Acox1 and Cyp4a10, both markers of activation of transcription factor PPARα, were also significantly correlated (Figure 2.7B). These data suggest that inter-strain differences in TCE metabolism may be associated with TCE-mediated responses in CC mice. Notably, liver levels of TCA did not correlate with either basal or TCE-affected protein levels or activity of Cyp2e1, Cyp1a1, ADH, or Aldh, an observation that is similar to the findings of (Yoo, Bradford, Kosyk, Uehara, et al., 2015).

QTL mapping

To identify genomic regions associated with inter-strain differences in TCE metabolism and transcriptional changes, we mapped QTL using a model that considered each of the eight founder alleles separately using liver TCA and Acox1 transcript levels in the highest treatment group. We identified quantitative trait loci (QTL) on chromosome 2 for each of the phenotypes (Figs. 2.8A and 2.8C). Further, we observed that NOD/ShiLTJ and WSB/EiJ founder alleles have most pronounced effects on QTLs associated with TCA formation and Acox1 induction (Figs. 2.8B and 2.8D).

There are many protein-coding genes in the locus associated with the variability in liver TCA levels across the population (Table 2.1). From this list, candidate genes were selected based on the available information for their function that could be linked to the effects of TCE. We chose acyl-coenzyme A thioesterase 8 (Acot8) and Fat Storage Inducing Transmembrane protein 2 (Fitm2) as candidate genes for further analysis because of their role in PPAR signaling, as well as several neighboring genes not involved in PPAR signaling or metabolism, Cluster of Differentiation 40 (Cd40) and Topoisomerase 1 (Top1). We performed RT-PCR to further examine whether transcript levels of the candidate and neighboring genes are associated with the phenotype, level of TCA in liver, used for mapping. Induction of Acot8 and Fitm2 expression was significantly positively correlated with liver TCA; Cd40 and Top1 transcript levels showed no correlation with this phenotype (Figure 2.9).

The QTL associated with strain-specific variability in TCE-induced liver expression of Acox1 (Table 1.1) contained only one protein coding gene, Low Density Lipoprotein Receptor-Related Protein 1B (Lrp1b). Even though, Lrp1b is a tumor suppressor gene regulated via the PPARγ signaling pathways (Liu, Musco, Lisitsina, Yaklichkin, & Lisitsyn, 2000), it was neither expressed in livers of the mice included in this study, nor was it induced by TCE.

To further explore the role of PPARα signaling in the variability associated with TCE metabolism, we considered the potential contribution from the genetic variants of PPARα. There are two non-synonymous coding SNPs (rs16820391 and rs16820392) in PPARα in the CC founder strains. The frequency of distribution of A/G missense substitution for both SNPs was around 50% across CC strains included in this study. No statistically significant difference was observed in liver TCA levels among strains with PPARα genotypes (A/G) for either SNP (data not shown). It is well established that retinoid X receptor alpha (RXRα), a type II nuclear receptor is capable of

interacting with PPARα and PPARγ by forming heterodimers thereby mediating fatty acid and lipid metabolism (Berger & Moller, 2002; Chandra et al., 2008). A nonsynonymous SNP (rs16817900) generating a C/T missense substitution was identified among the CC founder strains and was also present in 4 out of 45 CC strains examined. Interestingly, we found that in strains with RXRα C genotype, liver TCA levels were about 2-fold lower (in both mean and median) than in T allele strains (Supplementary Figure 2.4). Although, no statistical significant difference was observed between C/T genotypes and liver TCA levels because only 4 strains harbor the C allele this finding suggests PPAR-RXR signaling as contributing to differences in oxidative metabolism of TCE among CC strains.

IV. Discussion

The focus of this study was on characterizing the extent of population-level variability in chemically mediated responses in a diverse population, as well as on exploring the mechanisms of such variability using genetic mapping. Although several previous studies used classical inbred strains to assess inter-individual variability in TCE metabolism and toxicity, they were limited in the degree of genetic diversity. In the CC mouse population, genetic variants are randomly distributed across the genome, creating a mosaic genome with potentially significant differences in cellular functions as compared with those in the founder strains. Consequently, the CC lines permit high-resolution QTL mapping, enabling the identification of the genes that may be associated with the phenotypic variability at the genome level.

Using a CC mouse population, we aimed to increase precision of the estimates for the extent of inter-individual variability in TCE metabolism. Data from this study was compared with a previous study (Bradford et al., 2011) where a multi-strain panel was used to assess variability in

TCE metabolism. In the Bradford et al. (2011) study, inter-strain differences in the TCA levels in serum at 24 h post-dosing at 2,100 mg/kg TCE were around 4- to 6-fold across strains. In CC population, we observed more than an order of magnitude differences in the level of TCA at 24 h in tissues (using 800 mg/kg TCE dose data), further supporting the importance of genetic variability in TCE metabolism. We also found that select strains are low, intermediate or high "metabolizers" of TCE to TCA. To determine the concordance in population-level variability among two population-based studies, median estimates of TCA levels were derived using a PBPK model (Chiu et al., 2014a) and compared with the data in this study. We found that inter-strain variability in TCA levels in the CC mice was concordant with PBPK model predictions at lower doses across tissues. However, at the 800 mg/kg dose, nearly half of all strains were above the predicted ranges across different tissues. Metabolism of TCE in the rat is a saturable process at doses around 1,000 mg/kg, but in the mouse TCE metabolism is linear up to a dose of 2,000 mg/kg (Prout, Provan, & Green, 1985). Thus, our results are unlikely to be due to metabolic saturation and suggest that genetic diversity among CC mice may play a role in inter-strain differences in TCE toxicokinetics. The fact that model-derived median predictions were about one half to an order of magnitude below the observed values across all tissues examined is an indication that our data may be useful for updating the model with a larger population and data from additional tissues. In addition, further exploration of strain-dependent variability in concentration–time responses is needed. One additional test for the hypothesis that genetic diversity plays a role in inter-strain differences in toxicokinetics would be selection of strains representing population-level variability in TCA levels for a toxicokinetic study that will evaluate TCE metabolite levels at concentration–time across various tissues.

Several enzymes are involved in the oxidative metabolism of TCE to TCA (Lash et al., 2000). Genes associated with CYP, ADH, and ALDH families are known to be polymorphic and to result in inter-individual differences in their activity among individuals (Pastino, Yap, & Carroquino, 2000). Little evidence for the inter-individual differences in TCE metabolism through oxidation exist in human populations or in experimental animal studies. Most studies examined the role of polymorphisms in CYP2E1 and ADH/ALDH pathway, genes that are known not only to be polymorphic, but also contain polymorphisms that have known linkages to human cancer susceptibility (Li, Zhao, Sun, Luo, & Xiao, 2016). CYP2E1 is the principal enzyme responsible for metabolism of TCE in humans and rodents (Pastino et al., 2000). Other CYP isoforms including CYP1A1 have also been associated with TCE metabolism. We observed little difference in CYP2E1 and CYP1A1 activity levels in both TCE- and vehicle-treated mice. Yoo et al. (2015a) reported suggestive, but only marginally significant (P ¼ .06) correlation between liver TCA and basal CYP2E1 protein levels in a panel of 7 mouse inbred strains that are parental strains for CC. In the present study, we did not find a correlation between TCA and basal CYP2E1 protein levels in liver suggesting that a more complex milieu of oxidative enzymes may be responsible for TCE metabolism to TCA.

Interestingly, 10-fold or greater inter-strain differences were observed in ADH and ALDH activities in both vehicle- and TCE-treated animals. We also observed significant increases in ALDH and ADH activity with TCE exposure. Further, the extent of variability in these enzymes across mouse strains was consistent with previously reported variability in ALDH and ADH activity in human cryopreserved hepatocytes (Bronley-DeLancey et al., 2006). However, no association was observed between TCA levels and activity of ADH or ALDH, again suggesting that multiple factors may be responsible for the observed differences in TCA levels. We also

observed no correlations between TCE-metabolizing enzyme levels or activity, indicating lack of potential additive interactions among these enzymes in certain strains. Thus, while mouse population-derived data demonstrate the utility of the CC mouse population in capturing the population-level variability observed in humans, they also show the complexities of the oxidative metabolism of TCE whereby multiple enzymes play a role in TCE toxicokinetics.

TCA and other products of oxidative metabolism of TCE are well known to be PPARα agonists and peroxisome proliferation is one mechanism of liver toxicity and carcinogenesis of TCE (Bull et al., 1990; Rusyn et al., 2014). In our study, we hypothesized that strains with higher TCA levels would exhibit greater effects on PPARα-mediated signaling. Indeed, we observed significant induction and positive correlation in the transcription of PPARα-responsive Acox1 and Cyp4a10 genes with TCE treatment, with levels of Acox1 transcripts and TCA levels in liver also positively correlated. This is an important finding as it demonstrates the association between TCE metabolism and toxicodynamics. It also confirms the findings reported in Bradford et al. (2011) that peroxisome proliferator activated receptor-mediated molecular networks, consisting of the metabolism genes known to be induced by TCE, represent some of the most pronounced molecular effects of TCE treatment in mouse liver that are dependent on genetic background. These results are also consistent with findings that Acox1 and Cyp4a10 transcript levels are induced with repeated exposure to TCE and are positively correlated with each other and with liver TCA levels (Yoo, Bradford, Kosyk, Uehara, et al., 2015).

While a strong and reproducible concordance between liver TCA levels and induction of peroxisome proliferation at a population level confirms the traditional sequence of events: metabolism of TCE to TCA which then acts as a PPARα ligand and induces peroxisomal proliferation, the outcome of the haplotype-associated mapping afforded by CC population

suggests that a feedback loop also exists. A novel outcome of this study is the identification of candidate genes at QTLs associated with TCE metabolism to TCA. Among several protein-coding genes in the locus significantly associated with liver TCA levels among strains, Acot8 and Fitm2 were identified as candidate genes and were significantly correlated with TCA levels. These results are intriguing as Acot8 and Fitm2 are PPAR-responsive genes, suggesting the role of PPAR signaling in TCE metabolism, in addition to the role of TCE metabolites in peroxisome proliferation. A recent study showed significantly lower levels of TCA in the liver and kidney in PPARα-null and -humanized mice after either single or repeated exposures to TCE, suggesting a direct role of PPARα signaling in TCE toxicokinetics (Yoo, Cichocki, et al., 2015).

Another indication that genetic variants associated with PPARα signaling are associated with TCE metabolism to TCA is the observation that strains carrying a non-synonymous SNP variant (C genotype) in RXRα are associated with relatively low levels of TCA. PPARs are nuclear receptors that require dimerization with the nuclear receptor RXRα to form a heterodimer. The C genotype of RXRα is carried in the CAST/Eij strain among the CC founders. Although, no statistically significant differences in TCA levels were observed between C and T genotypes of RXRα, strains with C genotype demonstrated 2-fold lower mean and median TCA levels compared with strains carrying the T genotype. Results of previous studies also suggest that the CAST-specific alleles may be a significant contributor to the variability associated with TCE metabolism. (Yoo, Bradford, Kosyk, et al., 2015a; Yoo, Bradford, Kosyk, Uehara, et al., 2015) found that TCA levels in serum, liver and kidneys after exposure to TCE were the lowest in CAST/Eij strain as compared with other CC parental strains. A similar observation was reported by Bradford et al. (2011) in a comparison of 15 mouse inbred strains. Despite differences in dose and study designs, consistently low TCA levels in CAST/Eij strains across studies are highly reproducible, supporting

the suggestion that genetic variants in RXRα and other genes may contribute to the observed inter-strain variability in TCE metabolism.

This study, while informative with respect to quantitation and discovery of the genetic drivers of inter-individual variability, has a number of limitations. First, while we surveyed a dose–response in a large population of CC strains, we did not examine intra-strain reproducibility. In order to maximize the power of the study design with respect to mapping, we maximized the number of strains, not replicates (Kaeppler, 1997). Consistency of dose–response curves within each strain and concordance of major effects and relationships among the phenotypes with other multi-strain studies suggests that strain-specific effects are reproducible; however, this needs to be tested in subsequent studies. Studies also need to examine toxicokinetics of TCE in a concentration–time study design. Second, this study examined only a single time point and a more complete understanding of the effects that inter-strain differences in TCE metabolism may have on the apical toxicity phenotypes is needed though sub-chronic and chronic studies. Our data on strain-specific metabolism of TCE will be crucial for selection of strains for follow up longer term studies because it is unlikely that such studies can be done in a comparably large mouse population. While highly informative, population-based studies are challenging in terms of cost and logistics; thus, acute treatment-based surveys in large populations will likely be a very useful approach for narrowing the number of strains while preserving the extend of population variability through data-driven study designs and strain selection.

In summary, our results show that the CC mouse population is a valuable tool for assessing inter-individual variability and for investigating the genetic basis of the phenotypic differences. The mosaic genomes of CC enabled identification of the candidate genes underlying differences in TCE metabolism and support a role for PPAR signaling not only in TCE toxicity, but also in

TCE metabolism. This observation further supports the need for caution suggested by (Yoo, Cichocki, et al., 2015) in interpreting apparent species differences in PPAR signaling, because they may result from not only receptor-mediated toxicodynamic effects, but also modulation of toxicokinetics. Consequently, these results suggest the need to investigate interplay between varying genetic backgrounds and interspecies differences, and thereby improve the ability of experiment studies to predict risks to human populations.

V. Figures and Tables

Figure 2.1. Schematic representation of metabolism of trichloroethylene (TCE) via oxidative pathway. Names of metabolites that are chemically unstable or reactive are shown in brackets. Major enzymatic pathways are identified for cytochrome P450 enzymes (CYPs), aldehyde dehydrogenase (ALDH), alcohol dehydrogenase (ADH), UDP-glucuronosyltransferase (UGT), and GSH S-transferase zeta (GSTZ).

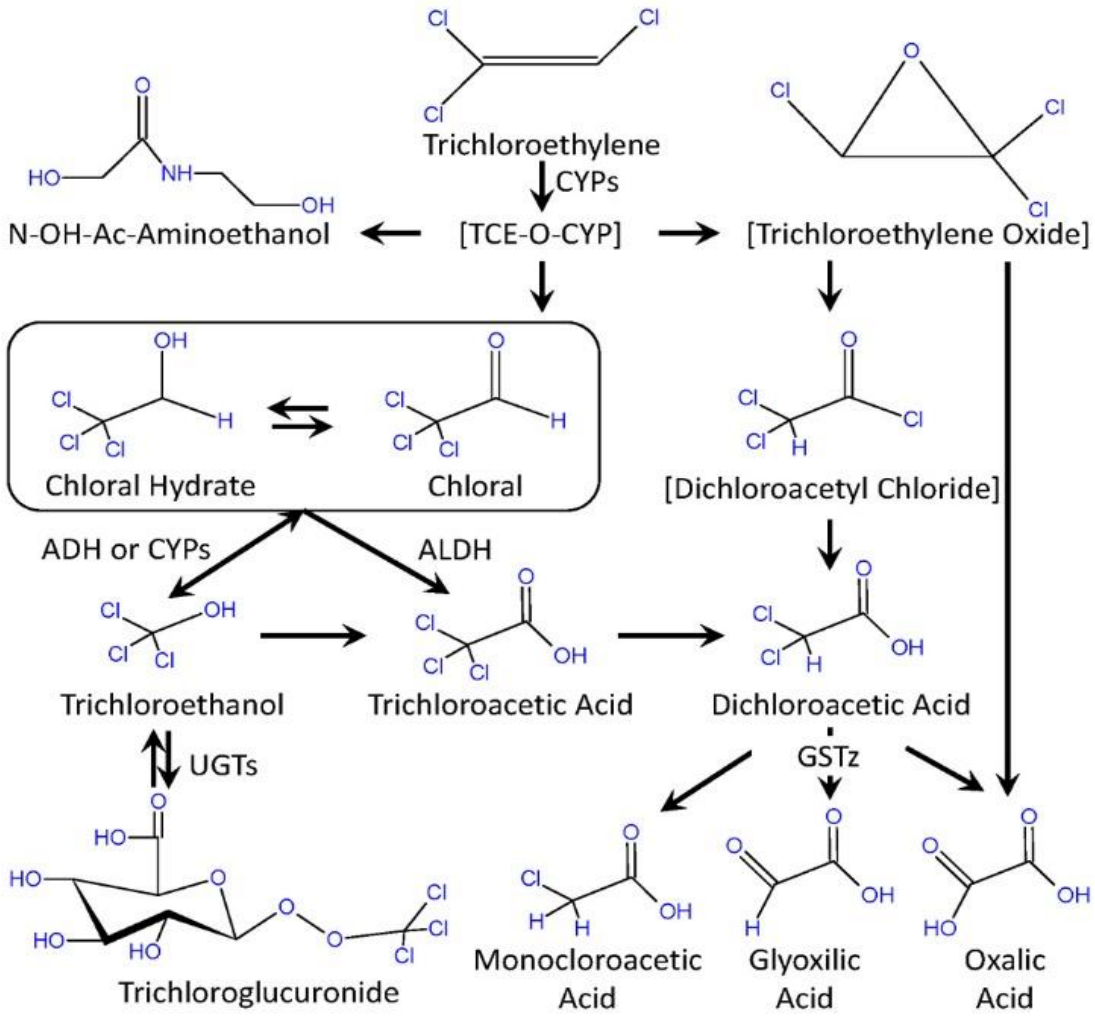

Figure 2.2. Liver TCA levels in CC mice 24 h after oral administration of a dose of 24 (A), 80 (B), 240 (C), or 800 (D) mg/kg of TCE. Bars colored in red, green, and blue represent strains that exhibit high, intermediate and low, respectively, levels of TCA across different treatment groups.

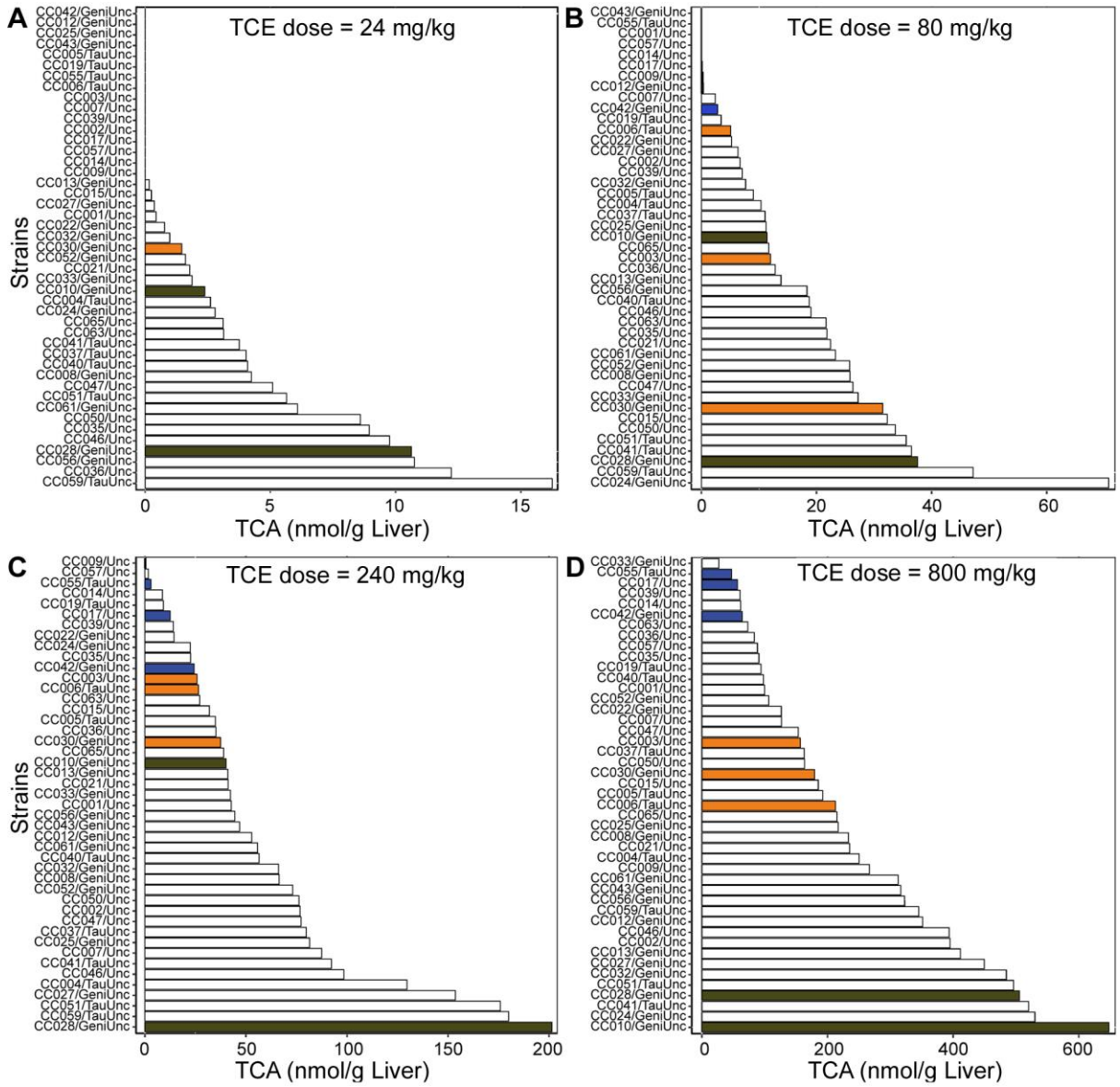

Figure 2.3. Inter-strain variability in formation of TCA in liver (A), kidney (B), and serum (C) 24 h after oral administration of a dose of 24, 80, 240, or 800 mg/kg of TCE. Each dot represents TCA level in a CC strain, horizontal black line indicates median value for each dose-tissue combination among CC strains. Red box and whiskers are PBPK model-derived (Chiu et al., 2014) population estimates. The boxes and the horizontal line represent 5, 95, and 50% median TCA levels. The whiskers represent upper and lower bound confidence interval for 95 and 5%, respectively, median TCA levels.

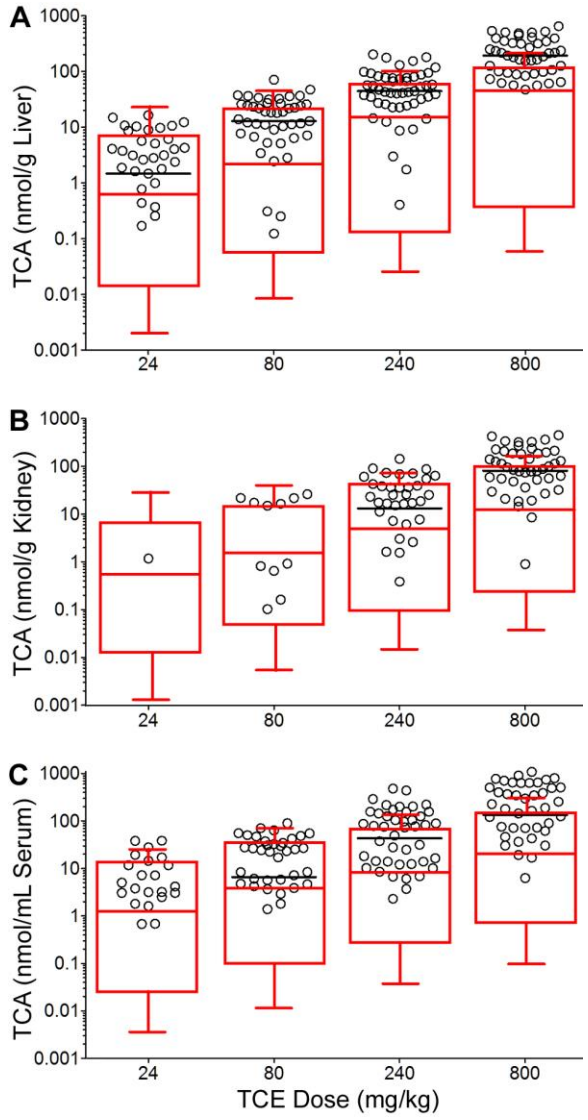

Figure 2.4. Inter-strain differences in liver Cyp2e1 protein expression (A–B) and Cyp1a1 activity (C–D) in CC mice administered vehicle (black circles) or a single oral dose of TCE (800 mg/kg, red circles). Panels (B) and (D) are box and whiskers plots of population variability where a horizontal line represents the median, the box shows 1st and 3rd quartile ranges and the whiskers represent standard errors of the mean.

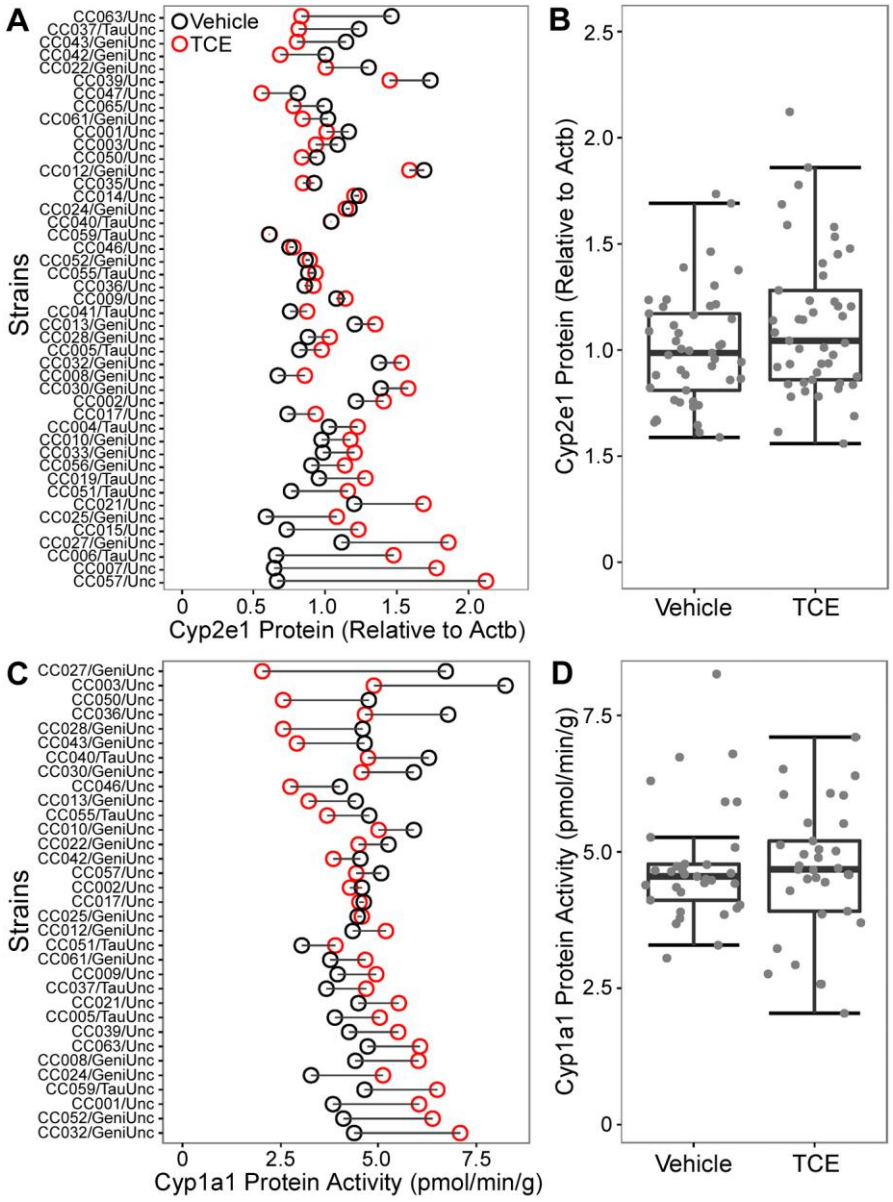

Figure 2.5. Inter-strain differences in liver ADH (A–B) and ALDH (C–D) activity in CC mice administered vehicle (black circles) or a single oral dose of TCE (800 mg/kg, red circles). Panels (B) and (D) are box and whiskers plots of population variability where a horizontal line represents the median, the box shows 1st and 3rd quartile ranges and the whiskers represent standard errors of the mean. The asterisks (*) denote statistical significant differences (P < .05) between TCE and vehicle treated groups (Mann–Whitney test).

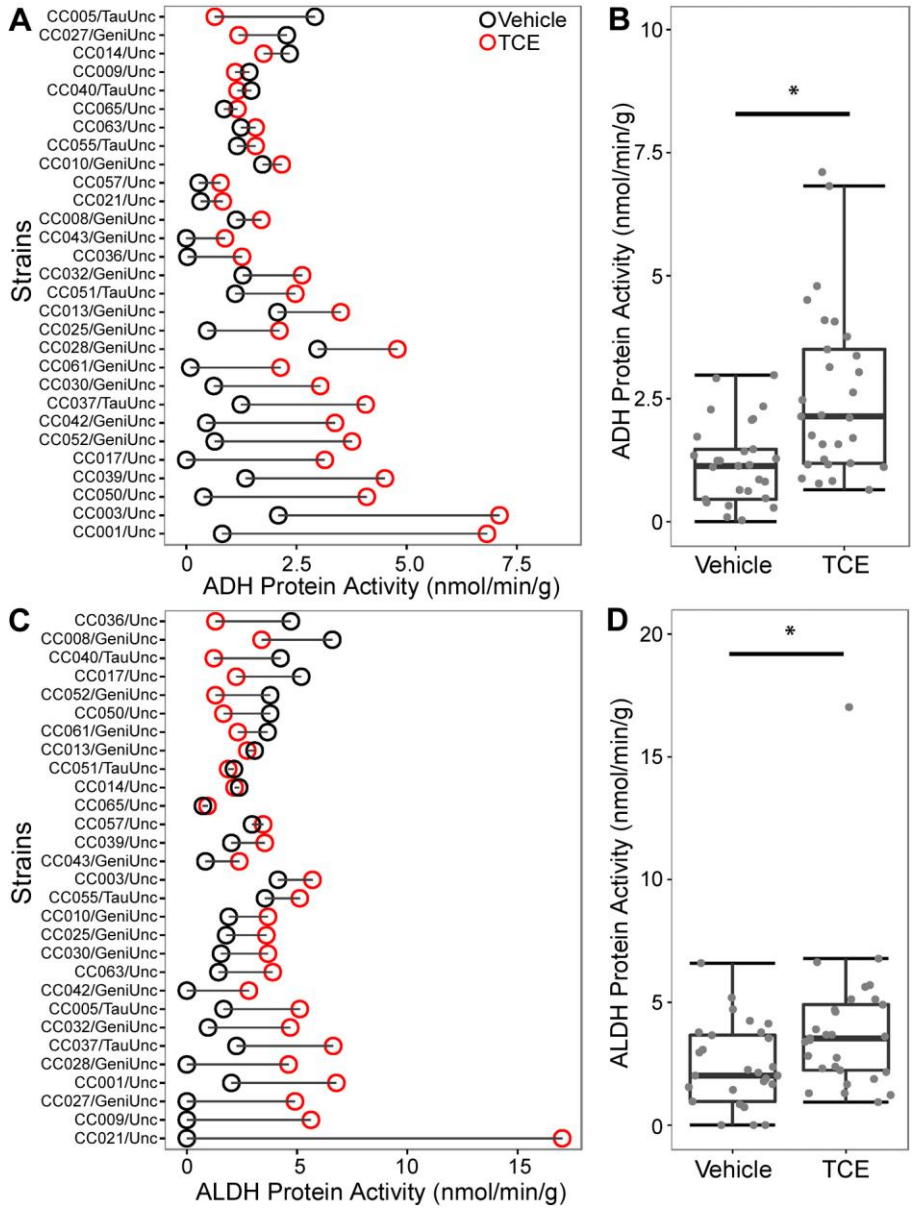

Figure 2.6. Inter-strain differences in liver Acox1 (A–B) and Cyp4a10 (C–D) transcript levels in CC mice administered vehicle (black circles) or a single oral dose of TCE (800 mg/kg, red circles). Panels (B) and (D) are box and whiskers plots of population variability where a horizontal line represents the median, the box shows 1st and 3rd quartile ranges and the whiskers represent standard errors of the mean. The asterisks (*) denote statistical significant differences ($P < .05$) between TCE and vehicle treated groups (Mann–Whitney test).

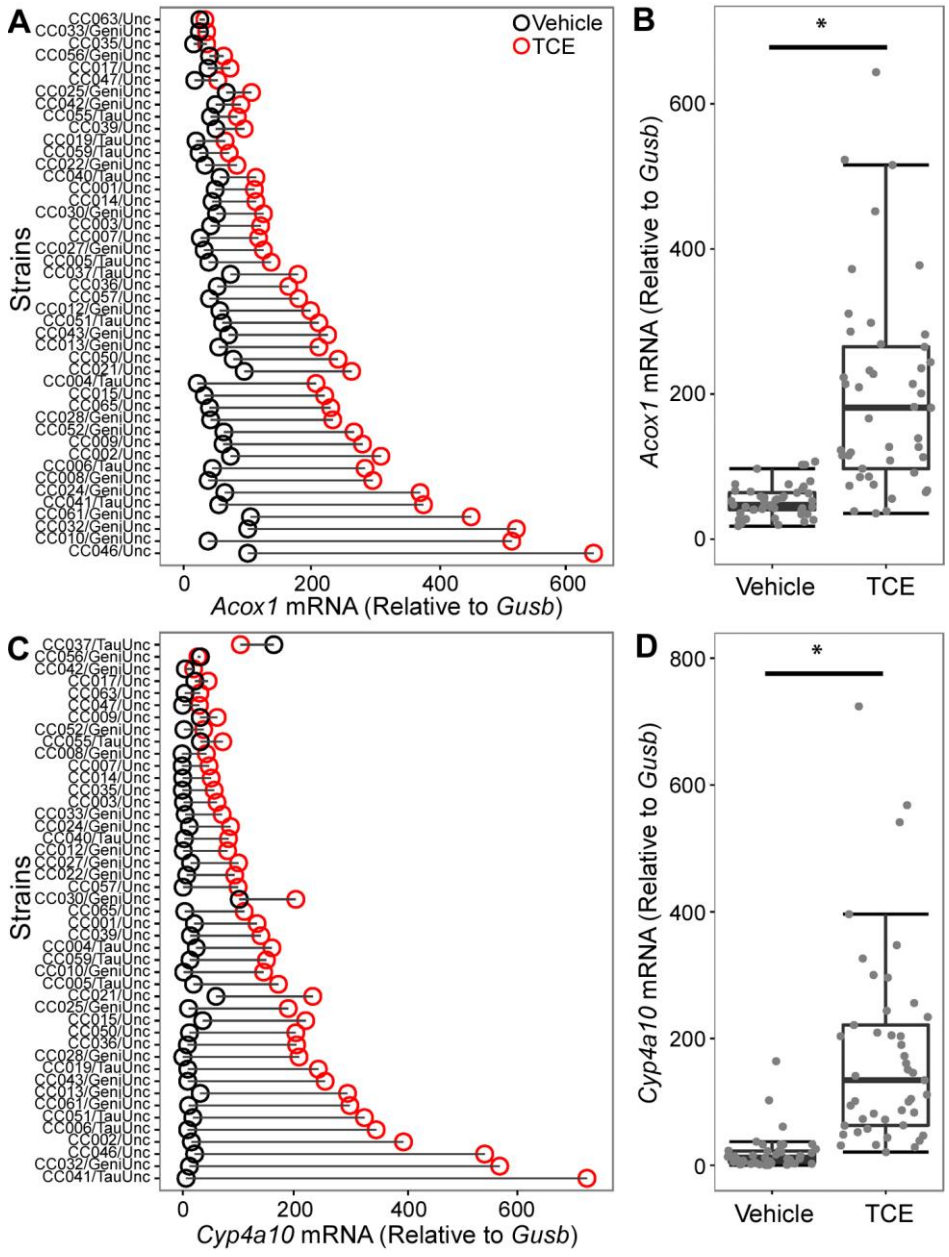

Figure 2.7. Correlation analysis (Spearman) among toxicokinetic and toxicodynamic phenotypes across the population of CC strains. A, Scatter plots of TCA levels at 24 h after dosing with 800 mg/kg of TCE in multiple tissues of 45 CC strains. Trend lines and corresponding r and P-values are shown. B, Correlation between expression of Acox1, Cyp4a10, and liver TCA levels in responses to TCE treatment. Full correlation matrix is included as Supplementary Table 1.

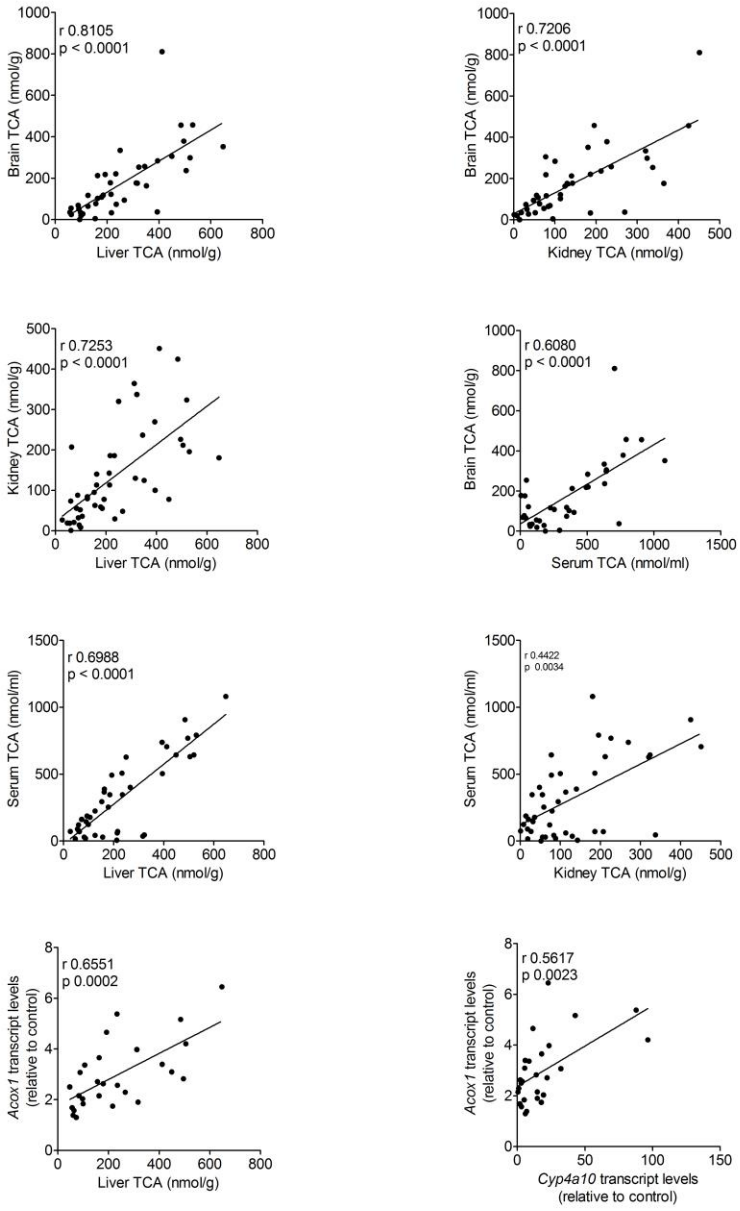

Figure 2.8. QTL mapping of TCE toxicokinetic and toxicodynamic phenotypes. Log transformed liver TCA (A–B) and Acox1 (C–D) transcript levels measured at 24-h time point in CC mice administered with a single oral dose of TCE (800 mg/kg) were mapped to the mouse genome polymorphisms among CC strains. Panels A and C show logarithmic odds ratio (LOD) scores across the whole mouse genome (chromosomes 1 through X). The red line represents a permutation-based significance threshold (n ¼ 1000 permutations). Plots B and D show the effect of the CC founder strain alleles on chromosome 2 (top) and a zoom-in on the significant regions with corresponding LOD scores.

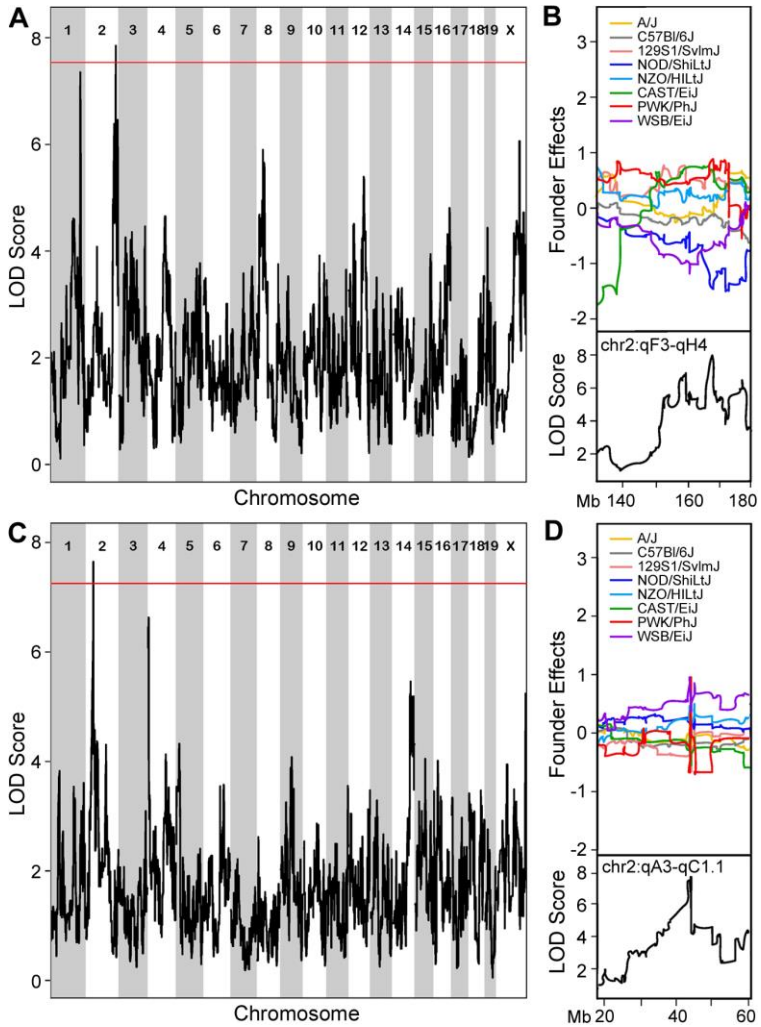

Figure 2.9. QTL region on distal chromosome 2 associated with liver TCA levels. RefSeq genes that are located on chr2 [qH2-qH3] in the region between 160,640,000 and 165,200,000 (a sub-set of the entire QTL, see Table 1) are shown with a position marked for the candidate genes (abbreviation, full name and physical genomic location are shown) that were examined for the relationship between TCE-induced expression and TCA level in livers of CC mice treated with a single oral dose of 800 mg/kg of TCE. Scatter plots show correlation among gene expression for Top1, Fitm2, Acot8, and Cd40 and liver TCA levels. Best fit linear regression lines are plotted and corresponding r and P values are depicted on each plot.

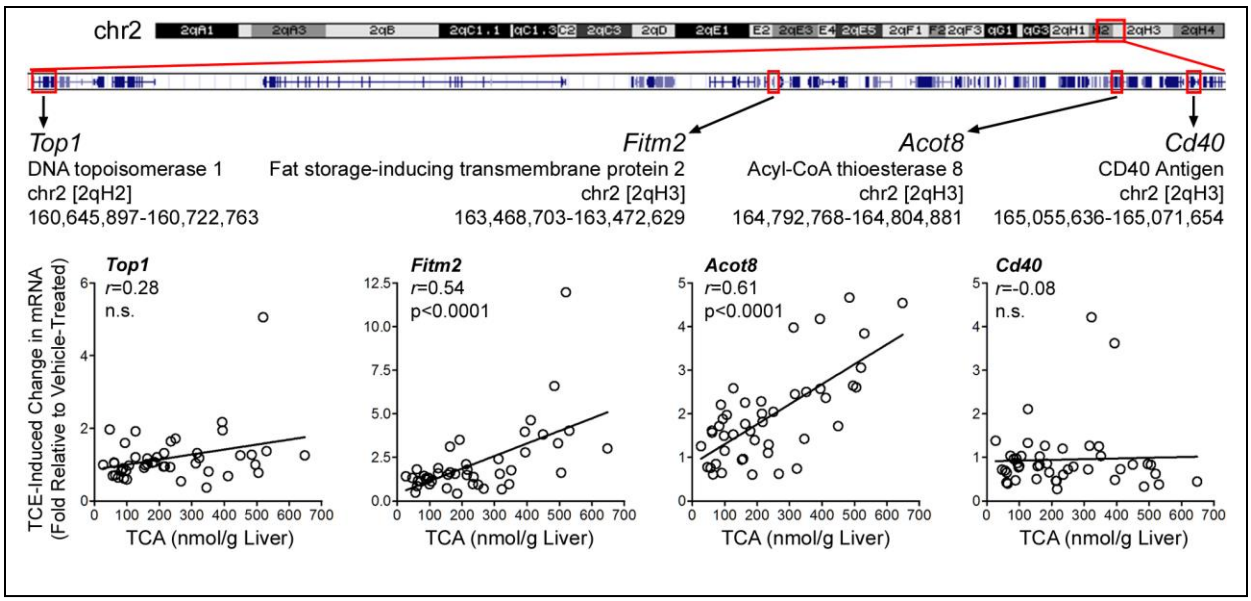

Table 2.1 Significant quantitative trait loci and genes in these loci that were associated with inter-strain differences in Liver TCA and TCE-Induced Induction in Acox1 Expression in Liver

Phenotype	**Genomic position (Mb)**	**Protein coding genes in the locus**
TCA	Chr 2: 157.685-180.142 Mb	*CTNNBL1, VSTM2L, TTI1, RPRD1B, TGM2, BPI, LBP, SNHG11, RALGAPB, ADIG, ARHGAP40, SLC32A1, ACTR5, PPP1R16B, FAM83D, DHX35, MAFB,* ***TOP1,*** *PLCG1, ZHX3, LPIN3, EMILIN3, CHD6, PTPRT, CISD3B, SRSF6, L3MBTL1, SGK2, IFT52, MYBL2, GTSF1L, TOX2, JPH2, OSER1, GDAP1L1,* ***FITM2,*** *R3HDML, HNF4A, TTPAL, SERINC3, PKIG, ADA, WISP2, KCNK15, RIMS4, YWHAB, PABPC1L, TOMM34, STK4, KCNS1, WFDC5, WFDC12, WFDC15A, WFDC15B, SVS2, SVS3B, SVS4, SVS3A, SVS6, SVS5, SLPI, MATN4, RBPJL, SDC4, SYS1, TRP53TG5, DBNDD2, PIGT, WFDC2, SPINT3, WFDC6A, EPPIN, WFDC8, WFDC6B, WFDC16, WFDC9, WFDC10, WFDC11, WFDC13, SPINT4, SPINT5, WFDC3, DNTTIP1, UBE2C, TNNC2, SNX21,* ***ACOT8****, ZSWIM3, ZSWIM1, SPATA25, NEURL2, CTSA, PLTP, PCIF1, ZFP335, MMP9, SLC12A5, NCOA5,* ***CD40,*** *CDH22, SLC35C2, ELMO2, ZFP663, ZFP334, OCSTAMP, SLC13A3, TRP53RKA, SLC2A10, EYA2, ZMYND8, NCOA3, SULF2, PREX1, TRP53RKB, ARFGEF2, CSE1L, STAU1, DDX27, ZNFX1, KCNB1, PTGIS, B4GALT5, SLC9A8, SPATA2, RNF114, SNAI1, UBE2V1, TMEM189, CEBPB, PTPN1, FAM65C, PARD6B, ADNP, DPM1, MOCS3, KCNG1, NFATC2, ATP9A, SALL4, ZFP64, TSHZ2, ZFP217, BCAS1, CYP24A1, PFDN4, DOK5, CBLN4, MC3R, FAM210B, AURKA, CSTF1, CASS4, RTFDC1, GCNT7, FAM209, TFAP2C, BMP7, SPO11, RAE1, RBM38, CTCFL, PCK1, ZBP1, PMEPA1, ANKRD60, RAB22A, VAPB, STX16, NPEPL1, NELFCD, CTSZ, TUBB1, ATP5E, SLMO2, ZFP831, EDN3, ETOHI1, ZFP931, PHACTR3, SYCP2, PPP1R3D, FAM217B, CDH26, CDH4, TAF4, LSM14B, PSMA7, SS18L1, MTG2, HRH3, OSBPL2*
Acox1 **induction by TCE in liver**	Chr 2: 41.836-43.374 Mb	*LRP1B*

Supplemental Figure 2.1. Dose-response plots of liver, kidney, serum and brain TCA levels in CC mice 24 h after oral administration of TCE (24-800 mg/kg). Lines colored in red, green, and blue represent strains that exhibit high, intermediate and low levels of TCA across different treatment groups. Dotted lines represent other strains. Lines connect values across doses from a strain.

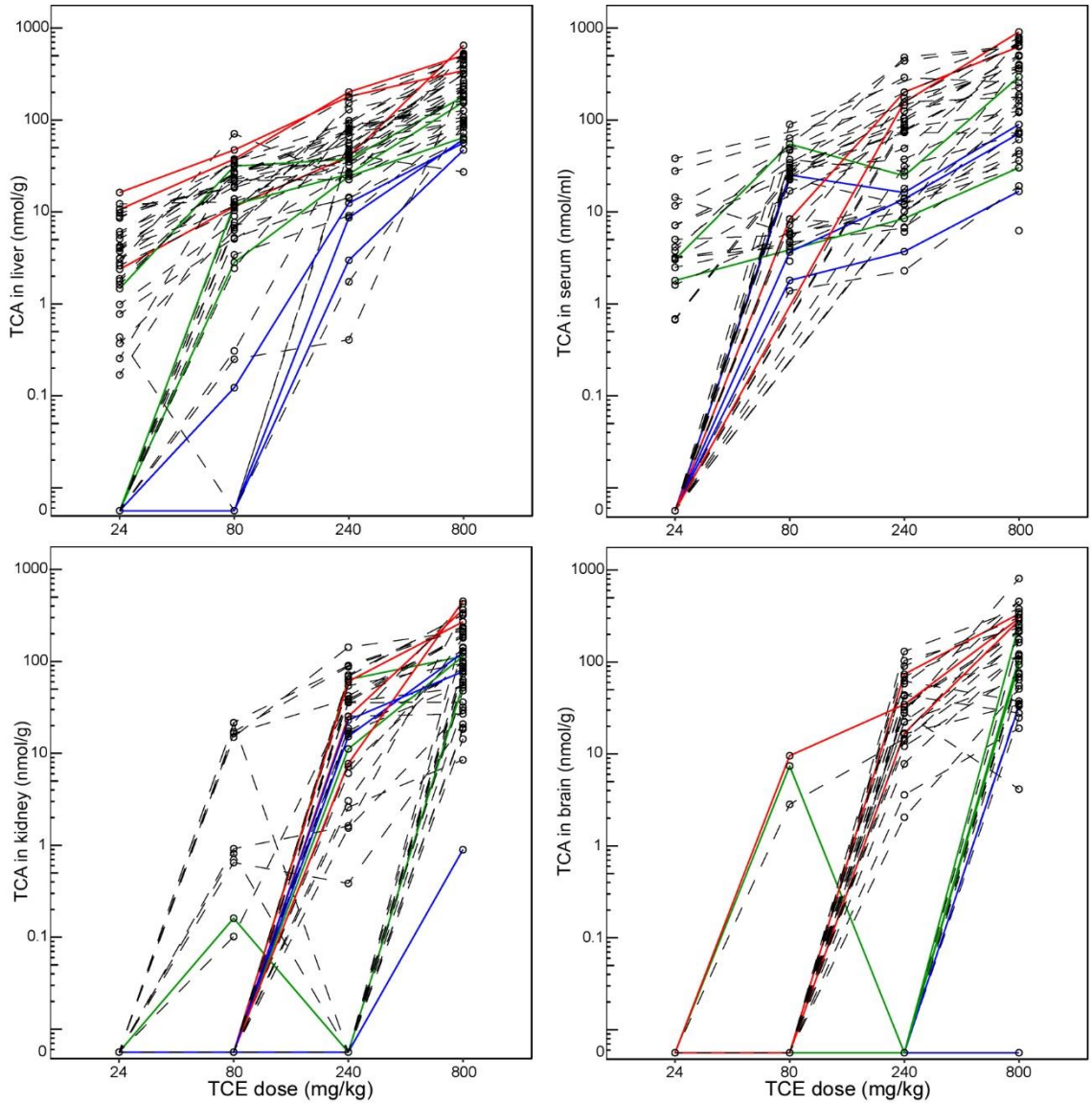

Supplemental Figure 2.2. Serum TCA levels in CC mice 24 h after oral administration of a dose of 80 (A), 240 (B), or 800 (C) mg/kg of TCE. Bars colored in red, green, and blue represent strains that exhibit high, intermediate and low levels of TCA across different treatment groups. The order of strains is in accordance with rank ordering of strains for liver TCA (800 mg/kg TCE).

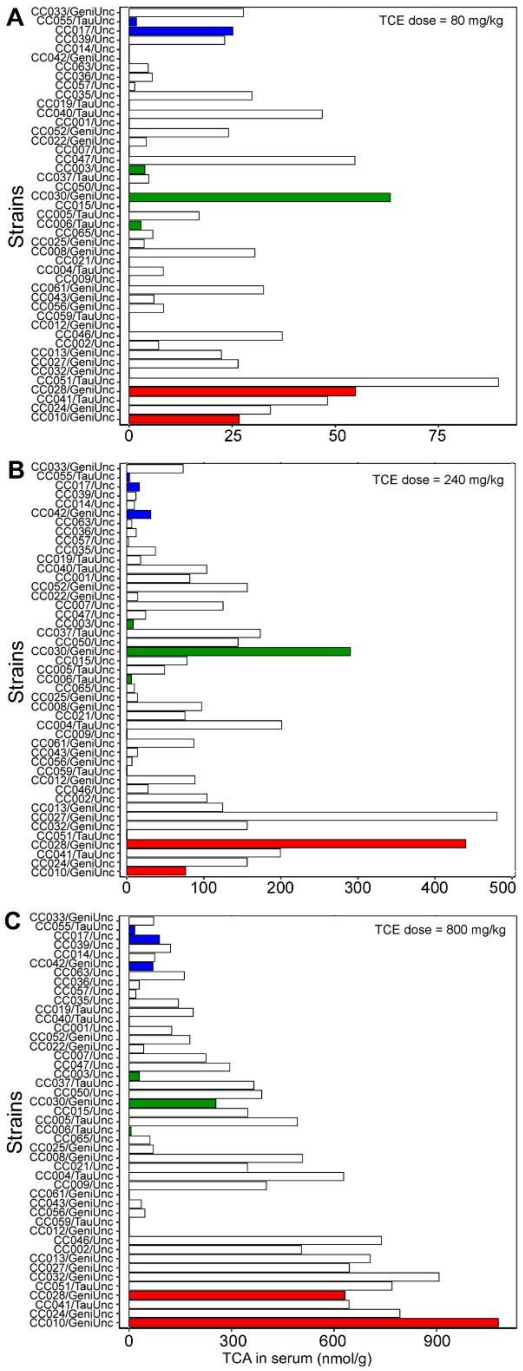

Supplemental Figure 2.3. Kidney (A-B) and brain (C-D) TCA levels in CC mice 24 h after oral administration of a dose of 240 or 800 mg/kg of TCE. Bars colored in red, green, and blue represent strains that exhibit high, intermediate and low levels of TCA across different treatment groups. The order of strains is in accordance with rank ordering of strains for liver TCA (800 mg/kg TCE).

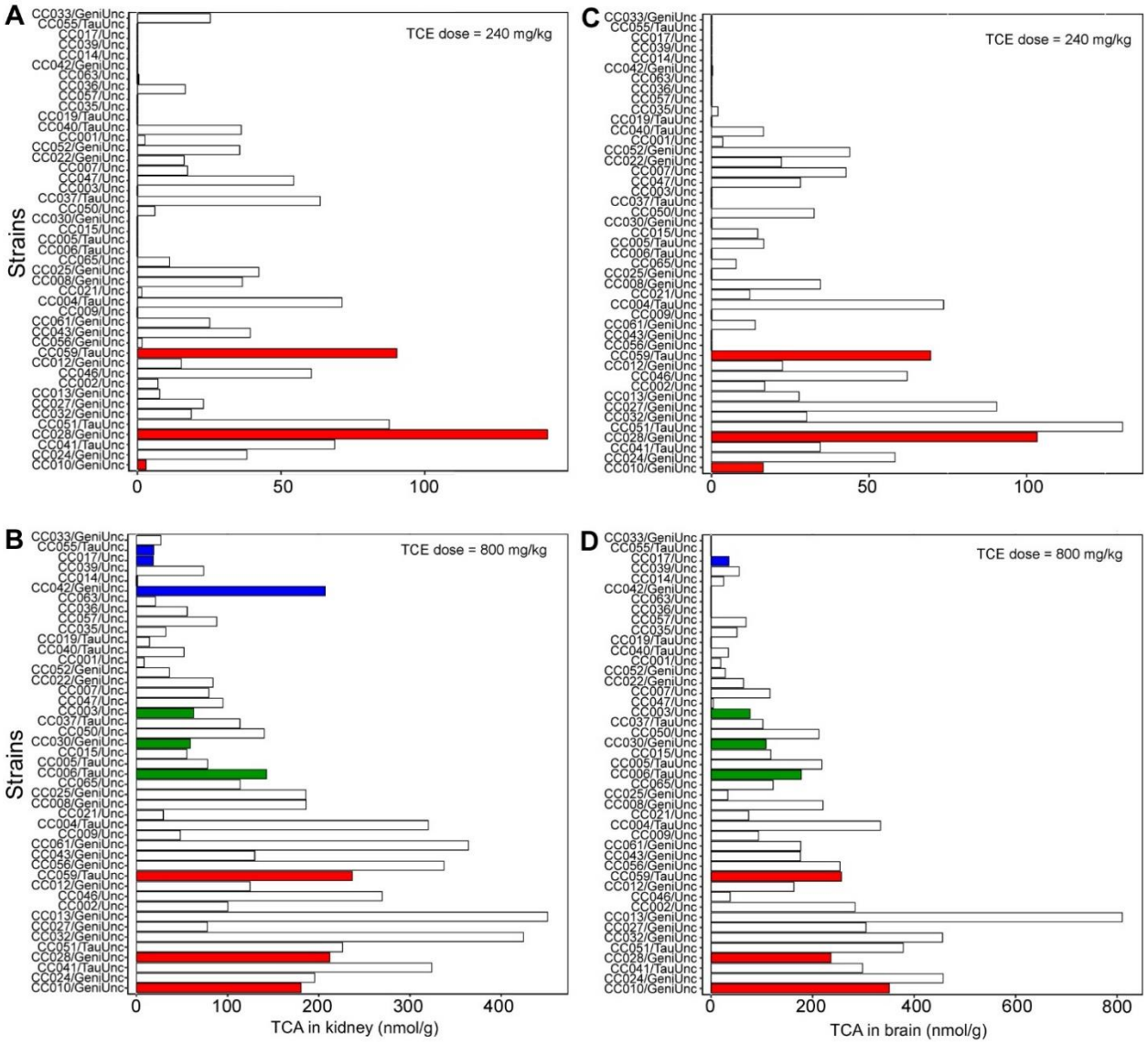

Supplemental Figure 2.4. Liver TCA levels in RXRα variants among CC mice orally administered with 800 mg/kg of TCE. The box shows 1st and 3rd quartile ranges and the whiskers represent standard error of the mean.

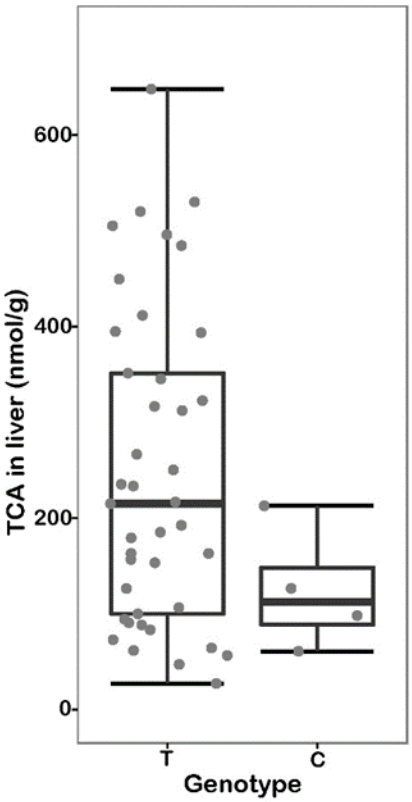

Supplemental Table 2.1. P-values (uncorrected) for Spearman correlation among phenotypes collected in this study (Top). Bonferroni-corrected p-values for Spearman correlation among phenotypes collected in this study (bottom).

	ADH_TCE	ADH_veh	ALDH_TCE	ALDH_Veh	Cyp1a1_TCE	Cyp1a1_Veh	Cyp2e1_TCE	Cyp2e1_Veh	Cyp4a10	Acox1	TCA
ADH_TCE	1	0.4429	0.9729	0.3232	0.9988	0.4138	0.3736	0.2598	0.9422	0.8715	0.7074
ADH_veh	0.4429	1	0.0289	0.2457	0.5914	0.9747	0.123	0.2243	0.6074	0.0901	0.0962
ALDH_TCE	0.9729	0.0289	1	0.0061	0.1959	0.5327	0.1998	0.0479	0.1249	0.9928	0.5551
ALDH_Veh	0.3232	0.2457	0.0061	1	0.6935	0.5704	0.1606	0.0453	0.2583	0.6617	0.0402
Cyp1a1_TCE	0.9988	0.5914	0.1959	0.6935	1	0.0873	0.8918	0.2455	0.7692	0.9928	0.5289
Cyp1a1_Veh	0.4138	0.9747	0.5327	0.5704	0.0873	1	0.5159	0.9002	0.4147	0.7959	0.3158
Cyp2e1_TCE	0.3736	0.123	0.1998	0.1606	0.8918	0.5159	1	0.5542	0.7901	0.2392	0.0977
Cyp2e1_Veh	0.2598	0.2243	0.0479	0.0453	0.2455	0.9002	0.5542	1	0.0737	0.2126	0.8656
Cyp4a10	0.9422	0.6074	0.1249	0.2583	0.7692	0.4147	0.7901	0.0737	1	0.0023	0.0588
Acox1	0.8715	0.0901	0.9928	0.6617	0.9928	0.7959	0.2392	0.2126	0.0023	1	0.0002
TCA	0.7074	0.0962	0.5551	0.0402	0.5289	0.3158	0.0977	0.8656	0.0558	0.0002	1

	ADH_TCE	ADH_veh	ALDH_TCE	ALDH_Veh	Cyp1a1_TCE	Cyp1a1_Veh	Cyp2e1_TCE	Cyp2e1_Veh	Cyp4a10	Acox1	TCA
ADH_TCE	1	1	1	1	1	1	1	1	1	1	1
ADH_veh	1	1	0.289	1	1	1	1	1	1	0.901	0.962
ALDH_TCE	1	0.289	1	0.061	1	1	1	0.479	1	1	1
ALDH_Veh	1	1	0.061	1	1	1	1	0.453	1	1	0.402
Cyp1a1_TCE	1	1	1	1	1	0.873	1	1	1	1	1
Cyp1a1_Veh	1	1	1	1	0.873	1	1	1	1	1	1
Cyp2e1_TCE	1	1	1	1	1	1	1	1	1	1	0.977
Cyp2e1_Veh	1	1	0.479	0.453	1	1	1	1	0.737	1	1
Cyp4a10	1	1	1	1	1	1	1	0.737	1	0.023	0.588
Acox1	1	0.901	1	1	1	1	1	1	0.023	1	0.002
TCA	1	0.962	1	0.402	1	1	0.977	1	0.558	0.002	1

CHAPTER 3: CHARACTERIZATION OF GENETIC BACKGROUND, DOSE, AND THEIR COMBINATORY EFFECTS ON LIVER GENE EXPRESSION RESPONSES WITH TCE EXPOSURE[2]

I. Introduction

Gene expression profiling is widely used in the field of toxicology and provides important molecular insights into the mechanisms of adverse health effects from chemical exposure (Burczynski et al., 2000; Harrill & Rusyn, 2008). Transcriptomic signatures of chemical exposures have been widely used in chemical safety evaluation and large reference databases exist to enable comparative analyses and predictive modeling (Fostel, 2008; Ganter et al., 2005; Uehara et al., 2010). In addition, many studies demonstrate the value of transcriptomic data-derived dose-response information for both hazard identification and quantitative risk assessment (Andersen et al., 2008; Thomas, Philbert, et al., 2013a) and pathway-based dose-response analysis of transcriptomic data displayed concordance with traditional apical endpoints (Thomas et al., 2007b; Thomas et al., 2011; Thomas, Philbert, et al., 2013a; Y. H. Zhou et al., 2017). Indeed, toxicogenomics data are making their way into decision making for both drugs and environmental chemicals (Sauer et al., 2017; J. Xu, Thakkar, Gong, & Tong, 2016).

The majority of available gene expression data in toxicology has been collected in genetically homogenous (e.g., a single strain or cell line) or undefined (e.g., outbred strains or mixtures of

[2] The text of this chapter is reproduced with permission from Mammalian Genome 29 (1-2): 168-181 (2018). Springer Nature © 2018

cells from multiple individuals) model systems. However, it is well established that gene expression, both basal and disease/treatment-perturbed, is heavily impacted by genetic variation among individuals (Bradford et al., 2011; Bystrykh et al., 2005; Chesler et al., 2003; D. Gatti et al., 2007; Harrill, Ross, Gatti, Threadgill, & Rusyn, 2009; Schadt et al., 2008; Schadt et al., 2003). Early studies of expression quantitative trait loci (eQTL) were conducted in panels of inbred mouse strains or human cell lines where population stratification was a challenge (D. M. Gatti, Harrill, Wright, Threadgill, & Rusyn, 2009) and recent studies in more heterogeneous mouse models such as Diversity Outbred (DO) and Collaborative Cross (CC) show greater promise of characterizing and replicating eQTLs (Crowley et al., 2015).

Studies of chemical effects using population-based models, both *in vivo* and *in vitro*, are increasingly common (Abdo, Xia, et al., 2015; Church et al., 2015; Cichocki et al., 2017; Eduati et al., 2015; French et al., 2015; Luo, Furuya, Chiu, & Rusyn, 2018; Mosedale et al., 2017; Venkatratnam et al., 2017). Powered by the balanced genetic diversity represented in the DO (Churchill et al., 2012) and CC (Threadgill, Miller, Churchill, & de Villena, 2011) populations, these mouse models enable exploration of causal variants driving variability in molecular mechanisms that result in phenotypic differences (Harrill & McAllister, 2017). Furthermore, characterization of the genetics-dependent and -independent transcriptional responses to chemical exposure is valuable for elucidating the extent and mechanisms of variability (Church et al., 2015; Harrill, Ross, et al., 2009; Mosedale et al., 2017).

The ensuing challenge in toxicology and environmental health is combining the mechanistic power of gene expression and genetics studies of chemical exposures with the need to understand the dose-response relationships. The complexity and cost of population-based studies that include multiple doses and parallel characterization of multiple dimensions of

toxicokinetics, toxicodynamics and inter-individual variability present unique challenges and may be best addressed using case studies of well-characterized toxicants (Rusyn, Gatti, Wiltshire, Kleeberger, & Threadgill, 2010). Thus, we chose trichloroethylene (TCE), a ubiquitous contaminant and a known carcinogen in both humans and rodents (Rusyn et al., 2014). TCE is a chemical with known variability in toxicokinetics (Chiu et al., 2014a) and toxicodynamics (Bradford et al., 2011). The objective of this study was to evaluate and characterize genetic background-, dose- and interaction-effects of TCE on liver gene expression, and to determine variability in dose-pathway relationships in a large genetically-diverse mouse population. Liver transcriptomic data from 50 strains of CC mice that were treated acutely with one of four doses of TCE were modeled to identify genes and pathways that exhibited significant strain, dose, or strain by dose interaction effects.

II. Materials and methods

Animals and Treatments. The in life portion of the study and tissue collection was detailed in (Venkatratnam et al., 2017). In brief, adult male mice (8-12 weeks old) from 50 CC strains were orally administered a single dose of 0, 24, 80, 240 or 800 mg/kg TCE (Sigma Aldrich, St. Louis, MO) in 5% Alkamuls EL-620 vehicle (Solvay, Deptford, NJ). Mice were sacrificed 24 h after treatment and tissues were flash frozen in liquid nitrogen and stored at -80^{o}C until analysis.

TCA level in liver. Analyses were performed by a modification of US EPA method 552.2 (Domino et al., 2003) as detailed in (Venkatratnam et al., 2017). Data on TCA levels in liver across all CC strains was reported in (Domino et al., 2003)(Venkatratnam et al., 2017).

RNA extraction and sequencing. Left-lobe of livers was pulverized with pestle and mortar pre-chilled in liquid nitrogen. RNA was extracted from ~20 mg of pulverized tissue using RNeasy

Qiagen mini Kit (Qiagen, Valencia, CA). Concentration of extracted RNA was measured using NanoDrop 2000 (Thermo Fisher Scientific, Wilmington, DE). RNA libraries were prepared using Illumina TruSeq Stranded Total RNA kit (Illumina, San Diego, CA) with Ribo-Zero Gold rRNA removal kit (Illumina). RNA-Seq of 50 base-pair single-end reads was conducted using Illumina HiSeq 2500 instrument (Illumina) at the depth of ~50 million reads/sample. Raw reads were trimmed for any sequencing adaptors and low quality bases using Trimmomatic (Bolger, Lohse, & Usadel, 2014). Reference genomes and inferred marker founder origin for CC mice were downloaded from University of North Carolina Systems Genetics Core Facility (http://csbio.unc.edu/CCstatus/index.py?run=Pseudo). Filtered reads were mapped to each of the corresponding CC reference genome using TopHat version 2.0.3 (D. Kim, Langmead, & Salzberg, 2015). Resulting alignments were re-mapped to reference mm10 assembly coordinates using lapels (https://github.com/shunping/lapels). HTSeq (Anders, Pyl, & Huber, 2015) was used to generate raw read counts per gene using intersection-nonempty parameter to account for ambiguous read mappings. Differential gene expression tests were then performed with DESeq2 (Love, Huber, & Anders, 2014).

Statistical analyses. Normalized count data on 23,948 genes for 246 combinations for four TCE and one vehicle treatments from CC strains was generated with R (version 3.3) package DESeq2 as detailed above. Genes with < 2 counts across all treatments were removed, leaving 19,870 genes for analysis. The "dose" vector was linearized by first replacing the vehicle (i.e., zero) TCE dose with 8 (the average distance between doses was 1/3 the prior dose) followed by a natural log transformation. DESeq2 was used to derive *p*-values and adjusted *p*-values for the main effects of dose and strain, as well as their interaction. In brief, counts were first modeled as: counts ~ strain + ln(dose). Genes exhibiting a linear dose effect were identified with a likelihood ratio test

comparing a reduced model of counts ~ strain. Similarly, genes exhibiting a strain effect were identified with a likelihood ratio test comparing a reduced model of counts ~ ln(dose) to the full model. Lastly, genes with an interaction effect were identified comparing a reduced model of counts ~ strain + ln(dose) to a full model of counts ~ strain + ln(dose) + strain*ln(dose). In a similar fashion, these analyses were repeated using the natural log of measured liver TCA metabolite concentration in nmol/g (with a +1 offset to guard against taking logarithm of zero) as a predictor instead of TCE dose. Differential expression gene results were subjected to multiple comparison adjustment by computing Benjamini-Hochberg false-discovery *q*-values as implement in DESeq2. Due to the large number of significant findings, stringent significance criteria ($q<0.001$) and absolute counts (read counts > 10) were used as criteria for further analysis.

Pathway analyses. Pathway enrichment analysis was conducted using The Database for Annotation, Visualization, and Integrated Discovery (DAVID) (Dennis et al., 2003). The top 3000 or fewer genes with Bonferroni corrected p values ($q < 0.001$) were uploaded to DAVID to identify pathways influenced by dose-, strain-, or interaction-effects.

Comparison of Transcriptomic Benchmark Doses with Apical Data. For dose-response expression studies, the BMDExpress software (Yang, Allen, & Thomas, 2007) has been used to evaluate benchmark doses for expression changes of individual genes with exposure. Although the current study has a large sample size, the sample size of 5 per strain presents a challenge in computing strain-specific benchmark doses, and in fact many of the models provided in BMDExpress would suffer from extreme overfitting with such small sample sizes. To best accord with our differential expression analyses and to benefit from the variance shrinkage models used in expression analyses, we devised the following approach to compute a strain-specific pathway BMD analogue. First, we used the strain-specific linear modeling routine from DESeq2 as

described to obtain slope ($\hat{\beta}_1$) and intercept ($\hat{\beta}_0$) estimates from the software's modeling of logarithmic gene expression, as well as the Wald-like *t*-statistic (which utilizes variance shrinkage estimation). Next, an artificial model standard deviation $\hat{\sigma}$ was computed from the model in order to be consistent with the reported *p*-value. Specifically, if *t** represents the shrunken t-statistic, $\hat{\sigma} = \frac{\hat{\beta}_1}{t^*}\sqrt{\sum_i (x_i - \bar{x})^2}$ for *x*=ln (dose). Finally, we have the per-gene BMD=ln (control dose) $+sign(\hat{\beta}_1)\ \hat{\sigma}/\hat{\beta}_1$. The final BMD reflects the point at which the dose-response fit is estimated to exhibit a 1 standard-deviation departure from control expression, using shrunken estimates of variation that are obtained from the DESeq2 modeling. To compute a pathway (gene set) BMD, we used the median BMD of all genes assigned to the pathway.

Previous studies have suggested that transcriptomic points of departure (PODs) correlated with those for apical endpoints, and that therefore transcriptional BMD values have the potential to serve as POD for quantitative risk assessment (Thomas et al., 2011). We therefore compared transcriptomic BMDs with apical BMDLs used for liver effects in the U.S. EPA's Toxicological Review for TCE (U.S. EPA, 2011a, 2011b). Specifically, U.S. EPA selected increased liver/body weight ratio BMDLs in mice and rats for liver non-cancer effects, and increased carcinomas in mice for liver cancer. Because apical endpoint PODs were derived from both rats and mice, each with differing toxicokinetics, we standardized all dose units to human equivalent doses (HEDs) based on equivalent liver oxidative metabolism, using the most up-to-date multi-species physiologically-based pharmacokinetic (PBPK) model (Chiu & Ginsberg, 2011; Chiu, Okino, & Evans, 2009). Median estimates of each internal dose metric from Chiu et al. (2009) were used. An additional reason for this standardization is that margins of exposure can be readily computed and compared based on the human equivalent dose. Apical endpoint HEDs were then compared to median transcriptional BMDL values.

Genetic mapping and eQTL analyses: In principle, mapping of traits in CC lines can be performed by analysis of variance, using for each locus the ancestral origin from each of the 8 founding CC lines as a categorical predictor. In practice, for many loci slight uncertainties of CC line origin remain, due to incomplete information on crossover events in the CC breeding outcomes. Hidden Markov modeling enables probabilistic statements of the parental line of origins for each locus, expressed as probabilities (summing to 1.0) for the eight founder lines. For the vast majority of loci and CC lines, a very large probability (greater than 0.95) is placed on the most likely parental origin for the locus. We performed regression modeling using trait as a response, and the probability vector as a predictor for a model with 8 degrees of freedom. Each trait, whether a phenotype such as TCE dose or TCA level, or an expression trait, was first transformed using rank-inverse normal transformation (GTEx Consortium, 2015) to ensure robustness to outliers. eQTL analysis was performed separately for each dosage group using the R package DOQTL1, and results were compared to direct likelihood ratios computed using regression F-statistics as described below to ensure correct computation. Expression traits were used only if they had both a mean number of reads ≥5 and a nonzero read proportion of at least 10%.

To accord with standard linkage mapping, the $\log_{10}$ likelihood ratio (LOD score) for the fitted model vs. the null was used to represent mapping evidence. At each locus, a *p*-value can be obtained from LOD scores via chi-square testing and standard likelihood ratio theory. However, initial investigation by permutation showed that p-values based on normal theory regression *F*-statistics were superior, i.e. were more nearly uniform under the null, and so were used for multiple comparisons as described below.

To facilitate multiple comparisons and to acknowledge that cis-eQTLs are more common than trans-eQTLs, we obtained separate cis- and trans- *p*-values for each expression trait as

follows. First, 1000 permutations of a normally-distributed "phenotype" were performed, and the linkage F-statistics computed across the genome. As the rank-inverse normal transformation produces identical transformed values for any trait (provided there are no ties), the permutations formed a generic set of sampling outcomes that are applicable to any quantitative trait. For each permutation, the maximum F-statistic was recorded for each chromosome. Thus, for each chromosome we obtained a set of 1000 maxima on the chromosome (cis) and 1000 maxima on the remaining chromosomes (trans). For each of these 40 sets of permutations (20 chromosomes, both cis and trans), the maximum F-statistic was modeled via maximum likelihood fitting to a Gompertz extreme value distribution, providing the basis for cis- and trans- p-values for each expression trait. By construction, these p-values control for multiple comparisons across different loci. In order to control for multiple comparisons across different genes, each of the sets of cis p-values and trans p-values were adjusted using the *qvalue* package in R, resulting in false discovery *q*-values for both cis and trans. For non-expression traits such as TCA levels, the overall maximum F-statistic distribution was used in the extreme value modeling to obtain a genome-wide *p*-value.

III. Results

Dose-, strain- and interaction-related effects of TCE on liver gene expression

Previous studies of inter-strain variability of TCE effects demonstrated that liver transcriptomic responses are strongly dependent on genetic background and that peroxisome proliferator-activated receptor-associated pathways represented some of the most pronounced genetic-background dependent molecular effects of TCE treatment in mouse liver (Bradford et al., 2011). Although this earlier study provided greater understanding of the mechanisms of TCE-induced toxicity anchored on genotype-phenotype correlations, it included only 15 inbred strains

and did not examine dose-response relationships. In an effort to further elucidate how TCE responses differ by genetic background- and dose-expression relationships, we utilized liver gene expression data from 50 CC strains and 4 dose groups (plus vehicle).

Dose, strain, and interaction effects were modeled for each transcript for both TCE dose and liver levels of TCA in each mouse. Exemplar plots of genes that were significant for one or several of these relationships are displayed in Figure 3.1, panel A shows the dose-response relationships for the administered dose of TCE and panel B for a correlation with liver TCA level in each individual mouse. For example, we observed that expression of UDP-glucuronosyltransferase family 2 member A3 (*Ugt2a3*) was down-regulated with TCE dose, but this effect on gene expression was strain independent, with no dose by strain interaction effect. The effects of TCE on UDP-glucuronosyltransferase enzymes is not well characterized, but it is known that glucuronidation of trichloroethanol, a major oxidative metabolite of TCE, is a detoxification mechanism (Chiu, Micallef, Monster, & Bois, 2007). Baseline expression levels of alcohol dehydrogenase 1 (*Adh1*) varied dramatically by strain but did not exhibit a significant dose-response to TCE or a dose by strain effect. Alcohol dehydrogenases are involved in the biotransformation of TCE metabolites chloral and chloral hydrate to trichloroethanol (Lash et al., 2014) and our finding of a high degree of inter-individual variability is consistent with previous observations in both humans and mice (Bronley-DeLancey et al., 2006; Venkatratnam et al., 2017). In contrast to the *Ugt2a3* and *Adh1* examples, the expression of acyl-CoA thioesterase 7 (*Acot7*) exhibited not only a strong baseline strain effect, but also a strain by dose interaction effect. *Acot7* is a PPARα-responsive gene (Rakhshandehroo, Knoch, Muller, & Kersten, 2010). Indeed, PPARα-signaling plays a critical role in the effects of TCE in rodent liver (Rusyn et al., 2014). Of note, all three example genes depicted in Figure 3.1 exhibited highly significant dose, strain and interaction effects regardless

whether TCE dose, or liver TCA concentrations were used as the "dose", demonstrating that at least for these exemplars, that TCA plays a key role in transcriptional responses to TCE in mouse liver, likely through its agonism to PPARα (Maloney & Waxman, 1999).

Overall, we found that 5,285 transcripts were significant (after multiple testing correction as described) for the effect of TCE dose, 11,820 for the effect of strain, and 2,140 for the interaction between the two (Figure 3.2, left column of Venn diagrams). When liver TCA was used as an input into the model, 4,769 transcripts were significant for TCA, 13,920 for strain, and 2,242 for interaction (Figure 3.2, right column). Interestingly, a very small number of transcripts was purely dose-dependent, without an effect of strain or interaction, only less than 1% of the transcriptome. In contrast, the effect of strain on the transcriptome was a major factor, representing in excess of the 50% of all transcripts that were mapped. This observation is consistent with the dominant effect of genetic variability on transcription in the liver (D. Gatti et al., 2007; Schadt et al., 2008), and general findings on the impact of genetic variation in expression regulation (GTEx Consortium, 2013, 2015).

Whether analyzing the effects of TCE dose on expression in liver, or the relationship between liver TCA concentration and liver expression, we found significant overlap in expression signatures. This finding is not completely unexpected, as there is strong correlation ($r=0.78$, $p=0.86$) between TCE dose and liver TCA levels (Figure 3.3A). However, this observation points to the important, but not exclusive, role of TCA as the "effector" metabolite of TCE in rodent liver which is largely realized through transcriptional and other downstream effects. The importance of including the dose-response considerations in the analysis of the population-wide transcriptional response to toxicity is illustrated in Figure 3.3B. While there is a significant positive correlation ($r=0.49$, $p<0.001$) between the number of significantly perturbed transcripts and liver TCA at the

highest TCE dose level, this relationship is highly strain-variable whereby many strains with the highest liver TCA were not the most "responsive" transcriptionally.

Dose-, strain- and interaction-related effects of TCE on liver pathways

Next, we examined the molecular pathways perturbed by TCE in mouse liver in a dose-, strain-, or interaction-dependent manner. To examine concordance in pathways between TCE dose and liver TCA, significant Gene Ontology and KEGG pathways/category enrichment was examined using DAVID/EASE (q-value<0.001), for lists of transcripts with significant dose (Figure 3.3C), strain (Figure 3.3D), or interaction (Figure 3.3E) effects. Most pathways for the dose and strain effects were shared between TCE dose and liver TCA analyses (marked in green), and their level of significance was highly concordant (slopes close to 1).

Due to the high degree of concordance, we show the pathway results for TCE dose for using DAVID/EASE (Tables 3.1 and 3.2). Pathways from significant dose-related transcripts are shown in Table 1. Pathways with strong TCE dose-response relationships included lipid and fatty acid metabolism. Most of these were also significant for the strain effect and they are closely related to PPARα signaling, a finding consistent with our understanding of the major molecular effects of TCE in the rodent liver (Rusyn et al., 2014). Another prominent group of dose-responsive pathways was the effect on cell-cell adhesion and gap junctional intercellular communication, also consistent with previous findings that exposure to TCE and TCA inhibits gap junctional communications in mouse hepatocytes (Klaunig, Ruch, & Lin, 1989).

While there was a greater number of genes that exhibited strain-specific changes in gene expression, enrichment analysis yielded fewer discernable significantly enriched pathways (Table 3.2). Two translation-related pathways were significant for strain alone and not dose or interaction.

Pathways that were both strain- and dose-dependent were largely similar to those in Table 3.1, showing that the large part of TCE dose-response response is highly dependent on the genetic background.

Comparison of PODs for transcriptional and apical effects of TCE in mouse liver

Next we sought to compare transcriptomics-derived dose-response effects of TCE in this acute exposure study in genetically diverse CC mice to the traditional apical endpoint-derived PODs for the same tissue but in other animal models. Specifically, we based these comparisons on the effects of TCE on liver transcriptome in B6C3F1 strain (Y. H. Zhou et al., 2017) and the liver non-cancer and cancer endpoints used by U.S. EPA to derive toxicity values (U.S. EPA, 2011a, 2011b). For this comparison, we converted both types of PODs to human equivalent doses using a multi-species PBPK models, as described in Methods, and the results are shown in Figure 3.4A. Because of the lack of PBPK models specifically for CC mice, we used the median estimates for mice from the PBPK model, which was calibrated using data from Swiss and B6C3F1 mice (Chiu et al., 2014a; M. V. Evans, Chiu, Okino, & Caldwell, 2009). The transcriptional PODs covered the same range of human equivalent doses as the apical endpoints, with the most sensitive median BMDL (KEGG_mmu00071, fatty acid degradation) being nearly the same as the most sensitive apical endpoint-derived BMDL (B6C3F1 mouse liver carcinomas). Overall, the median transcriptional BMDLs across all pathways in CC mice were within 10-fold of the apical PODs for TCE effects in the liver.

A corollary of this analysis is a question of whether data from the CC population are more informative as compared to the analysis of the dose-response gene and pathway effects of TCE in B6C3F1 hybrid strain. Thus, we constructed strain-specific distributions using the data for the

same pathways (Figure 3.4B). We find that B6C3F1 strain-derived data fall into the upper tertile of the overall population variability distribution, above the apical data-derived PODs. Furthermore, the analysis of strain-specific effects of TCE on mouse liver transcriptome that is afforded by the CC population shows that certain strains are more sensitive (e.g., CC004/TauUnc) or resistant (e.g., CC039/Unc, CC023/GeniUnc and CC018/Unc) and may be selected for further studies in sub-chronic and chronic exposure scenarios. Interestingly, although the most sensitive strain CC004/TauUnc had transcriptional PODs that were 10-fold lower than those of B6C3F1 mice, the median transcriptional POD for this strain was within 2-fold of the most sensitive apical POD.

Genetic mapping of the transcriptional effects of TCE in mouse liver

To further elucidate whether the CC model provides sufficient resolution to dissect the genetic underpinnings of TCE susceptibility, we conducted genome-wide linkage mapping to identify loci associated with variability in liver TCA levels for the highest TCE dose group. As reported previously (Venkatratnam et al., 2017), we identified a significant QTL on distal chromosome 2 (Figure 3.5A) associated with variability in liver TCA levels, although the robust mapping methods used here differ from the previous report. The previous study also reported that expression of PPARα-response gene *Fitm2* (Fat Storage Inducing Transmembrane Protein-2) which resides in this locus (red arrowhead) was positively correlated with liver TCA levels for the highest TCE dose exposure group.

In the current study, the availability of whole-transcriptomic expression data enabled a more comprehensive examination of this locus for the potential association between genetic polymorphisms and gene expression. A linkage scan for expression of *Fitm2* co-localized with the

TCA peak region (Figure 3.5B) and indicates a strong eQTL. Among the genes in a 1.5-LOD support interval for this locus, *Fitm2* had the highest correlation with TCA levels (Figure 3.5C). Further, effects of CC founder alleles in this region revealed that presence of M.m.castaneous alleles in this region is associated with higher expression of *Fitm2* (Figure 3.5C). However, TCA levels and *Fitm2* expression were substantially correlated *within* sets of CC strains sharing regional diplotypes, indicating possible additional sources of positive correlation and signaling potential additional complexities with confidently pointing to the genetic underpinnings of inter-individual variability in liver TCA levels.

To conduct a more comprehensive analysis of the genetic underpinnings of variation in response to TCE, we additionally performed an analysis using, for each gene and CC strain, the *slope* of the expression response (β_1 in a dose-response linear model) to TCE as a trait for linkage mapping. To be comprehensive, we performed the analysis using β_1 values from both simple linear regression of expression vs. ln(dose), as well as β_1 values from the DESeq2 analyses. Separate cis and trans *p*-values and corresponding false discovery *q*-values were obtained as described in Methods. In terms of *q*-values (which are corrected for multiple comparisons), none of the results were significant.

Finally, to identify genetic loci driving variability in transcriptomic responses, we performed expression quantitative trait locus (eQTL) analysis at each dose group. We observed trans-bands (or instances where expression of several genes are driven by a common locus) in chromosomes 3, 11, and 12 in the vehicle treatment group. No trans-bands were observed at lower dose groups, but few trans-bands were observed at higher dose groups (data not shown). Figure 3.5D reports the numbers of significant local (cis) eQTLs at each dose group in a Venn diagram,

illustrating variation by dose, but also considerable commonality, with 2285 genes significant at $q<0.05$ for all doses.

IV. Discussion

It is widely acknowledged in the fields of toxicology and risk assessment that population variability is one of the key challenges that begets uncertainty in human health assessments of environmental chemicals (Zeise et al., 2013). Drug safety evaluation is usually more informed through studies in humans at various phases of the clinical trials, still the challenge of idiosyncratic adverse drug reactions is also prominent and subject to active investigations (Atienzar et al., 2016). Solutions to these challenges are currently few, despite the abundance of experimental models from cells, to animals, to human studies. For instance, the tools for studies of genetics in experimental model systems have been originally developed by geneticists (Churchill et al., 2012; The International HapMap Consortium, 2003; Threadgill et al., 2011) and only fairly recently these models have been used in studies of acute and repeat-dose exposure to drugs and chemicals (French et al., 2015; Harrill & McAllister, 2017). The potential for how these new animal models can inform risk assessment is great, though example applications of incorporating these data into decision-making remain small in number (Chiu & Rusyn, 2018). For instance, evaluation of toxicity using population-based *in vitro* and *in vivo* models can potentially reduce both false positive and false negative signals and improve hazard identification. Enhanced ability to perform genetic mapping allows for the identification of key biological pathways and mechanisms that may be involved in toxicity and/or susceptibility. In addition, population-based toxicity data can serve as a surrogate for human variability, and thus be used to quantitatively estimate the degree of human toxicokinetic/toxicodynamic variability and thereby increase confidence in the dose-response step of risk assessment that sets health-protective exposure limits.

The difficulty in translating the data from studies in population-based experimental models to real decisions is due not only to the complexities of the relationships between genotypes and phenotypes, but also because of impediments resulting from "cultural" differences between the research questions in genetics, decades-old "standard practices" in toxicology studies, and the needs of decision-makers. Specifically, there appears to be a chasm in what constitutes the most valuable outcome(s) of a toxicology study in a population model. Is it a susceptibly locus, the molecular determinant(s) of inter-individual variability that may be used as a biomarker, a quantitative estimate of the extent of inter-individual variability, a better "model" (*i.e.*, strain or cell line) for susceptible humans, or all of the above.

This study takes the "*all of the above*" point of view. It adds to the body of knowledge on the utility of the mouse population-based experimental models in toxicology and risk assessment by examining transcriptomic data obtained from a study in CC mice for characterization of strain-dependent and -independent mechanisms of TCE toxicity, discovery of the potential susceptibility loci, as well as dose-response assessment and derivation of POD values. This study provides further evidence of the relative impact of dose and strain variation on transcription, and is among the largest studies to date that have combined large populations, transcriptomics and toxicity phenotyping.

We found that all known pathways of liver toxicity of TCE (Cichocki et al., 2016; Rusyn et al., 2014) are perturbed in both strain- and dose-dependent manner. Even though strain effects were predominant in terms of liver transcriptome among CC strains, TCE effects were prominent and largely dependent on the formation of TCA. However, despite high concordance in dose-, strain- and interaction-effects between TCE dose and liver TCA levels, the inter-individual variability likely depends on factors other than metabolism to TCA. This finding is highly

informative with respect to not only the interpretation of the strain differences in the mouse, but also the extrapolation of these data to humans. The diversity of the pathways involved and the complexity of the signaling mechanisms that were largely strain-dependent caution against over-reliance on studies in knockout and/or transgenic animals as more informative, or human-like, models. This study also supports the utility of the information on the molecular pathways, rather than individual genes, for cross-species translation and biomarker discovery, similar to the conclusions of the study of tolvaptan-induced liver injury in CC population (Mosedale et al., 2017).

Additionally, studies in genetically defined population-wide models enable discovery of the susceptibility loci through genetic mapping. There are a number of published examples where susceptibility loci and candidate genes were successfully identified for drug and chemical-associated toxicity phenotypes (French et al., 2015; Harrill, Watkins, et al., 2009; Mosedale et al., 2017; Venkatratnam et al., 2017). Despite some success, these studies have pointed out that chemical-induced toxicities are highly complex traits and thus are polygenic in nature. Our study confirms this sentiment by also exploring the gene expression dimension. We found that TCE-mediated transcriptional responses in mouse liver may be highly polygenic in nature, so that mapping multiple susceptibility loci may be difficult with the sample size of 50 CC strains. One possible solution is to increase the number of strains (Kaeppler, 1997), or replicates per strain in future studies; however, the cost and complexity of these studies is likely prohibitive and not proportionate to the value of information that may be obtained. While the knowledge of the exact susceptibility genes/loci may be of use for drugs in the context of "precision medicine," even if such are discovered they are likely to be less informative in the context of human health assessment of TCE and other chemicals for which genetic testing prior to exposure is highly improbable.

An outcome of this study that is most likely to be of use for human health risk assessment is the exploration of dose-response relationships in response to TCE at the transcriptomic and population levels. The seminal paper by French and co-workers (French et al., 2015) was the first to demonstrate the value of mouse population studies for quantitative dose-response modeling that is directly applicable for risk assessment. Similarly, we have shown previously for TCE that population-based estimates of toxicokinetic parameters from a study in mice are concordant to those for data from humans (Chiu et al., 2014a). Hence, our study explored the quantitative aspects of molecular sequelae of exposure to TCE in a mouse population and used gene expression to derive PODs for various pathways and strains. Thomas and coworkers have demonstrated that pathway-based POD based on gene expression data from short-term exposure studies are well correlated with the POD on the apical endpoints derived from traditional 90 day and 2 year animal studies (Farmahin et al., 2017; Thomas et al., 2011; Thomas, Wesselkamper, et al., 2013).

We recently reported that in B6C3F1 mice, transcriptional PODs for TCE correlated well with PODs for apical endpoints, after correcting for toxicokinetics (Zhou et al. 2017). Here, we found a similar correspondence to apical endpoint PODs using transcriptomic data from a genetically diverse mouse population. Previously, it was found that the transcriptional POD were more conservative, generally within one order of magnitude (Thomas et al., 2011). In our earlier study in B6C3F1 mice, transcriptional PODs for TCE were also within 10-fold of apical PODs, but the differences were in both directions, i.e. not consistently conservative. Here, in CC mice, the transcriptional and apical endpoint PODs for TCE substantially overlapped, a large number of transcriptional pathways, including the most sensitive falling *within the range* of the apical endpoint PODs. This greater apparent correlation suggests that using CC mice may provide a more robust transcriptional POD because of the incorporation of genetic diversity that reduces the

potential impact of outliers, but this hypothesis needs to be tested for additional chemicals and target tissues. Moreover, as was the case with Zhou et al. (2017), conversion to human equivalent doses has the additional utility of being directly comparable to human exposure estimates and derivation of the margins of exposure. These results provide further evidence that transcriptomic data can be used as surrogates for *in vivo* PODs, and suggest that a population-based approach might be more robust than using a single strain.

In summary, our study is among the first to explore the linkages between gene expression and genetic polymorphisms in a toxicological context. This innovative approach extends the common method to analyzing toxicity pathway perturbations to the population level, allowing for an exploration of gene-environment interactions, which are thought to be the basis of phenotypic variation across the population. Using the CC population and TCE liver effects as a prototypical example, we have demonstrated that adding the dimension of genetic diversity has multiple potential benefits. First, by identifying pathways that are dependent on strain, treatment, or their interaction, we obtain deeper insights into toxicological mechanisms. Second, it enables the possibility of genetic mapping to identify susceptibility loci, although this may be challenging for polygenic traits such as TCE-induced liver effects. Finally, at least in this case, conducting gene expression dose-response analysis across a population appears to be more robust than using a single strain in terms of the correlation between transcriptional and apical PODs. Overall, our study demonstrates the utility of mouse population-based studies in addressing the key issue of inter-individual variability in the human health risk assessment of chemical exposures.

V. Figures and Tables

Figure 3.1. Examples of genes (*Ugt2a3, Adh1*, and *Acot7*) that were affected by exposure to TCE in mouse liver in genetic background-, dose- or interaction-dependent manner. Top panel **(A)** shows correlation with administered TCE dose; bottom panel **(B)** is correlation with liver TCA levels at 24 hrs after dosing. Each circle represents gene expression in a CC mouse. Each line represents a linear dose-response fit for each CC strain. The y-axis represents normalized counts of the expression. The x-axis in the top panel represents administered TCE dose (mg/kg) and in the bottom panel represents liver TCA levels (nmol/g) in the CC population. False discovery *q*-values (q≤0.001) for dose and strain main effects, as well as their interaction, are displayed in each box.

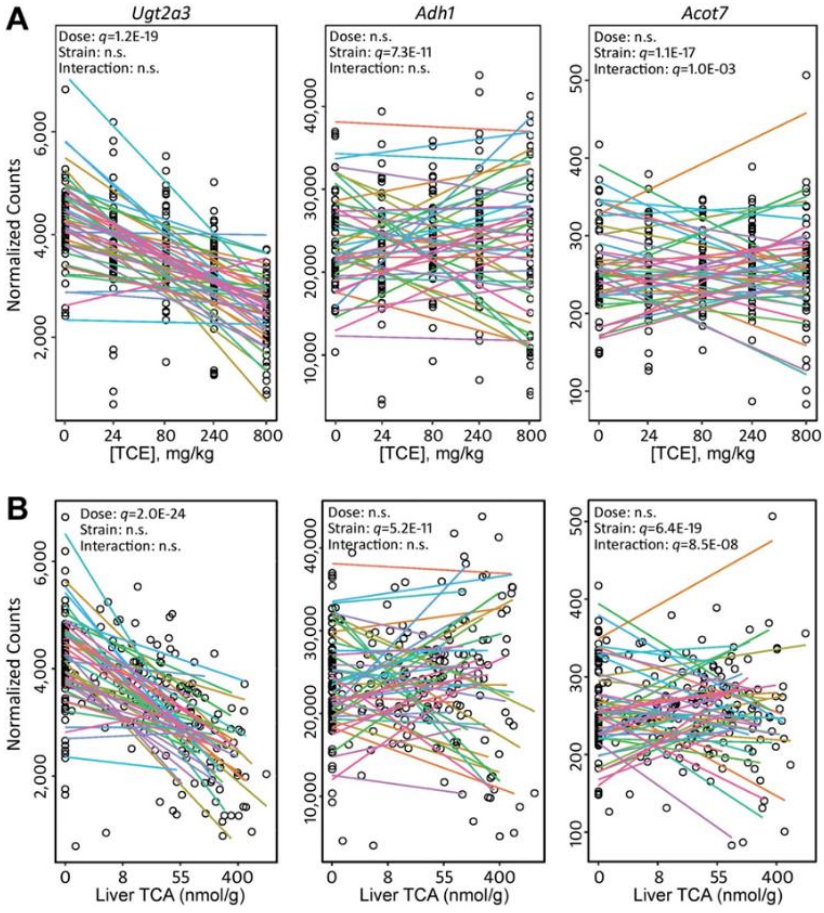

Figure 3.2. Venn diagrams representing total number of transcripts from the transcriptome that are strongly influenced by genetic background-, dose-, or interaction-effects with administered TCE dose (left panel) or liver TCA (right panel) as dose inputs. Numbers within each sector of circles represents either unique or common transcripts. Percentages represent the total percent of transcripts from the liver transcriptome that are common between TCE dose and TCA level analyses.

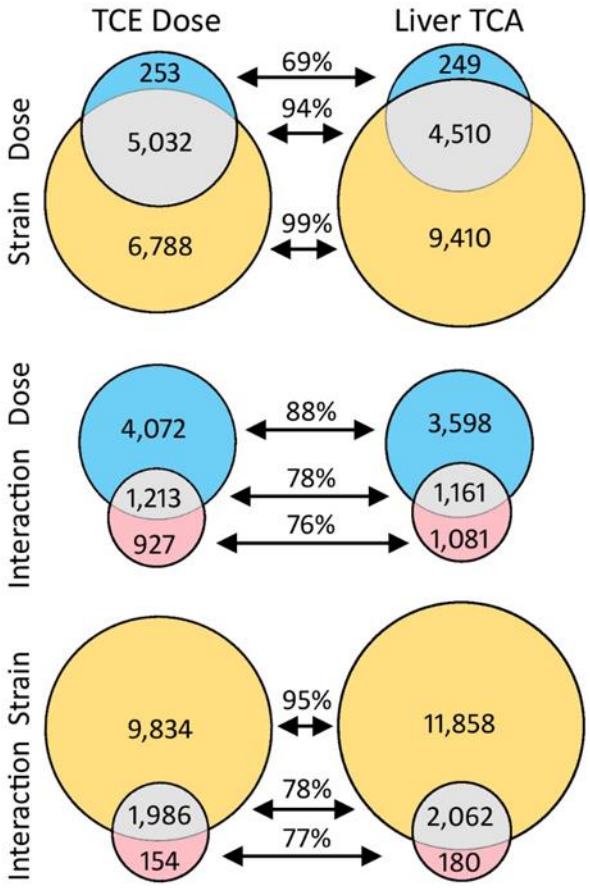

Figure 3.3. Concordance between TCE dose and liver TCA levels based on gene- and pathway-based analyses. **(A)** Scatter-plot showing individual animal's liver TCA (nmol/g) as compared to the administered TCE dose (mg/kg). The inset shows the results of the correlation analysis of these data. **(B)** A relationship between liver TCA levels and the number of significantly ($q<0.05$) perturbed transcripts by the TCE (800 mg/kg) in each CC strain. The inset shows the results of the correlation analysis of these data. **(C)** Concordance in pathways that were significantly ($q<0.01$) associated with dose (top), strain (middle), or interaction (bottom) for the analyses where TCE dose (x-axis) or liver TCA (y-axis) were used as dose inputs. Each dot is a KEGG or GO pathway/category. Pathways that were significant only for TCE are colored black, only for liver TCA are colored red and pathways that were significant for both are colored green.

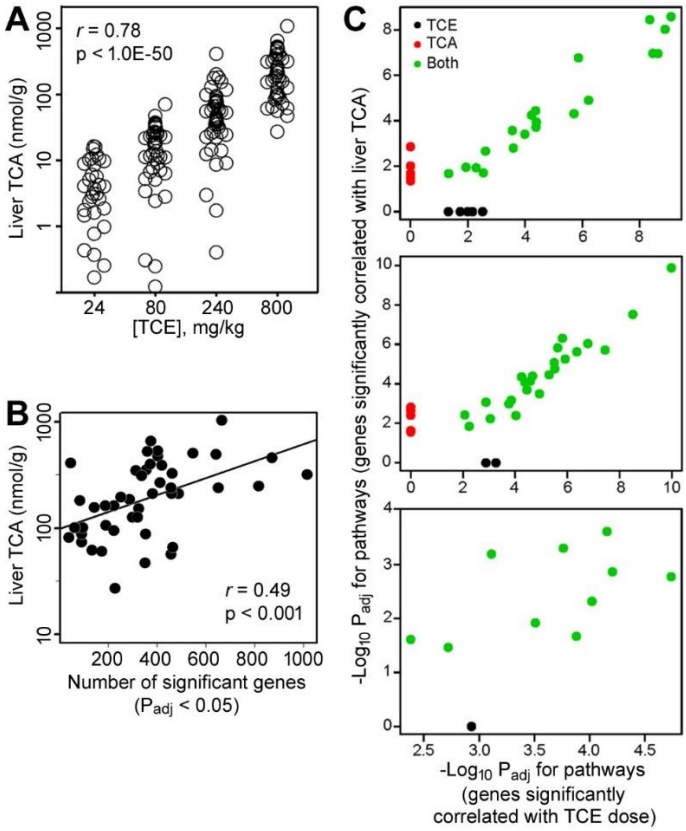

Figure 3.4. Comparison of point of departures (PODs) across significantly (q<0.001) perturbed pathways due to genetic background-, dose-, and interaction-effects in the CC model with apical endpoints from sub-chronic or chronic TCE studies in B6C3F1. Box plots represent PODs, converted to human equivalent dose (mg/kg-d) using mouse and human physiologically-based pharmacokinetic models, for the following: apical endpoints (black); transcriptional PODs for B6C3F1 mice from Zhou et al. (2017) (green); transcriptional PODs for CC mice aggregated across pathways and strains (blue, panel **A** only); transcriptional PODs for individual pathways, aggregated across CC strains (red, panel **A**); or transcriptional PODs for individual CC strains, aggregated across pathways (red, panel **B**). See Supplemental Table 6 for full listing of abbreviations used.

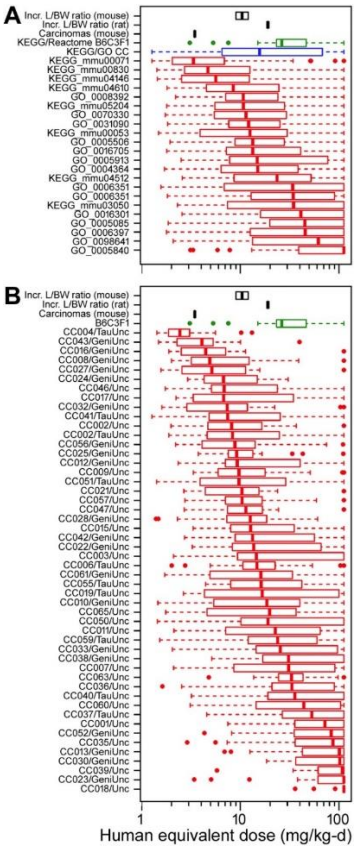

Figure 3.5. **(A)** A genome-wide linkage scan for liver TCA levels at the highest TCE dose (800 mg/kg) in 50 CC lines identifies a significant QTL on chromosome 2. Location of a candidate gene *Fitm2* is marked with a red arrowhead. (**B**) Genome-wide linkage scan of *Fitm2* gene expression shows a cis-eQTL localizing in the same region as for (A). (**C**) Scatter plot representing liver TCA (nmol/g) levels versus normalized *Fitm2* expression, with dots representing CC founder alleles in the peak region. (**D**) Venn diagrams displaying unique local eQTLs by administered TCE dose.

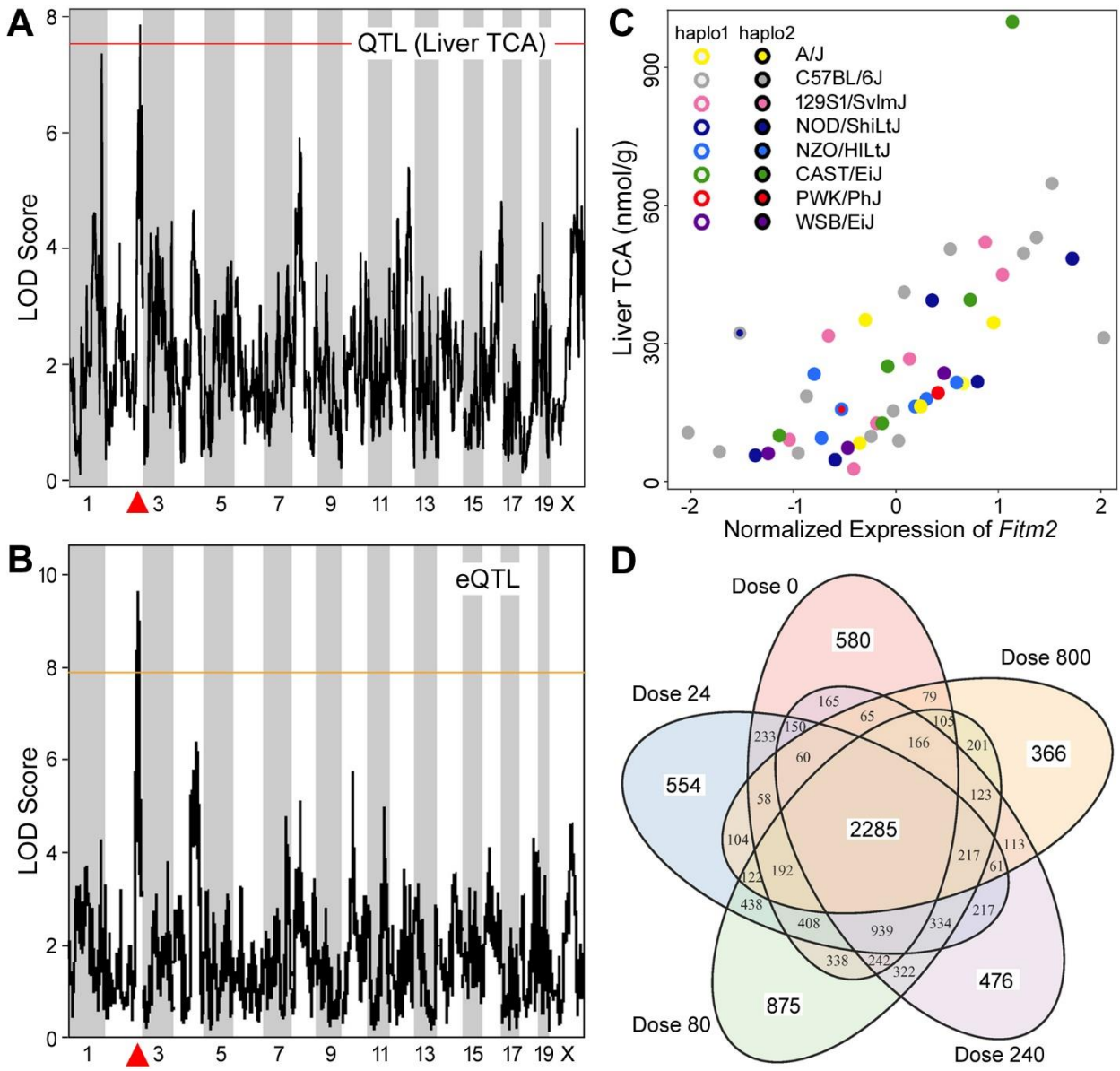

Table 3.1. Pathways that are significantly associated with dose-, dose-/interaction-effects, and dose /strain-effects.

Category	Term	Count	pValue	qValue*
Pathways from genes that were significantly (q<0.001) correlated with TCE dose[&]				
KEGG_PATHWAY	mmu04146:Peroxisome	42	5.96E-13	8.65E-11
KEGG_PATHWAY	mmu00071:Fatty acid degradation	27	1.46E-09	8.49E-08
KEGG_PATHWAY	mmu03050:Proteasome	29	1.72E-12	1.66E-10
GOTERM_BP_DIRECT	GO:0055088~lipid homeostasis	22	2.21E-08	1.85E-05
KEGG_PATHWAY	mmu04610:Complement and coagulation cascades	33	3.03E-08	1.46E-06
GOTERM_CC_DIRECT	GO:0005913~cell-cell adherens junction	71	3.01E-05	9.95E-04
KEGG_PATHWAY	mmu00830:Retinol metabolism	33	2.16E-06	6.96E-05
GOTERM_MF_DIRECT	GO:0016740~transferase activity	293	7.95E-10	3.24E-07
GOTERM_BP_DIRECT	GO:0006637~acyl-CoA metabolic process	18	1.33E-07	9.76E-05
KEGG_PATHWAY	mmu00053:Ascorbate and aldarate metabolism	15	1.38E-05	3.08E-04
GOTERM_CC_DIRECT	GO:0034364~high-density lipoprotein particle	12	3.08E-05	9.79E-04
Pathways significantly (q<0.001) perturbed with dose effect				
GOTERM_BP_DIRECT	GO:0006351~transcription, DNA-templated	50	1.19E-08	1.34E-05
Pathways from genes that had a significant (q<0.001) dose and strain interaction effect[$]				
GOTERM_MF_DIRECT	GO:0016301~kinase activity	114	1.04E-07	2.32E-05
GOTERM_MF_DIRECT	GO:0098641~cadherin binding involved in cell-cell adhesion	60	5.71E-08	1.49E-05
GOTERM_BP_DIRECT	GO:0006351~transcription, DNA-templated	270	9.62E-09	9.64E-06
GOTERM_BP_DIRECT	GO:0006397~mRNA processing	62	2.18E-06	9.94E-04
Pathways from genes that were significantly (q<0.001) correlated with TCE dose that were also strain-dependent[@]				
KEGG_PATHWAY	mmu03050:Proteasome	29	1.45E-12	2.09E-10
KEGG_PATHWAY	mmu04146:Peroxisome	32	1.05E-06	6.02E-05
KEGG_PATHWAY	mmu04610:Complement and coagulation cascades	35	1.38E-09	1.33E-07
KEGG_PATHWAY	mmu00830:Retinol metabolism	33	1.86E-06	8.94E-05
GOTERM_CC_DIRECT	GO:0005913~cell-cell adherens junction	74	7.54E-06	2.98E-04
GOTERM_MF_DIRECT	GO:0016740~transferase activity	300	2.69E-10	1.09E-07
KEGG_PATHWAY	mmu00053:Ascorbate and aldarate metabolism	15	1.28E-05	4.08E-04

[&], Full list of the significant pathways is in Supplemental Table 1 (5285 genes)

[$], Full list of the significant pathways is in Supplemental Table 2 (2140 genes)

[@], Full list of the significant pathways is in Supplemental Table 3 (5032 genes)

Table 3.2. Pathways that are significantly perturbed by either strain- or strain- and dose-effects.

Category	Term	Count	pValue	qValue*
Pathways from genes that were significantly (q<0.001) correlated with strain effect[&]				
GOTERM_CC_DIRECT	GO:0005840~ribosome	62	8.97E-12	1.68E-09
GOTERM_MF_DIRECT	GO:0005085~guanyl-nucleotide exchange factor activity	48	3.35E-08	3.05E-05
Pathways from genes that were significantly (q<0.001) correlated with strain that were also dose-dependent[@]				
GOTERM_MF_DIRECT	GO:0016705~oxidoreductase activity	41	2.11E-11	1.32E-08
GOTERM_MF_DIRECT	GO:0008392~arachidonic acid epoxygenase activity	26	9.61E-11	4.50E-08
KEGG_PATHWAY	mmu00830:Retinol metabolism	38	1.17E-09	6.65E-08
GOTERM_MF_DIRECT	GO:0005506~iron ion binding	61	6.92E-09	1.30E-06
GOTERM_CC_DIRECT	GO:0031090~organelle membrane	35	1.68E-08	1.24E-06
GOTERM_MF_DIRECT	GO:0070330~aromatase activity	20	2.07E-08	3.52E-06
GOTERM_CC_DIRECT	GO:0005840~ribosome	59	2.80E-10	3.10E-08
KEGG_PATHWAY	mmu05204:Chemical carcinogenesis	45	7.83E-14	2.23E-11
GOTERM_MF_DIRECT	GO:0004364~glutathione transferase activity	20	2.94E-09	6.89E-07
KEGG_PATHWAY	mmu04512:ECM-receptor interaction	31	6.44E-06	1.15E-04

[&], Full list of the significant pathways is in Supplemental Table 4 (5285 genes)

[@], Full list of the significant pathways is in Supplemental Table 5 (2140 genes)

Supplemental Table 3.1. Pathways from genes that were significantly (q<0.001) correlated with TCE dose.

Annotation Cluster 1	Enrichment Score: 10.44963901183211											
Category	Term	Count	%	PValue	Genes	List Total	Pop Hits	Pop Total	Fold Enric	Bonferron	Benjamini	FDR
KEGG_PATHWAY	mmu04146:Peroxisome	42	1.432958	5.96E-13	ACOX2, A(	1214	83	7720	3.21788	1.73E-10	8.65E-11	7.93E-10
GOTERM_CC_DIRECT	GO:0005777~peroxisome	51	1.74002	2.83E-12	ACOX2, A(	2709	131	19662	2.825645	2.52E-09	2.80E-10	4.40E-09
GOTERM_CC_DIRECT	GO:0005778~peroxisomal membrane	25	0.852951	2.66E-08	ACOX1, M	2709	53	19662	3.423598	2.37E-05	1.48E-06	4.14E-05
Annotation Cluster 2	Enrichment Score: 8.114739464455717											
GOTERM_BP_DIRECT	GO:0006635~fatty acid beta-oxidation	28	0.955305	6.60E-13	ACOX2, A(	2568	44	18082	4.480813	3.87E-09	7.75E-10	1.28E-09
KEGG_PATHWAY	mmu00071:Fatty acid degradation	27	0.921187	1.46E-09	ACOX1, A(	1214	49	7720	3.504018	4.25E-07	8.49E-08	1.95E-06
Annotation Cluster 3	Enrichment Score: 7.553384683229137											
KEGG_PATHWAY	mmu03050:Proteasome	29	0.989423	1.72E-12	PSMB10, F	1214	45	7720	4.098115	4.97E-10	1.66E-10	2.28E-09
GOTERM_CC_DIRECT	GO:0000502~proteasome complex	34	1.160014	2.20E-12	PSMB10, F	2709	66	19662	3.738985	1.96E-09	2.46E-10	3.43E-09
REACTOME_PATHWAY	R-MMU-1236978:R-MMU-1236978	30	1.023541	5.04E-11	PSMB10, F	1278	50	7575	3.556338	4.38E-08	4.38E-08	7.83E-08
REACTOME_PATHWAY	R-MMU-450408:R-MMU-450408	33	1.125896	5.73E-11	PSMB10, F	1278	59	7575	3.31523	4.97E-08	2.48E-08	8.88E-08
REACTOME_PATHWAY	R-MMU-350562:R-MMU-350562	31	1.05766	1.03E-10	PSMB10, F	1278	54	7575	3.402669	8.93E-08	2.98E-08	1.60E-07
REACTOME_PATHWAY	R-MMU-187577:R-MMU-187577	34	1.160014	1.73E-10	PSMB10, F	1278	64	7575	3.148841	1.50E-07	3.74E-08	2.68E-07
REACTOME_PATHWAY	R-MMU-195253:R-MMU-195253	36	1.22825	2.43E-10	PSMB10, F	1278	71	7575	3.005356	2.11E-07	4.23E-08	3.78E-07
REACTOME_PATHWAY	R-MMU-5358346:R-MMU-5358346	33	1.125896	3.16E-10	PSMB10, D	1278	62	7575	3.154816	2.75E-07	4.58E-08	4.91E-07
REACTOME_PATHWAY	R-MMU-382556:R-MMU-382556	40	1.364722	3.52E-10	ABCF1, PS	1278	85	7575	2.789285	3.06E-07	4.37E-08	5.46E-07
GOTERM_CC_DIRECT	GO:0022624~proteasome accessory complex	15	0.511771	3.87E-10	PSMD14, F	2709	17	19662	6.404143	3.45E-07	2.66E-08	6.03E-07
REACTOME_PATHWAY	R-MMU-1169091:R-MMU-1169091	35	1.194132	7.30E-10	PSMB10, N	1278	70	7575	2.963615	6.34E-07	7.92E-08	1.13E-06
REACTOME_PATHWAY	R-MMU-69481:R-MMU-69481	30	1.023541	1.12E-09	PSMB10, F	1278	55	7575	3.233035	9.72E-07	1.08E-07	1.74E-06
REACTOME_PATHWAY	R-MMU-69017:R-MMU-69017	30	1.023541	1.12E-09	PSMB10, F	1278	55	7575	3.233035	9.72E-07	1.08E-07	1.74E-06
REACTOME_PATHWAY	R-MMU-174113:R-MMU-174113	31	1.05766	1.82E-09	PSMB10, F	1278	59	7575	3.114307	1.58E-06	1.58E-07	2.82E-06
REACTOME_PATHWAY	R-MMU-4641257:R-MMU-4641257	31	1.05766	1.82E-09	PSMB10, F	1278	59	7575	3.114307	1.58E-06	1.58E-07	2.82E-06
REACTOME_PATHWAY	R-MMU-69229:R-MMU-69229	30	1.023541	1.95E-09	PSMB10, F	1278	56	7575	3.175302	1.69E-06	1.54E-07	3.03E-06
REACTOME_PATHWAY	R-MMU-349425:R-MMU-349425	30	1.023541	1.95E-09	PSMB10, F	1278	56	7575	3.175302	1.69E-06	1.54E-07	3.03E-06
REACTOME_PATHWAY	R-MMU-5607761:R-MMU-5607761	32	1.091778	2.76E-09	PSMB10, F	1278	63	7575	3.010657	2.39E-06	2.00E-07	4.28E-06
REACTOME_PATHWAY	R-MMU-5676590:R-MMU-5676590	32	1.091778	2.76E-09	PSMB10, F	1278	63	7575	3.010657	2.39E-06	2.00E-07	4.28E-06
REACTOME_PATHWAY	R-MMU-69601:R-MMU-69601	30	1.023541	3.34E-09	PSMB10, F	1278	57	7575	3.119595	2.90E-06	2.23E-07	5.18E-06
REACTOME_PATHWAY	R-MMU-5610780:R-MMU-5610780	31	1.05766	5.06E-09	PSMB10, F	1278	61	7575	3.012199	4.39E-06	3.14E-07	7.85E-06
REACTOME_PATHWAY	R-MMU-5610785:R-MMU-5610785	31	1.05766	8.24E-09	PSMB10, F	1278	62	7575	2.963615	7.15E-06	4.77E-07	1.28E-05
REACTOME_PATHWAY	R-MMU-4608870:R-MMU-4608870	31	1.05766	1.32E-08	PSMB10, F	1278	63	7575	2.916574	1.15E-05	7.18E-07	2.05E-05
REACTOME_PATHWAY	R-MMU-2871837:R-MMU-2871837	37	1.262368	1.61E-08	PSMB10, F	1278	84	7575	2.610804	1.39E-05	8.20E-07	2.49E-05
REACTOME_PATHWAY	R-MMU-174084:R-MMU-174084	32	1.091778	1.79E-08	PSMB10, A	1278	67	7575	2.830916	1.56E-05	8.64E-07	2.78E-05
REACTOME_PATHWAY	R-MMU-4641258:R-MMU-4641258	30	1.023541	2.42E-08	PSMB10, F	1278	61	7575	2.915031	2.10E-05	1.11E-06	3.76E-05
REACTOME_PATHWAY	R-MMU-202424:R-MMU-202424	39	1.330604	3.10E-08	PSMB10, F	1278	93	7575	2.485613	2.69E-05	1.35E-06	4.82E-05
REACTOME_PATHWAY	R-MMU-5668541:R-MMU-5668541	33	1.125896	3.52E-08	PSMB10, T	1278	72	7575	2.716647	3.05E-05	1.45E-06	5.46E-05
REACTOME_PATHWAY	R-MMU-5607764:R-MMU-5607764	36	1.22825	4.19E-08	PSMB10, F	1278	83	7575	2.570847	3.64E-05	1.65E-06	6.50E-05
REACTOME_PATHWAY	R-MMU-68827:R-MMU-68827	30	1.023541	5.96E-08	PSMB10, F	1278	63	7575	2.82249	5.17E-05	2.25E-06	9.25E-05
REACTOME_PATHWAY	R-MMU-5687128:R-MMU-5687128	34	1.160014	9.28E-08	PSMB10, C	1278	78	7575	2.583664	8.05E-05	3.35E-06	1.44E-04
REACTOME_PATHWAY	R-MMU-174154:R-MMU-174154	32	1.091778	9.51E-08	PSMB10, A	1278	71	7575	2.671428	8.26E-05	3.30E-06	1.48E-04
REACTOME_PATHWAY	R-MMU-5658442:R-MMU-5658442	31	1.05766	3.68E-07	PSMB10, F	1278	71	7575	2.587946	3.19E-04	1.23E-05	5.71E-04
REACTOME_PATHWAY	R-MMU-174178:R-MMU-174178	32	1.091778	6.04E-07	PSMB10, A	1278	76	7575	2.495676	5.24E-04	1.94E-05	9.37E-04
REACTOME_PATHWAY	R-MMU-174184:R-MMU-174184	32	1.091778	6.04E-07	PSMB10, A	1278	76	7575	2.495676	5.24E-04	1.94E-05	9.37E-04
REACTOME_PATHWAY	R-MMU-68949:R-MMU-68949	31	1.05766	1.50E-06	PSMB10, F	1278	75	7575	2.449922	0.001302	4.65E-05	0.002328
GOTERM_CC_DIRECT	GO:0005839~proteasome core complex	13	0.443535	1.95E-06	PSMB10, F	2709	20	19662	4.717719	0.001739	9.16E-05	0.003038
GOTERM_CC_DIRECT	GO:0008540~proteasome regulatory particle, base subcomplex	10	0.34118	7.44E-06	PSMC6, PS	2709	13	19662	5.583099	0.006619	2.89E-04	0.01159

Annotation Cluster 4	Enrichment Score: 6.151312649143183											
GOTERM_BP_DIRECT	GO:0055088~lipid homeostasis	22	0.750597	2.21E-08	CEBPA, AC	2568	41	18082	3.778246	1.30E-04	1.85E-05	4.27E-05
GOTERM_MF_DIRECT	GO:0000062~fatty-acyl-CoA binding	20	0.682361	3.44E-08	ACOX2, SC	2498	35	17446	3.99085	6.99E-05	6.99E-06	5.92E-05
GOTERM_MF_DIRECT	GO:0050660~flavin adenine dinucleotide binding	30	1.023541	5.93E-08	ACOX2, CY	2498	72	17446	2.909995	1.21E-04	1.10E-05	1.02E-04
GOTERM_MF_DIRECT	GO:0016627~oxidoreductase activity, acting on the CH-CH group of donors	17	0.580007	1.62E-07	TM7SF2, A	2498	28	17446	4.240278	3.29E-04	2.53E-05	2.79E-04
GOTERM_BP_DIRECT	GO:0033539~fatty acid beta-oxidation using acyl-CoA dehydrogenase	13	0.443535	1.24E-06	ACOX2, AC	2568	19	18082	4.817716	0.007281	7.30E-04	0.002408
Annotation Cluster 5	Enrichment Score: 6.056714025644405											
GOTERM_CC_DIRECT	GO:0022624~proteasome accessory complex	15	0.511771	3.87E-10	PSMD14, F	2709	17	19662	6.404143	3.45E-07	2.66E-08	6.03E-07
GOTERM_CC_DIRECT	GO:0005838~proteasome regulatory particle	9	0.307062	4.45E-06	PSMC5, PS	2709	10	19662	6.532226	0.003963	1.89E-04	0.00693
Annotation Cluster 6	Enrichment Score: 4.038471186113166											
KEGG_PATHWAY	mmu04610:Complement and coagulation cascades	33	1.125896	3.03E-08	MBL2, C7,	1214	76	7720	2.761207	8.79E-06	1.46E-06	4.03E-05
Annotation Cluster 7	Enrichment Score: 3.8057916038977835											
GOTERM_CC_DIRECT	GO:0022624~proteasome accessory complex	15	0.511771	3.87E-10	PSMD14, F	2709	17	19662	6.404143	3.45E-07	2.66E-08	6.03E-07
GOTERM_CC_DIRECT	GO:0031595~nuclear proteasome complex	8	0.272944	6.57E-06	PSMC6, PS	2709	8	19662	7.258029	0.005845	2.66E-04	0.010232
GOTERM_CC_DIRECT	GO:0008540~proteasome regulatory particle, base subcomplex	10	0.34118	7.44E-06	PSMC6, PS	2709	13	19662	5.583099	0.006619	2.89E-04	0.01159
Annotation Cluster 9	Enrichment Score: 3.555823482528236											
GOTERM_CC_DIRECT	GO:0005913~cell-cell adherens junction	71	2.422381	3.01E-05	RTN4, PVF	2709	316	19662	1.63076	0.026516	9.95E-04	0.046897
Annotation Cluster 10	Enrichment Score: 3.528918602785428											
Category	Term	Count	%	PValue	Genes	List Total	Pop Hits	Pop Total	Fold Enric	Bonferron	Benjamini	FDR
KEGG_PATHWAY	mmu00830:Retinol metabolism	33	1.125896	2.16E-06	CYP2C44, (	1214	89	7720	2.357885	6.26E-04	6.96E-05	0.00287
KEGG_PATHWAY	mmu00140:Steroid hormone biosynthesis	32	1.091778	3.86E-06	HSD3B2, C	1214	87	7720	2.338995	0.00112	1.12E-04	0.005137
Annotation Cluster 11	Enrichment Score: 3.271383522695853											
GOTERM_MF_DIRECT	GO:0016740~transferase activity	293	9.996588	7.95E-10	HGSNAT, S	2498	1472	17446	1.390155	1.62E-06	3.24E-07	1.37E-06
Annotation Cluster 12	Enrichment Score: 2.9132565804072748											
GOTERM_BP_DIRECT	GO:0006637~acyl-CoA metabolic process	18	0.614125	1.33E-07	ACADSB, A	2568	31	18082	4.088484	7.80E-04	9.76E-05	2.57E-04
Annotation Cluster 14	Enrichment Score: 2.390627404278099											
KEGG_PATHWAY	mmu00053:Ascorbate and aldarate metabolism	15	0.511771	1.38E-05	UGT2B1, A	1214	27	7720	3.532857	0.003997	3.08E-04	0.018359
KEGG_PATHWAY	mmu00040:Pentose and glucuronate interconversions	17	0.580007	4.00E-05	SORD, GU	1214	36	7720	3.002929	0.011524	8.28E-04	0.053121
Annotation Cluster 17	Enrichment Score: 2.000093327948195											
REACTOME_PATHWAY	R-MMU-193368:R-MMU-193368	15	0.511771	1.80E-05	ACOX2, AE	1278	26	7575	3.419556	0.015496	5.38E-04	0.02791
Annotation Cluster 23	Enrichment Score: 1.6673154033674744											
GOTERM_CC_DIRECT	GO:0034364~high-density lipoprotein particle	12	0.409417	3.08E-05	APOA4, A	2709	21	19662	4.147445	0.027063	9.79E-04	0.047877

Supplemental Table 3.2. Pathways from genes that had a significant (q<0.001) dose and strain interaction effect.

Annotatio	Enrichment Score: 6.677482124251916											
Category	Term	Count	%	PValue	Genes	List Total	Pop Hits	Pop Total	Fold Enric	Bonferror	Benjamini	FDR
GOTERM_	GO:0005524~ATP binding	220	10.51625	4.17E-08	XRCC3, AD	1798	1507	17446	1.416497	6.53E-05	1.31E-05	6.97E-05
GOTERM_	GO:0006468~protein phosphorylation	102	4.875717	6.93E-08	RNASEL, T	1873	576	18082	1.709568	3.47E-04	4.96E-05	1.32E-04
GOTERM_	GO:0016301~kinase activity	114	5.449331	1.04E-07	TBK1, FAM	1798	674	17446	1.641161	1.62E-04	2.32E-05	1.73E-04
GOTERM_	GO:0004674~protein serine/threonine kinase activity	80	3.824092	1.86E-07	CDK18, TB	1798	428	17446	1.813645	2.90E-04	3.63E-05	3.10E-04
GOTERM_	GO:0016310~phosphorylation	104	4.971319	4.06E-07	TBK1, FAM	1873	612	18082	1.640554	0.002034	2.26E-04	7.73E-04
GOTERM_	GO:0004672~protein kinase activity	92	4.397706	7.01E-07	FASTKD3,	1798	531	17446	1.681123	0.001097	9.98E-05	0.001172
GOTERM_	GO:0016740~transferase activity	208	9.942639	1.14E-06	HGSNAT, (	1798	1472	17446	1.371077	0.001783	1.49E-04	0.001904
Annotatio	Enrichment Score: 5.987965957083108											
GOTERM_	GO:0005913~cell-cell adherens junction	64	3.059273	4.03E-08	CAST, VAF	1938	316	19662	2.054787	3.40E-05	2.83E-06	6.23E-05
GOTERM_	GO:0098641~cadherin binding involved in cell-cell adhesion	60	2.868069	5.71E-08	CAST, VAF	1798	279	17446	2.086667	8.94E-05	1.49E-05	9.54E-05
Annotatio	Enrichment Score: 4.467273080066286											
GOTERM_	GO:0006351~transcription, DNA-templated	270	12.90631	9.62E-09	MEF2A, AS	1873	1885	18082	1.382805	4.82E-05	9.64E-06	1.83E-05
Annotatio	Enrichment Score: 4.1088072504049125											
GOTERM_	GO:0006397~mRNA processing	62	2.963671	2.18E-06	RNASEL, R	1873	322	18082	1.858851	0.010881	9.94E-04	0.004156

Supplemental Table 3.3. Pathways from genes that were significantly (q<0.001) correlated with TCE dose that were also strain-dependent.

Annotation Clust	Enrichment Score: 7.531969476693256											
Category	Term	Count	%	PValue	Genes	List Total	Pop Hits	Pop Total	Fold Enric	Bonferror	Benjamini	FDR
KEGG_PATHWAY	mmu03050:Proteasome	29	0.983384	1.45E-12	PSMB10, P	1206	45	7720	4.125299	4.18E-10	2.09E-10	1.93E-09
GOTERM_CC_DIR	GO:0000502~proteasome complex	34	1.152933	3.36E-12	PSMB10, P	2750	66	19662	3.68324	3.06E-09	3.82E-10	5.24E-09
REACTOME_PATH	R-MMU-1236978:R-MMU-1236978	30	1.017294	4.75E-11	PSMB10, P	1275	50	7575	3.564706	4.14E-08	4.14E-08	7.38E-08
REACTOME_PATH	R-MMU-450408:R-MMU-450408	33	1.119023	5.37E-11	PSMB10, P	1275	59	7575	3.323031	4.68E-08	2.34E-08	8.34E-08
REACTOME_PATH	R-MMU-350562:R-MMU-350562	31	1.051204	9.69E-11	PSMB10, P	1275	54	7575	3.410675	8.44E-08	2.81E-08	1.50E-07
REACTOME_PATH	R-MMU-187577:R-MMU-187577	34	1.152933	1.62E-10	PSMB10, P	1275	64	7575	3.15625	1.41E-07	3.52E-08	2.51E-07
REACTOME_PATH	R-MMU-195253:R-MMU-195253	36	1.220753	2.28E-10	PSMB10, P	1275	71	7575	3.012428	1.98E-07	3.97E-08	3.53E-07
REACTOME_PATH	R-MMU-5358346:R-MMU-5358346	33	1.119023	2.97E-10	PSMB10, D	1275	62	7575	3.162239	2.59E-07	4.32E-08	4.61E-07
GOTERM_CC_DIR	GO:0022624~proteasome accessory complex	15	0.508647	4.75E-10	PSMD14, P	2750	17	19662	6.308663	4.32E-07	3.32E-08	7.41E-07
REACTOME_PATH	R-MMU-1169091:R-MMU-1169091	35	1.186843	6.84E-10	PSMB10, N	1275	70	7575	2.970588	5.96E-07	8.51E-08	1.06E-06
REACTOME_PATH	R-MMU-69481:R-MMU-69481	30	1.017294	1.06E-09	PSMB10, P	1275	55	7575	3.240642	9.21E-07	1.15E-07	1.64E-06
REACTOME_PATH	R-MMU-69017:R-MMU-69017	30	1.017294	1.06E-09	PSMB10, P	1275	55	7575	3.240642	9.21E-07	1.15E-07	1.64E-06
REACTOME_PATH	R-MMU-174113:R-MMU-174113	31	1.051204	1.72E-09	PSMB10, P	1275	59	7575	3.121635	1.50E-06	1.66E-07	2.67E-06
REACTOME_PATH	R-MMU-4641257:R-MMU-4641257	31	1.051204	1.72E-09	PSMB10, P	1275	59	7575	3.121635	1.50E-06	1.66E-07	2.67E-06
REACTOME_PATH	R-MMU-69229:R-MMU-69229	30	1.017294	1.84E-09	PSMB10, P	1275	56	7575	3.182773	1.61E-06	1.61E-07	2.86E-06
REACTOME_PATH	R-MMU-349425:R-MMU-349425	30	1.017294	1.84E-09	PSMB10, P	1275	56	7575	3.182773	1.61E-06	1.61E-07	2.86E-06
REACTOME_PATH	R-MMU-202424:R-MMU-202424	41	1.390302	2.10E-09	PSMB10, P	1275	93	7575	2.619228	1.83E-06	1.66E-07	3.26E-06
REACTOME_PATH	R-MMU-5676590:R-MMU-5676590	32	1.085114	2.60E-09	PSMB10, P	1275	63	7575	3.01774	2.26E-06	1.89E-07	4.04E-06
REACTOME_PATH	R-MMU-5607761:R-MMU-5607761	32	1.085114	2.60E-09	PSMB10, P	1275	63	7575	3.01774	2.26E-06	1.89E-07	4.04E-06
REACTOME_PATH	R-MMU-69601:R-MMU-69601	30	1.017294	3.16E-09	PSMB10, P	1275	57	7575	3.126935	2.75E-06	2.12E-07	4.90E-06
REACTOME_PATH	R-MMU-2871837:R-MMU-2871837	38	1.288572	3.81E-09	PSMB10, P	1275	84	7575	2.687675	3.32E-06	2.37E-07	5.91E-06
REACTOME_PATH	R-MMU-5610780:R-MMU-5610780	31	1.051204	4.78E-09	PSMB10, P	1275	61	7575	3.019286	4.16E-06	2.78E-07	7.42E-06
REACTOME_PATH	R-MMU-5610785:R-MMU-5610785	31	1.051204	7.79E-09	PSMB10, P	1275	62	7575	2.970588	6.78E-06	4.24E-07	1.21E-05
REACTOME_PATH	R-MMU-5607764:R-MMU-5607764	37	1.254663	1.02E-08	PSMB10, P	1275	83	7575	2.648476	8.92E-06	5.25E-07	1.59E-05
REACTOME_PATH	R-MMU-4608870:R-MMU-4608870	31	1.051204	1.25E-08	PSMB10, P	1275	63	7575	2.923436	1.09E-05	6.05E-07	1.94E-05
REACTOME_PATH	R-MMU-174084:R-MMU-174084	32	1.085114	1.69E-08	PSMB10, A	1275	67	7575	2.837577	1.47E-05	7.75E-07	2.63E-05
REACTOME_PATH	R-MMU-4641258:R-MMU-4641258	30	1.017294	2.29E-08	PSMB10, P	1275	61	7575	2.92189	2.00E-05	9.99E-07	3.56E-05
REACTOME_PATH	R-MMU-5668541:R-MMU-5668541	33	1.119023	3.32E-08	PSMB10, T	1275	72	7575	2.723039	2.89E-05	1.38E-06	5.15E-05
REACTOME_PATH	R-MMU-68827:R-MMU-68827	30	1.017294	5.65E-08	PSMB10, P	1275	63	7575	2.829132	4.92E-05	2.24E-06	8.77E-05
REACTOME_PATH	R-MMU-5687128:R-MMU-5687128	34	1.152933	8.75E-08	PSMB10, C	1275	78	7575	2.589744	7.62E-05	3.31E-06	1.36E-04
REACTOME_PATH	R-MMU-174154:R-MMU-174154	32	1.085114	9.00E-08	PSMB10, A	1275	71	7575	2.677713	7.84E-05	3.27E-06	1.40E-04
REACTOME_PATH	R-MMU-5658442:R-MMU-5658442	31	1.051204	3.49E-07	PSMB10, P	1275	71	7575	2.594035	3.04E-04	1.22E-05	5.41E-04
REACTOME_PATH	R-MMU-174184:R-MMU-174184	32	1.085114	5.73E-07	PSMB10, A	1275	76	7575	2.501548	4.99E-04	1.92E-05	8.89E-04
REACTOME_PATH	R-MMU-174178:R-MMU-174178	32	1.085114	5.73E-07	PSMB10, A	1275	76	7575	2.501548	4.99E-04	1.92E-05	8.89E-04
REACTOME_PATH	R-MMU-382556:R-MMU-382556	34	1.152933	9.61E-07	PSMB10, P	1275	85	7575	2.376471	8.36E-04	3.10E-05	0.001491

REACTOME_PATI	R-MMU-68949:R-MMU-68949	31	1.051204	1.43E-06	PSMB10, P	1275	75	7575	2.455686	0.001241	4.44E-05	0.002213
GOTERM_CC_DIR	GO:0005839~proteasome core complex	13	0.440827	2.30E-06	PSMB10, P	2750	20	19662	4.647382	0.002088	1.16E-04	0.003586
GOTERM_CC_DIR	GO:0008540~proteasome regulatory particle, base subcomplex	10	0.339098	8.45E-06	PSMC6, PS	2750	13	19662	5.49986	0.007662	3.20E-04	0.013192
Annotation Clust	Enrichment Score: 5.998152895410505											
GOTERM_CC_DIR	GO:0022624~proteasome accessory complex	15	0.508647	4.75E-10	PSMD14, P	2750	17	19662	6.308663	4.32E-07	3.32E-08	7.41E-07
GOTERM_CC_DIR	GO:0005838~proteasome regulatory particle	9	0.305188	5.00E-06	PSMC5, PS	2750	10	19662	6.434836	0.004539	2.27E-04	0.007804
Annotation Clust	Enrichment Score: 5.212192585189086											
KEGG_PATHWAY	mmu04146:Peroxisome	32	1.085114	1.05E-06	HACL1, EC	1206	83	7720	2.467981	3.01E-04	6.02E-05	0.001388
GOTERM_CC_DIR	GO:0005778~peroxisomal membrane	21	0.712106	1.48E-05	MAP2K2, I	2750	53	19662	2.832947	0.013348	5.17E-04	0.023047
GOTERM_CC_DIR	GO:0005777~peroxisome	38	1.288572	1.50E-05	HACL1, EC	2750	131	19662	2.073993	0.013522	5.04E-04	0.02335
Annotation Clust	Enrichment Score: 4.565566805920566											
KEGG_PATHWAY	mmu04610:Complement and coagulation cascades	35	1.186843	1.38E-09	C7, MBL2,	1206	76	7720	2.947979	3.98E-07	1.33E-07	1.84E-06
Annotation Clust	Enrichment Score: 4.171495225730368											
KEGG_PATHWAY	mmu00140:Steroid hormone biosynthesis	33	1.119023	1.04E-06	HSD3B2, C	1206	87	7720	2.428089	3.01E-04	7.52E-05	0.001386
KEGG_PATHWAY	mmu00830:Retinol metabolism	33	1.119023	1.86E-06	CYP2C44, (	1206	89	7720	2.373526	5.36E-04	8.94E-05	0.002474
Annotation Clust	Enrichment Score: 3.9692013371459587											
GOTERM_CC_DIR	GO:0005913~cell-cell adherens junction	74	2.509325	7.54E-06	RTN4, PVR	2750	316	19662	1.674325	0.006837	2.98E-04	0.011768
Annotation Clust	Enrichment Score: 3.7938853163665858											
GOTERM_CC_DIR	GO:0022624~proteasome accessory complex	15	0.508647	4.75E-10	PSMD14, P	2750	17	19662	6.308663	4.32E-07	3.32E-08	7.41E-07
GOTERM_CC_DIR	GO:0031595~nuclear proteasome complex	8	0.271278	7.29E-06	PSMC6, PS	2750	8	19662	7.149818	0.006609	3.01E-04	0.011374
GOTERM_CC_DIR	GO:0008540~proteasome regulatory particle, base subcomplex	10	0.339098	8.45E-06	PSMC6, PS	2750	13	19662	5.49986	0.007662	3.20E-04	0.013192
Annotation Clust	Enrichment Score: 3.5015779212317044											
GOTERM_MF_DIR	GO:0016740~transferase activity	300	10.17294	2.69E-10	HGSNAT, S	2545	1472	17446	1.397081	5.46E-07	1.09E-07	4.63E-07
Annotation Clust	Enrichment Score: 2.3984888974712875											
KEGG_PATHWAY	mmu00053:Ascorbate and aldarate metabolism	15	0.508647	1.28E-05	UGT2B1, A	1206	27	7720	3.556293	0.00367	4.08E-04	0.016953

Supplemental Table 3.4. Pathways from genes that were significantly (q<0.001) correlated with strain effect.

Annotation Cluster 1	Enrichment Score: 3.634969842314665											
Category	Term	Count	%	PValue	Genes	List Total	Pop Hits	Pop Total	Fold Enric	Bonferron	Benjamini	FDR
GOTERM_CC_DIRECT	GO:0005840~ribosome	62	2.122561	8.97E-12	MRPL40, M	2614	188	19662	2.480595	8.40E-09	1.68E-09	1.40E-08
KEGG_PATHWAY	mmu03010:Ribosome	48	1.643273	1.56E-08	RPL19, MR	1099	145	7720	2.325374	4.47E-06	4.47E-06	2.07E-05
GOTERM_CC_DIRECT	GO:0030529~intracellular ribonucleoprotein complex	77	2.636084	2.25E-07	MRPL40, R	2614	320	19662	1.809934	2.10E-04	2.34E-05	3.52E-04
Annotation Cluster 2	Enrichment Score: 3.5476067509915032											
Category	Term	Count	%	PValue	Genes	List Total	Pop Hits	Pop Total	Fold Enric	Bonferron	Benjamini	FDR
GOTERM_MF_DIRECT	GO:0005085~guanyl-nucleotide exchange factor activity	48	1.643273	3.35E-08	FGD2, ALS	2330	156	17446	2.303863	6.10E-05	3.05E-05	5.70E-05

Supplemental Table 3.5. Pathways from genes that were significantly (q<0.001) correlated with strain that were also dose-dependent

Annotatio	Enrichment Score: 8.28658833569832											
Category	Term	Count	%	PValue	Genes	List Total	Pop Hits	Pop Total	Fold Enric	Bonferron	Benjamini	FDR
GOTERM_	GO:00167(	41	1.400752	2.11E-11	CYP2U1, C	2335	99	17446	3.094266	3.95E-08	1.32E-08	3.60E-08
REACTOM	R-MMU-2	26	0.888282	3.11E-11	CYP2D10,	1206	40	7575	4.082711	2.64E-08	2.64E-08	4.82E-08
GOTERM_	GO:00083	26	0.888282	9.61E-11	CYP2D10,	2335	47	17446	4.133181	1.80E-07	4.50E-08	1.64E-07
GOTERM_	GO:00083	27	0.922446	7.11E-10	CYP2U1, C	2335	54	17446	3.73576	1.33E-06	2.66E-07	1.21E-06
KEGG_PA	mmu0083	38	1.298258	1.17E-09	CYP3A25,	1164	89	7720	2.83177	3.32E-07	6.65E-08	1.55E-06
GOTERM_	GO:00200	55	1.879057	1.36E-09	CYP2D10,	2335	175	17446	2.348192	2.56E-06	4.26E-07	2.33E-06
GOTERM_	GO:00044	40	1.366587	1.88E-09	CYP2U1, C	2335	108	17446	2.76723	3.52E-06	5.03E-07	3.20E-06
KEGG_PA	mmu0014	37	1.264093	2.28E-09	CYP2D10,	1164	87	7720	2.820634	6.50E-07	1.08E-07	3.03E-06
GOTERM_	GO:00055(	61	2.084045	6.92E-09	CYP2D10,	2335	212	17446	2.149824	1.30E-05	1.30E-06	1.18E-05
GOTERM_	GO:00310	35	1.195764	1.68E-08	CYP2U1, C	2616	94	19662	2.798531	1.49E-05	1.24E-06	2.61E-05
GOTERM_	GO:00703	20	0.683293	2.07E-08	CYP2U1, C	2335	36	17446	4.150845	3.87E-05	3.52E-06	3.53E-05
GOTERM_	GO:00193	18	0.614964	2.96E-08	CYP2G1, C	2428	30	18082	4.468369	1.61E-04	3.21E-05	5.69E-05
GOTERM_	GO:00167	21	0.717458	8.33E-08	CYP2G1, C	2335	42	17446	3.73576	1.56E-04	1.30E-05	1.42E-04
Annotatio	Enrichment Score: 7.627679948810967											
KEGG_PA	mmu0301	57	1.947386	2.35E-12	RPL19, RPI	1164	145	7720	2.607181	6.68E-10	2.23E-10	3.11E-09
REACTOM	R-MMU-1	42	1.434916	3.86E-11	RPL19, RPI	1206	91	7575	2.898967	3.27E-08	1.63E-08	5.96E-08
REACTOM	R-MMU-1	47	1.60574	4.02E-11	RPL19, RPI	1206	109	7575	2.708362	3.40E-08	1.13E-08	6.21E-08
REACTOM	R-MMU-7	44	1.503246	5.64E-11	RPL19, RPI	1206	99	7575	2.791598	4.78E-08	1.19E-08	8.72E-08
REACTOM	R-MMU-7	47	1.60574	5.86E-11	RPL19, RPI	1206	110	7575	2.68374	4.97E-08	9.93E-09	9.07E-08
REACTOM	R-MMU-9	42	1.434916	5.91E-11	RPL19, RPI	1206	92	7575	2.867456	5.00E-08	8.34E-09	9.14E-08
GOTERM_	GO:00058	59	2.015716	2.80E-10	RPL19, MR	2616	188	19662	2.358762	2.48E-07	3.10E-08	4.35E-07
REACTOM	R-MMU-9	45	1.53741	2.35E-09	RPL19, RPI	1206	113	7575	2.501321	1.99E-06	2.84E-07	3.63E-06
GOTERM_	GO:00226	23	0.785787	3.52E-07	RPSA, RPS	2616	53	19662	3.261684	3.12E-04	2.08E-05	5.47E-04
GOTERM_	GO:00037	66	2.254868	5.27E-07	RPL19, RPI	2335	264	17446	1.86788	9.86E-04	6.58E-05	8.98E-04
GOTERM_	GO:00159	16	0.546635	8.51E-07	RPSA, MRI	2616	29	19662	4.146789	7.54E-04	4.72E-05	0.001324
REACTOM	R-MMU-7	23	0.785787	9.46E-07	RPSA, EIF	1206	48	7575	3.009691	8.01E-04	8.01E-05	0.001463
REACTOM	R-MMU-7	24	0.819952	2.60E-06	RPSA, EIF	1206	54	7575	2.791598	0.002203	1.84E-04	0.004027
GOTERM_	GO:00226	30	1.02494	3.72E-06	RPL19, RPI	2616	91	19662	2.47782	0.00329	1.83E-04	0.00578
REACTOM	R-MMU-7	24	0.819952	3.81E-06	RPSA, EIF	1206	55	7575	2.740841	0.003222	2.48E-04	0.005891
Annotatio	Enrichment Score: 7.358036938571448											
KEGG_PA	mmu0520	45	1.53741	7.83E-14	CYP3A25,	1164	92	7720	3.244061	2.23E-11	2.23E-11	1.04E-10
GOTERM_	GO:00043	20	0.683293	2.94E-09	GSTA2, GS	2335	33	17446	4.528194	5.51E-06	6.89E-07	5.02E-06
KEGG_PA	mmu0098	30	1.02494	1.64E-08	GSTM6, GS	1164	66	7720	3.014683	4.67E-06	5.84E-07	2.17E-05
KEGG_PA	mmu0098	29	0.990776	3.25E-08	GSTM6, GS	1164	64	7720	3.005262	9.27E-06	1.03E-06	4.31E-05
KEGG_PA	mmu0048	26	0.888282	7.06E-08	GSTA2, GS	1164	55	7720	3.13527	2.01E-05	1.83E-06	9.36E-05
REACTOM	R-MMU-1	13	0.444141	9.01E-06	MGST3, GS	1206	20	7575	4.082711	0.007601	5.45E-04	0.013931
Annotatio	Enrichment Score: 4.691431257499761											
KEGG_PA	mmu0051	13	0.444141	9.95E-07	AGA, GBA	1164	18	7720	4.789996	2.83E-04	2.36E-05	0.001319
Annotatio	Enrichment Score: 3.014257244766574											
KEGG_PA	mmu0451	31	1.059105	6.44E-06	TNC, NPN	1164	88	7720	2.336379	0.001834	1.15E-04	0.008537
Annotatio	Enrichment Score: 2.500606978553935											
GOTERM_	GO:00360	18	0.614964	1.02E-07	MUP5, MU	2335	32	17446	4.20273	1.91E-04	1.47E-05	1.74E-04

CHAPTER 4: EVALUATION OF INTER-INDIVIDUAL DIFFERENCES IN TCE METABOLISM AND TOXICITY IN A 90-DAY ORAL TOXICITY TESTING USING GENETICALLY- DIVERSE MOUSE POPULATIONS

I. Introduction

Toxicity testing of chemicals is often conducted on chemicals that may pose health risk to humans. Since the establishment of the National Toxicology Program (NTP), several standardized study designs and protocols have been established to assess the toxicological potential of chemicals. Among the different study designs to assess risk, the 90-day or pre-chronic toxicity studies are critical in making regulatory decisions and conducting further animal studies. Pre-chronic studies aid in identifying hazard, target organs, similarities and differences in responses between species and sexes, slope of dose-response relationships, and doses for chronic studies (Chhabra, Huff, Schwetz, & Selkirk, 1990). Historically, such studies are often conducted in rodent models with fixed genetic background. Toxicology and carcinogenesis studies contracted by NTP utilize B6C3F1 as the preferred strain which is derived by inter-crossing C57BL/6N with C3H/HEN^{mtv-} strains. Selection of such a genetic background for safety testing was based on the notion that the use of F1 hybrids would offer better reproducibility compared to outbred stocks and minimize loss of genetic variability as seen in inbred lines (Meek, 1987). Consequently, due to the homogeneous background traditional toxicity models employing B6C3F1 poorly capture diversity in toxic responses that arise due to genetic differences as is observed in humans.

Advances in mouse genetics has led to the development of different population-based rodent models that comprise of a large panel of genetically-diverse lines of mice derived from multi-parental crosses of classical inbred strains of mice (Churchill et al., 2004; Churchill et al., 2012; Threadgill & Churchill, 2012). The rationale for multi-parental breeding strategy is to randomize genetic variations so that all components of systems can be interrogated as allele frequencies for quantitative trait locus (QTL) mapping; these models are also sufficiently large to power analyses of modest interactions (Threadgill & Churchill, 2012). The Collaborative Cross (CC) mice are derived from eight genetically-diverse classical inbred strains of mice (Churchill et al., 2004; Threadgill, Hunter, & Williams, 2002). The CC recombinant intercrosses (RIXs) are F1 hybrids that offer more heterogeneity in comparison to the CC but retain the same level of reproducibility (Graham et al., 2015; Threadgill & Churchill, 2012). The Diversity Outbred mice are F2 crosses derived from CC; due to the random breeding schemes each individual DO mouse is genetically-unique and so reproducibility poses a challenge in the DO population (Bogue et al., 2015; Churchill et al., 2012).

Several reports have shown the utility of population-based rodent resources in biomedical applications with an emphasis on genetic analysis of complex traits (Church et al., 2015; Durrant et al., 2011; Rogala et al., 2014; Smallwood et al., 2014). For example, the CC model has helped reproduce hallmark symptoms of Ebola hemorrhagic fever that are otherwise not observed in existing mouse models (Rasmussen et al., 2014). More recently, studies have also shown the utility of these models in toxicological research on chlorinated solvents and industrial toxicants (Cichocki et al., 2017; French et al., 2015; Venkatratnam et al., 2017). Although the use of these population-based rodent resources are rapidly growing in toxicology, the quantitative extent of variability in toxic responses in these models have not been directly compared to B6C3F1 or between the

different population-based models in any study. The utility of these models derives from identifying genetically susceptible strains based on acute or single exposure studies in a population, ultimately these strains may serve as an alternative to B6C3F1 in carcinogenicity studies. In addition, there is lack of knowledge on whether classical toxicity markers are dependent on genetic background, dose, or an interaction effect between genetic background and treatment. To address these gaps in knowledge we aimed to conduct a toxicity study involving different population-based rodent models and B6C3F1.

Trichloroethylene (TCE) is a ubiquitous environmental toxicant and a known carcinogen in both humans and rodents (Guha et al., 2012). It has been well established that TCE metabolism plays a critical role in cancer and non-cancer toxicity (Lash et al., 2014). Oxidative metabolism of TCE has been shown to be highly driven by dose and genetic background in mice (Venkatratnam et al., 2017). Physiologically-based pharmacokinetic (PBPK) modeling has demonstrated comparable variability in TCE toxicokinetics between humans and classical inbred strains of mice (Chiu et al., 2014a). The objective of this study is to evaluate inter-strain variability in responses within and between CC, DO, CC-RIX, and B6C3F1 populations in a 90-day oral toxicity study with trichloroethylene (TCE) as a case study toxicant. We hypothesized that variability in TCE toxicokinetics and toxicodynamics within and between different populations will be larger than stochastic or intra-strain variability in responses in B6C3F1. This sub-chronic study was designed to follow closely the NTP study design and was conducted by following the Office of Economic Cooperation and Development (OECD) guidelines as closely as possible. Several traditional markers of toxicity and metabolism were examined in each of the mouse populations. We observed that most of these responses within the CC and CC-RIX populations were highly variable in comparison to the B6C3F1, with some strains showing clear susceptibility, suggesting that genetic

background may have a profound effect in dose-response assessments. Collectively, this study provides novel information on the application of population-based rodent models to address challenges in risk assessments pertaining to human genetic variability.

II. Materials and Methods

Animals and treatment. The NTP study design for pre-chronic study consists of testing chemicals in two species at five different doses and a control group. Each treatment group must have 10 animals per sex per species. Due to the inherent genetic structure of different mouse populations we replaced the ’10 animals per treatment’ criterion with 10 reproducible CC or CC-RIXs strains and 10 DO mice; this approach closely reflects that of the NTP sub-chronic study while allowing for the incorporation of population-based rodent models. Adult male mice (8-12 weeks) were selected for this study as previous studies have shown that metabolic capacity is higher in males than females (Lash et al., 2006). 10 CC strains with a known diverse TCE toxicokinetic and toxicodynamic profiles from Venkatratnam et al. 2017 were selected for this study. To evaluate intra-strain or stochastic variability 5 mice per CC strain per dose group were employed in this study. 10 CC-RIXs with one mouse per strain per treatment were arbitarily assigned for this study. CC and CC-RIX mouse populations were acquired in multiple batches from University of North Carolina Systems Genetics Core (Chapel Hill, NC). 60 Non-litter mate DO mice and B6C3F1 mice were purchased from The Jackson Laboratories (Bar Harbor, ME). All animals were housed individually and were allowed to acclimate to the room for at least 7 days prior to beginning experimentation. Prior to the start of the experiment, mice were anesthetized using isoflurane for microchip tagging with MUSSIC Identification system from Avid Identification systems, Inc (Norco, CA). Mice were orally administered with a daily dose of 0, 24, 40, 80, 160 or 240 mg/kg TCE (Sigma Aldrich, St. Louis, MO) in 5% Alkamuls EL-620 vehicle

(Solvay, Deptford, NJ) for a period of 90 weekdays. Due to the large number of mice in this study, animals representing each treatment group and population were split into a series of eight groups for daily administration of TCE or vehicle. Oral gavages were conducted between 8 am and 12 pm each day to minimize circadian effects on TCE metabolism. Mice were weighed each week to normalize dosing by weight and were housed in regular cages in a temperature-controlled (24 °C) room, with a 12/12-h light/dark cycle, and were allowed access to water and regular rodent diet ad libitum. Three days prior to necropsy, mice were fed 5-bromo-2′-deoxyuridine (BrdU) (Sigma Aldrich, St. Louis, MO) in drinking water (0.2 g/L) for evaluation of cell proliferation in different tissues. Mice were necropsied 24 h after last dosing. These studies were conducted under the approval of the Institutional Animal Care and Use Committees (IACUC) at Texas A & M University.

Sample collection and processing. Blood from portal vein was split into two vials – 1.1 mL serum collection tube (Sarstedt, Germany) for serum collection, and 300 uL Microvette collection vial (Sarstedt, Germany) for hematological analysis. Femur bones were clipped from vehicle- and TCE- (240 mg/kg) treated animals and a fresh smear was acquired on a slide for bone marrow histology analysis that was later conducted at the Texas A & M University Veterinary Medical Diagnostic Laboratory (College Station, TX). Remaining bone marrow was centrifuged and stored in vials at -80^{0}C. Complete blood count (CBC) profiles for all animals were acquired using VetScan VS2 (Abaxis, Union City, CA). Liver, kidney, bone marrow, brain, gonadal fat pad, lung, spleen, and tail from all animals were collected and flash frozen. Sections of left-lobe liver, kidney, and duodenum were placed in cassettes and formalin fixed overnight. Formalin was decanted and cassettes were rinsed in tap water for a period of 5 mins. The cassettes were then placed in a

solution of 70% ethanol and stored at 4^0 C for preparation of paraffin blocks at the Veterinary Integrative Biosciences Histology Lab (College Station, TX).

Kidney Injury Marker-1 (KIM-1) assay. Mouse TIM-1/KIM-1/HAVCR Quantikine ELISA Kit was purchased from R & D systems (Minneapolis, MN). In brief, 10 mg of kidney tissue was dissolved in 1mL of calibrator diluent RD5-26 buffer (provided by the manufacturer). Tissues were homogenized in 2 mL tubes with stainless steel beads for 30 seconds using Bead Ruptor 24 Elite (Omni International, Kennesaw, GA) and centrifuged at 10,000 rpm for 5 mins. The supernatant was used for analysis. The remaining steps in the analysis were conducted by following the manufacturer's protocol.

Trichloroacetic acid (TCA) measurements in tissues. Analyses were performed by a modification of US EPA method 552.2 (Domino et al., 2003) as detailed in Venkatratnam et al. 2017.

Statistics. Graph Pad Prism (La Jolla, CA) was used to perform statistical tests. R (v.3.1.2) was used to data plots (*ggplot2*) and conducting statistical analyses. For all tests, a $p < 0.05$ was set as statistical significance.

Hepatic and renal pathology examination. Hematoxylin and Eosin (H & E) stained slides were prepared by Veterinary Integrative Biosciences Histology Lab (College Station, TX). Kidneys were sectioned longitudinally and one half was routinely fixed in formalin, paraffin embedded, sectioned, and stained with hematoxylin and eosin (H&E). A portion of the left liver lobe was treated similarly. Light microscopic examination of H&E stained kidney and liver was performed by a board certified veterinary anatomic pathologist (AP). Only vehicle and highest treatment (TCE 240 mg/kg) groups were examined by the pathologist. The pathologist was blinded

to treatment and mouse strain information. The entirety of the kidney and liver sections on each slide were examined and scored for histologic lesions on an ascending numerical semi-quantitative scale as described by the National Toxicology Program where 1 = minimal and 4 = marked with levels 2 and 3 intermediate between these classifications. Diagnostic categories were defined as described in the National Toxicology Program Non-neoplastic Lesion Atlas (Cesta et al., 2014) (Seely and Brix 2014, Maronpot 2014) and the International Harmonization of Nomenclature and Diagnostic Criteria for Lesions in Rats and Mice (INHAND) Project. (Frazier et al., 2012). Although several histological findings were initially identified across all the populations, we removed spontaneous lesions that were inconsistent both within each strain or population and treatment from the analysis. We focused on the three histopathological findings that were more consistent in the liver and kidney across the different populations. These were chronic progressive nephropathy, tubular epithelial vacuolation, and tubular epithelial karyomegaly in the kidney, and centrilobular hypertrophy and karyomegaly, focal inflammation, and apoptosis or necrosis in the liver. A composite histopathology score was calculated for each animal by summing individual scores for each lesion category for each tissue.

III. Results

Oxidative metabolite levels of TCE in tissues. TCA is a major oxidative metabolite of TCE which has been shown to drive hepatocarcinogenesis via activation of peroxisome proliferation-activating receptor alpha (PPARα) in rodents (Lash et al., 2014) . Previous studies in classical inbred lines and CC strains have shown strong positive correlation between liver TCA levels and PPARα-responsive genes suggesting that individuals with higher levels of TCA may be relatively more susceptible to PPARα-driven adverse effects in a population (Venkatratnam et al., 2017; Yoo, Bradford, Kosyk, Uehara, et al., 2015). In this study, a more than 10-fold difference in liver

and kidney TCA levels was observed between strains within the CC and CC-RIX populations administered with TCE (240 mg/kg) (Figure 4.1). We also observed that within the CC and CC-RIX populations inter-strain variability was 10-foldwas greater than intra-strain variability. Interestingly, the extent of variability in liver and kidney TCA levels was comparable between B6C3F1 and DO mice (Figure 1). Although several strains from different populations showed large variability in TCA levels, in comparison to B6C3F1 no statistical significance was observed in hepatic and renal TCA levels (data not shown).

Renal injury in different populations. KIM-1 is a known marker for proximal tubular damage in the kidney (Han, Bailly, Abichandani, Thadhani, & Bonventre, 2002). As classical mouse models do not reflect kidney injury with TCE exposures as seen in humans (Rusyn et al., 2014), we measured KIM-1 levels from different mouse populations to evaluate the role of genetic differences in eliciting proximal tubular injury. KIM-1 levels between vehicle- and TCE-treated (240 mg/kg) mice were found to be less than 5-fold across strains but the differences within the CC and CC-RIX populations were appreciably larger than B6C3F1 and DO mice (Figure 2).

Strain and population differences in basal hematological, hematopoietic, and physiological endpoints.

Information on Complete Blood Count (CBC), bone marrow histopathology, and organ weights is often used to identify hazard and assess toxicodynamic effects of chemicals in a 90-day oral toxicity study. To understand whether genetic background has an influence on these biological endpoints we compared inter-strain differences for all the endpoints. We observed that 15 out of 20 hematological end points demonstrated significant differences across strains (Figure 3). Similarly, 9 out of 17 hematopoietic endpoints and all the other physiological endpoints were

significantly different across strains (Figure 3). Next, we also compared the extent of inter- versus intra-strain variability for all the endpoints (Figure 4). We observed that for majority of these endpoints inter-strain variability is greater than intra-strain variability (Figure 4).

To identify the population model that offers the most diverse responses we compared coefficient of variation (CV) for all the endpoints by population. We observed that CC and CC-RIX populations showed maximum diversity for 37 out of 44 endpoints (Figure 5). The DO population showed largest variability in responses among 5 out of 44 endpoints and also 2 out of 44 endpoints were highly variable in B6C3F1. As expected, B6C3F1 displayed the lowest CVs for more than 50% of the endpoints. Interestingly, the DO mice also showed the lowest CVs for several endpoints. Another key finding was that no significant differences between B6C3F1 and DO mice were observed in their responses for all the physiological endpoints except for one hematopoietic endpoint.

Among the endpoints that demonstrated significant inter-strain variability we directly compared the CVs of organ weights, body weights and organ-to-body weight ratios within each population. Changes in organ weights and organ-to-body weight ratios often provide information on target organ and treatment effects. We found that weights of gonadal fat deposit showed large CV within the CC-RIX population and showed appreciable inter-strain variability (Figures 4 and 6). On the other hand, liver-to-body and kidney-to-body weight ratios demonstrated smaller CV within populations despite significant inter-strain variability (Figure 4 and 6).

A similar trend was observed in hematological endpoints. For example, we observed that relatively higher variability in the percentage of neutrophils among the CC and CC-RIX populations in comparison to B6C3F1 and DO (Figure 7). However, other hematological

parameters such as relative percentage of lymphocytes and basal mean corpuscle volumes showed comparable variability across CC, CC-RIX, and DO populations. Hematopoietic endpoints such as percentages of lymphocytes and myeloid, and myeloid to erythroid ratios showed comparable variability across all mouse populations (Figure 8).

Histopathological assessments of liver and kidney sections. We observed some histopathological lesions showed high background incidences in specific strains and populations. For instance, in the kidney there was a high incidence of tubular epithelial vacuolation exclusively in B6C3F1 mice (Supplemental Table 1). Similarly, appreciable levels of chronic progressive nephropathy was observed across the CC population in comparison to the B6C3F1, CC-RIX population, and DO population (Supplemental Table 1). It is noteworthy that a majority of animals from the CC-RIX and DO populations showed little to no background incidences of any lesions in the kidney (Figure 9). Due to the higher incidence of tubular epithelial vacuolation in B6C3F1 total histopathological scores in kidney were significantly different compared to DO and a few strains within CC population (Figure 9). In the liver, centrilobular hypertrophy and karyomegaly was found across the different populations and B6C3F1 (Supplemental Table 1). This resulted in higher total histopathological scores in liver for all the vehicle treated mice.

Dose-response assessments of hematological and biological markers of toxicity. Dose-response relationships are often conducted using toxicity endpoints to derive point of departures (PoDs) and establish safe levels of exposures. In our study we observed more than 10-fold differences in dose-response derived slopes for several CBC parameters within the CC and CC-RIX populations (Figure 10). Interestingly, we also observed differences in slope direction for many markers suggesting that qualitative differences in such toxicodynamic responses may also exist within the CC and CC-RIX populations.

IV. Discussion

Rodent testing has been the historical approach to assess adverse or pharmacological effects of chemicals that are either natural or anthropogenic. There is a need to develop models in these species that reflect larger variability in phenotypic and toxicodynamic effects to better identify hazard and improve precision in dose-response assessments. It is generally accepted that inbred strains of rodents minimize intra-strain variability in toxicological responses due to their genetic homogeneity. The F1 hybrid rodent models are reproducible and offer relatively larger genetic variability than inbred lines. Outbred stocks offer large variability in their responses due to batch-to-batch differences in their genetic makeup. Despite fundamental differences in their genetic architecture, there is a need to compare inter-strain and intra-strain variability to account for variability in responses driven by genetic background. In this study, we aimed to incorporate different genetically-diverse mouse populations to better evaluate variability in metabolism and toxic effects, improve dose-response assessments, and identify an appropriate population model that may be better suited than B6C3F1 in future toxicity study designs. Despite the highly diverse toxicity endpoints that are routinely assessed in toxicity screenings, this investigation focused on hematological, hematopoietic, hepatic, nephrotic, and physiological endpoints relevant to our case study toxicant TCE.

We observed highly diverse oxidative metabolism of TCE as measured by TCA levels within the CC and CC-RIXs in comparison to the B6C3F1 revealing that toxicokinetic responses maybe strongly driven by genetic background. This trend was also consistent with previous studies with chlorinated solvents using CC model (Cichocki et al., 2017; Venkatratnam et al., 2017). A novel finding in this analysis is that population variability in liver and kidney TCA levels within the DO population was comparable to the B6C3F1. Despite the fact that the number of DO mice in each

treatment group was identical or comparable to the number of strains in the CC-RIX and CC, poor diversity in TCA levels in different tissues was observed in the DO population. One major reason for this is that the DO mice utilized in this study may lack the genetic diversity needed to compare with the CC and CC-RIX populations. To achieve comparable genetic diversity a large number of DO mice may need to be incorporated within each dose group. As previously observed (French et al., 2015), the total number of mice would be much larger than the current requirements of pre-chronic studies. Also, due to batch to batch differences in the genetic diversity represented in DO population it may be challenging to achieve reproducibility and consistency in the toxicity findings.

Inter-strain differences in peripheral blood count values are known to exist suggesting that baseline levels of these parameters may determine degree of variability in hematotoxic effects upon chemical exposures (Kile, Mason-Garrison, & Justice, 2003). Previous studies have associated TCE with hematopoietic alterations, decreased lymphocytic counts, and B-cell activation (Bassig et al., 2016; Lan et al., 2010). We also observed that across the different hematological, hematopoietic, and physiological endpoints, the majority of the phenotypes showed large basal differences within CC and CC-RIX populations compared to B6C3F1 and DO. Further, most of the endpoints demonstrated significant basal inter-strain differences across the populations informing the need to incorporate population approaches to address variability in these responses. Evaluating variability in these responses not only sheds light on toxic markers that are strongly influenced by genetic background but also shows the importance of conducting safety assessments in population-based models instead of single strain models.

Dose response assessments often aim to derive a PoD value which corresponds to a particular dose at which the toxic outcome occurs or is perceived to occur. Uncertainty factors are

often employed to address data gaps in variability in PoDs of toxicokinetic and toxicodynamic responses. Experimental data to address this variability in apical endpoints are often unavailable or unusable due to concerns with study design, route of administration of chemicals, and selection and spacing of doses. A previous study with the CC model showed more than 10-fold inter-strain differences in transcriptional PoDs suggesting that these differences may be consistent or greater in traditional toxicity endpoints from pre-chronic and chronic studies (Venkatratnam et al., 2018). In this study, dose-response assessments of biological and hematological endpoints revealed that qualitative differences in PoDs due to differences in genetic background among individuals in CC and CC-RIX populations. Next, inter-strain differences in the PoDs for some endpoints varied by more than 10-fold, suggesting that default safety factors may be underestimating risk associated with exposures. These experimental data provide strong evidences for incorporation of population-approaches in toxicity screening to better characterize variability in chemical responses and also select potentially susceptible strains for chronic study assessments.

Histopathological examination of tissues is critical in identifying hazard and the target organ of toxicity. It is well known that certain strains are more prone to background lesions than others (Igarashi et al., 2013). There are clear differences in basal incidences of tubular epithelial vacuolation between B6C3F1 and individual strains from the CC and DO populations demonstrating that genetic background can have profound effect on these lesions.

Based on the overall findings from this study we observe that the CC and CC-RIX populations offer large diversity in their responses to TCE exposures compared to B6C3F1 and DO. Despite the outcomes of this study, incorporation of population based rodent models into toxicity testing are not without limitations. First, chronic studies are often expensive due cost of purchasing animals, recruitment of pathologist and staff, and ancillary services. Incorporating

population-approaches to current chronic study designs will be both tedious and expensive. Next, information on survivability of strains from the CC and CC-RIX populations throughout a two-year cancer bioassay is unavailable, limiting its use in chronic cancer bioassays. Third, background incidence of lesions and other health issues associated with selected susceptible strains needs to be made more publicly available as additional data is generated.

In summary, this study shows promising results for incorporating population-based approaches in current toxicity study designs to address critical gaps in dose-response assessments and other aspects of risk assessment. Our study identifies CC and CC-RIX populations as useful population models that offer large diversity in responses that are routinely evaluated in safety assessments. Despite current challenges with these models, proper data curation and commercialization of these models may facilitate their use in the toxicology community in the near future.

V. Figures and Table

Figure 4.1. Box and whisker plots of liver and kidney TCA levels in CC, CC-RIX, and DO populations in comparison to B6C3F1. The horizontal line is the median and the box represents 1st and 3rd quartile ranges. The whiskers are the standard error of mean.

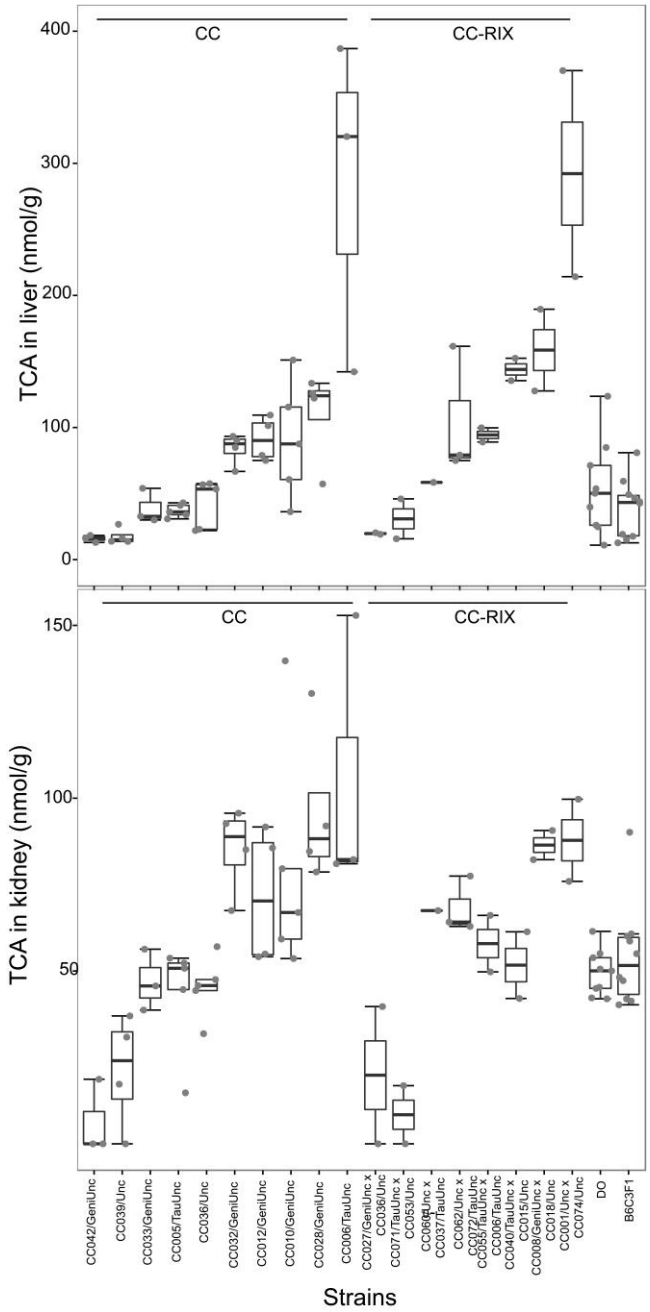

Figure 4.2. Line graph of average KIM-1 levels in vehicle (black circles) - and TCE (240 mg/kg, red circles) -treated CC, CC-RIX, and DO populations in comparison to B6C3F1.

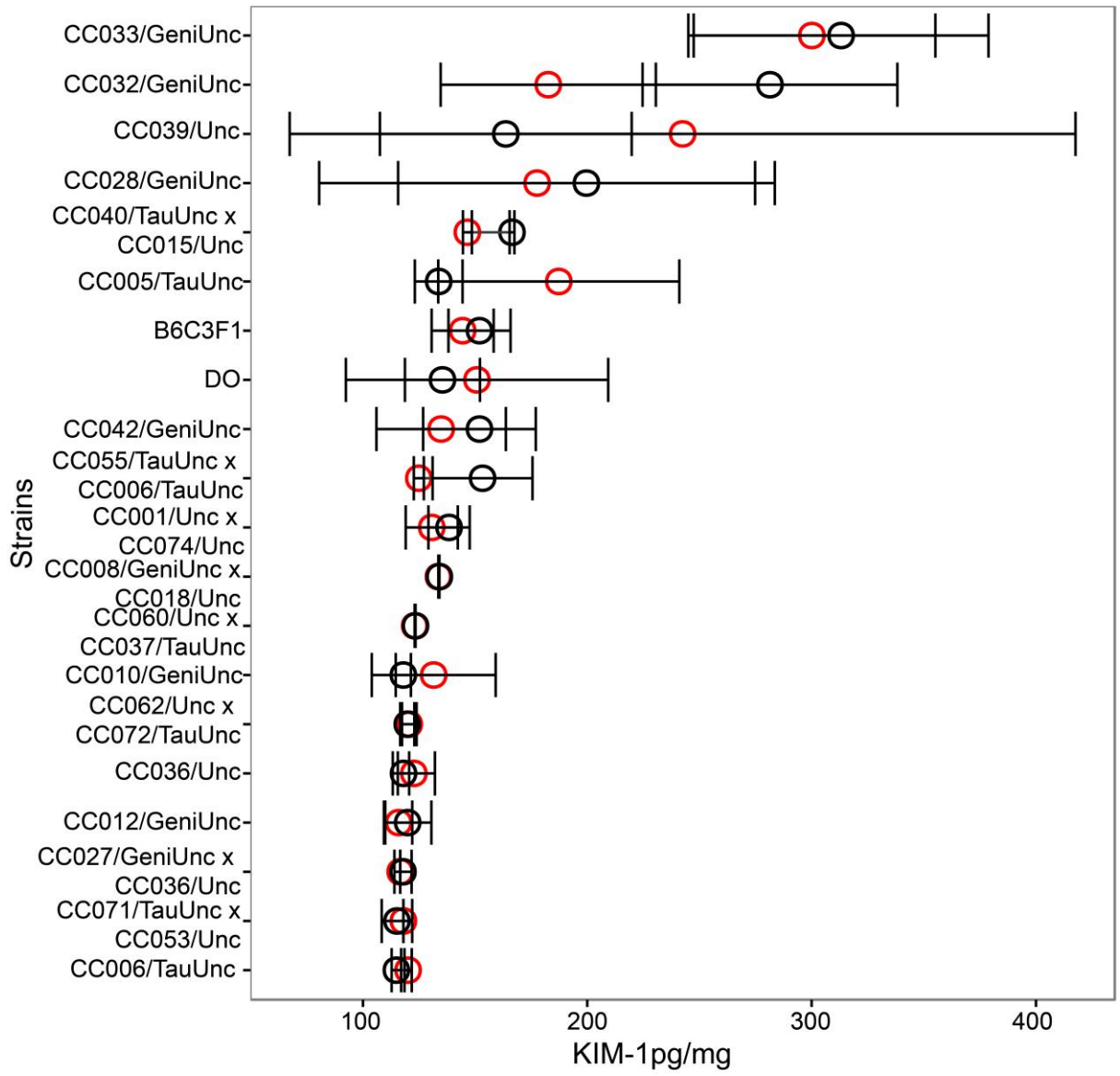

Figure 4.3. Line graph displaying negative $\log_{10}$ p values for inter-strain variability across CC, CC-RIX, and DO populations, and B6C3F1. The dashed line represents the threshold value of p <0.05.

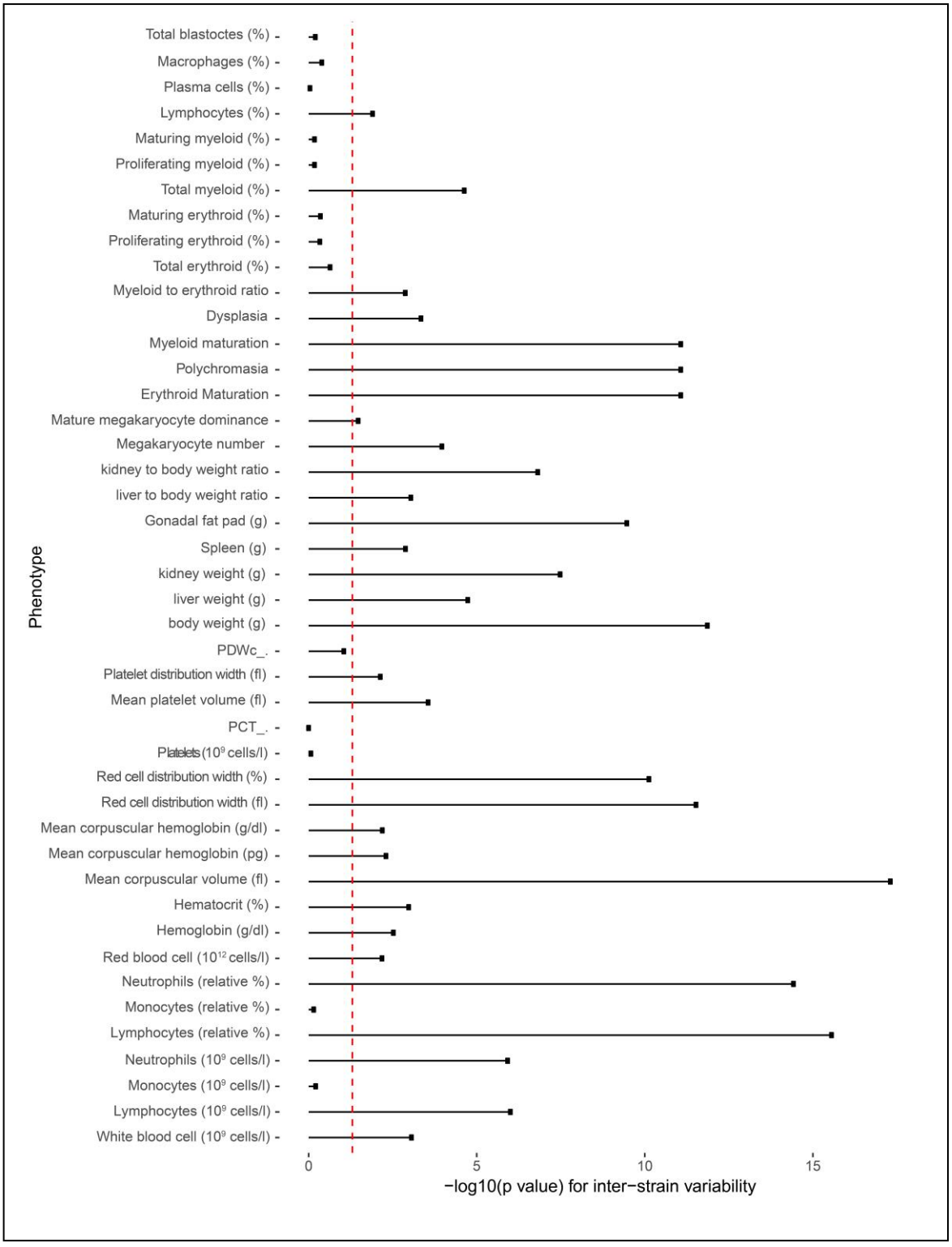

Figure 4.4. Bar graph representing coefficient of variation within CC, CC-RIX, and DO populations compared to B6C3F1 for different endpoints.

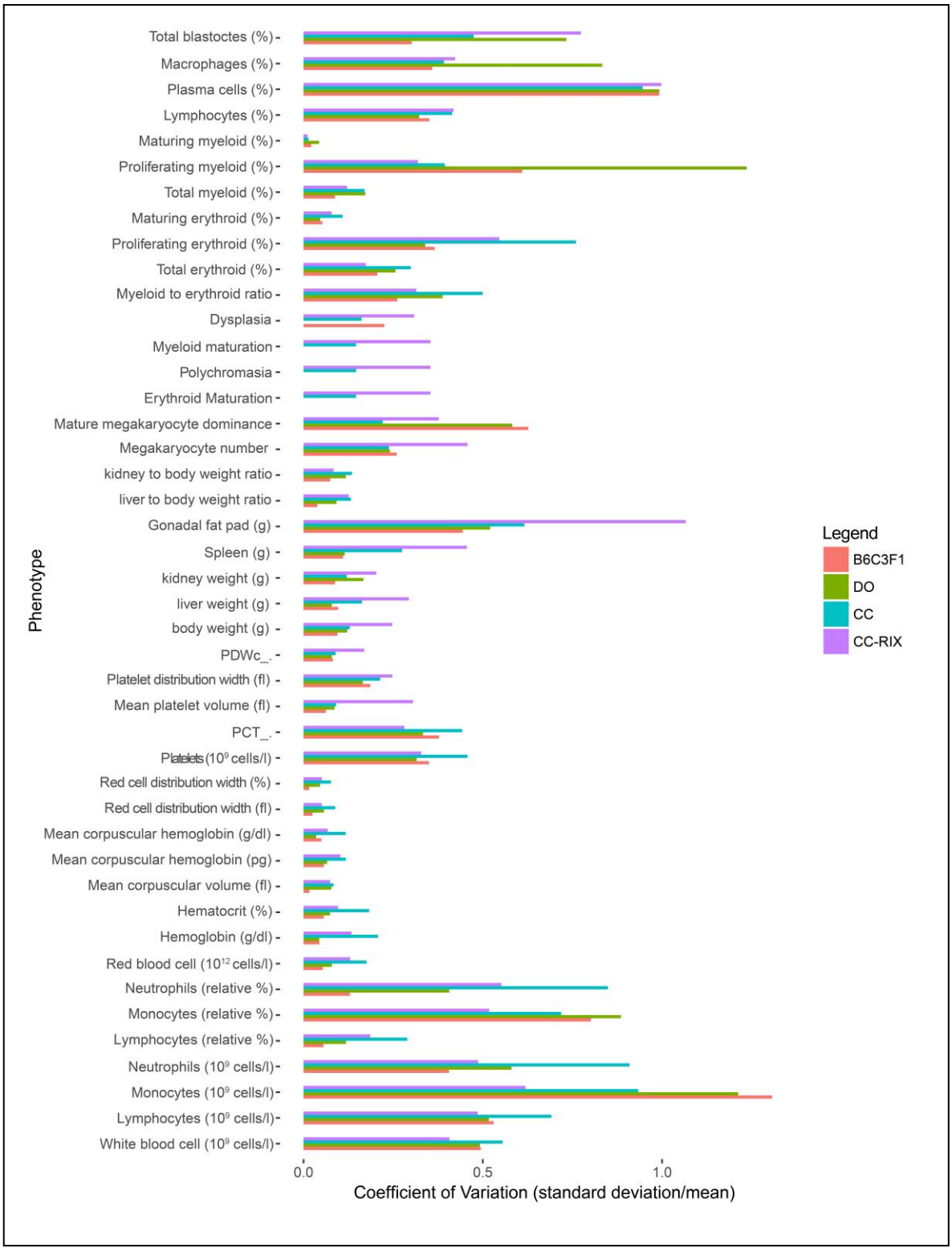

Figure 4.5. Bar graph comparing inter (red bar) - versus intra (blue bar)-strain variability for all the endpoints in all mouse populations and B6C3F1. *, **, and *** represents endpoints with significant (p values ≤ 0.05, ≤ 0.01, and ≤ 0.001) inter-strain differences.

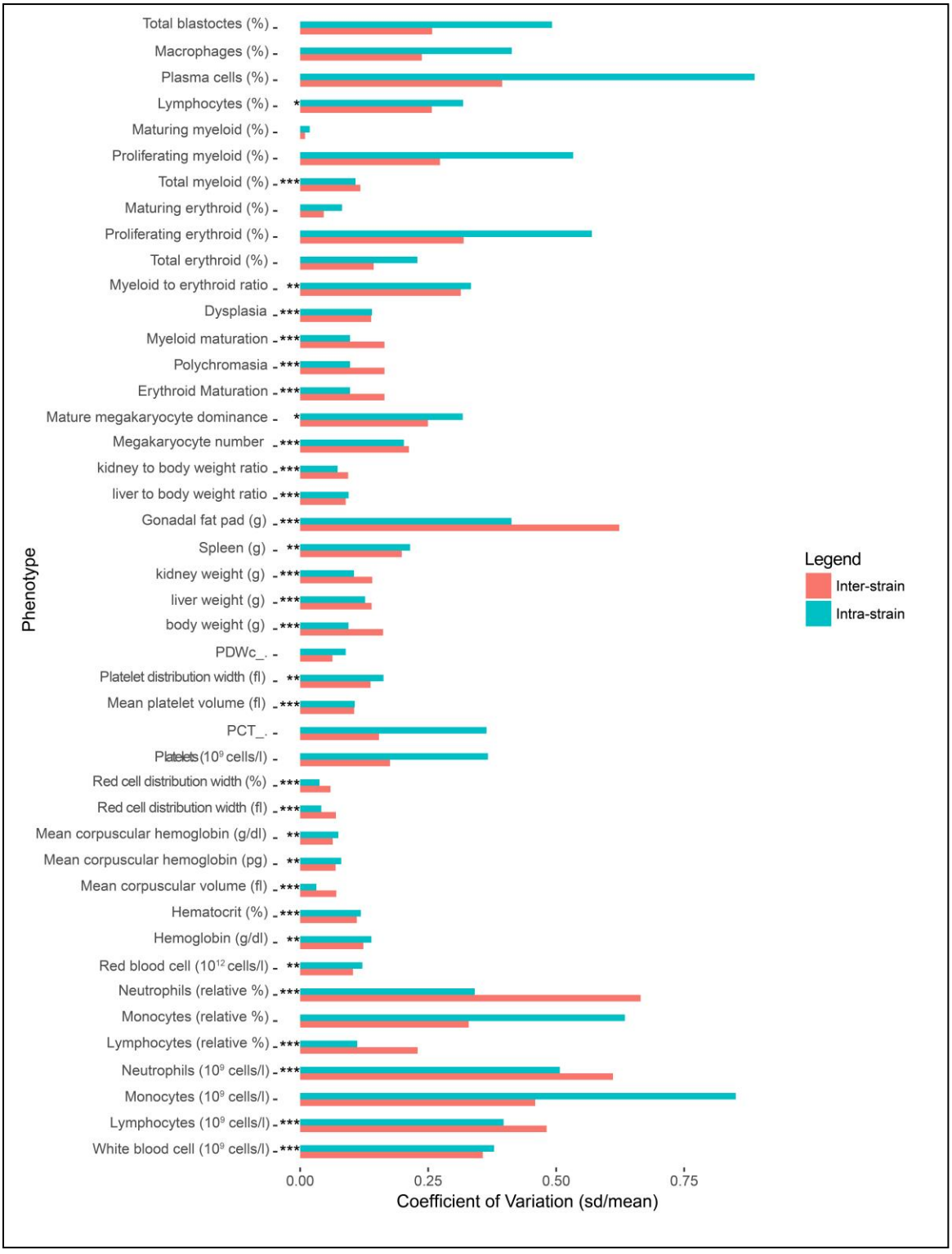

Figure 4.6. Box plots showing coefficient of variation on physiological endpoints with statistically-significant inter-strain differences in CC, CC-RIX, and DO populations, and B6C3F1. The horizontal line is the median and the box represents 1st and 3rd quartile ranges.

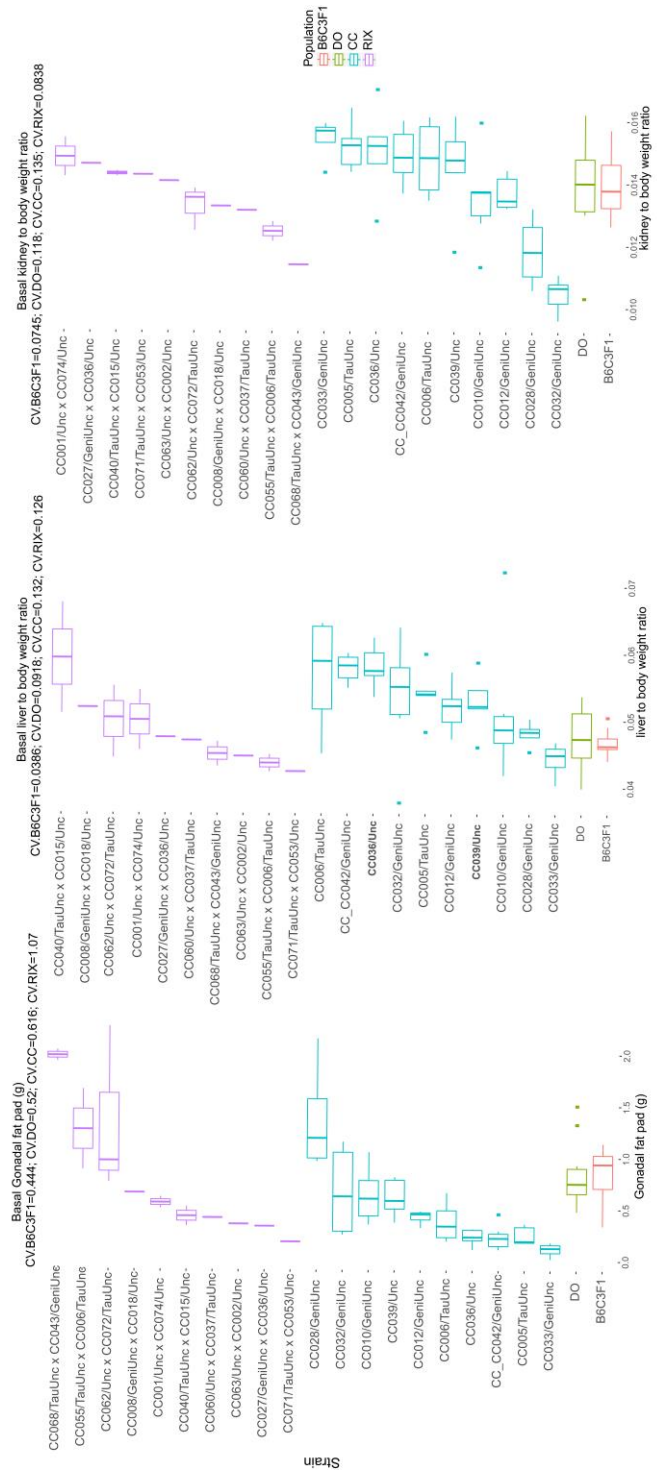

Figure 4.7. Box plots showing coefficient of variation on hematological endpoints with statistically-significant inter-strain differences in CC, CC-RIX, and DO populations, and B6C3F1. The horizontal line is the median and the box represents 1st and 3rd quartile ranges.

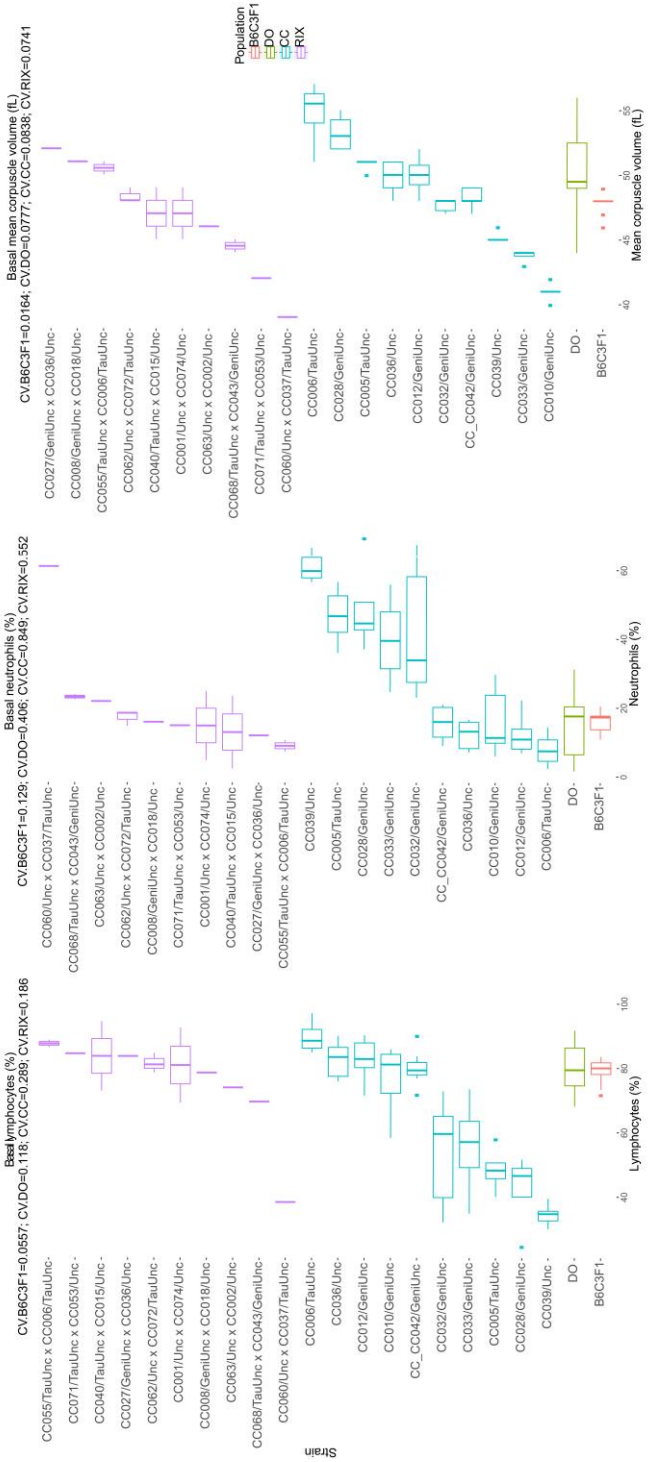

Figure 4.8. Box plots showing coefficient of variation on hematopoietic endpoints with statistically-significant inter-strain differences in CC, CC-RIX, and DO populations, and B6C3F1. The horizontal line is the median and the box represents 1st and 3rd quartile ranges.

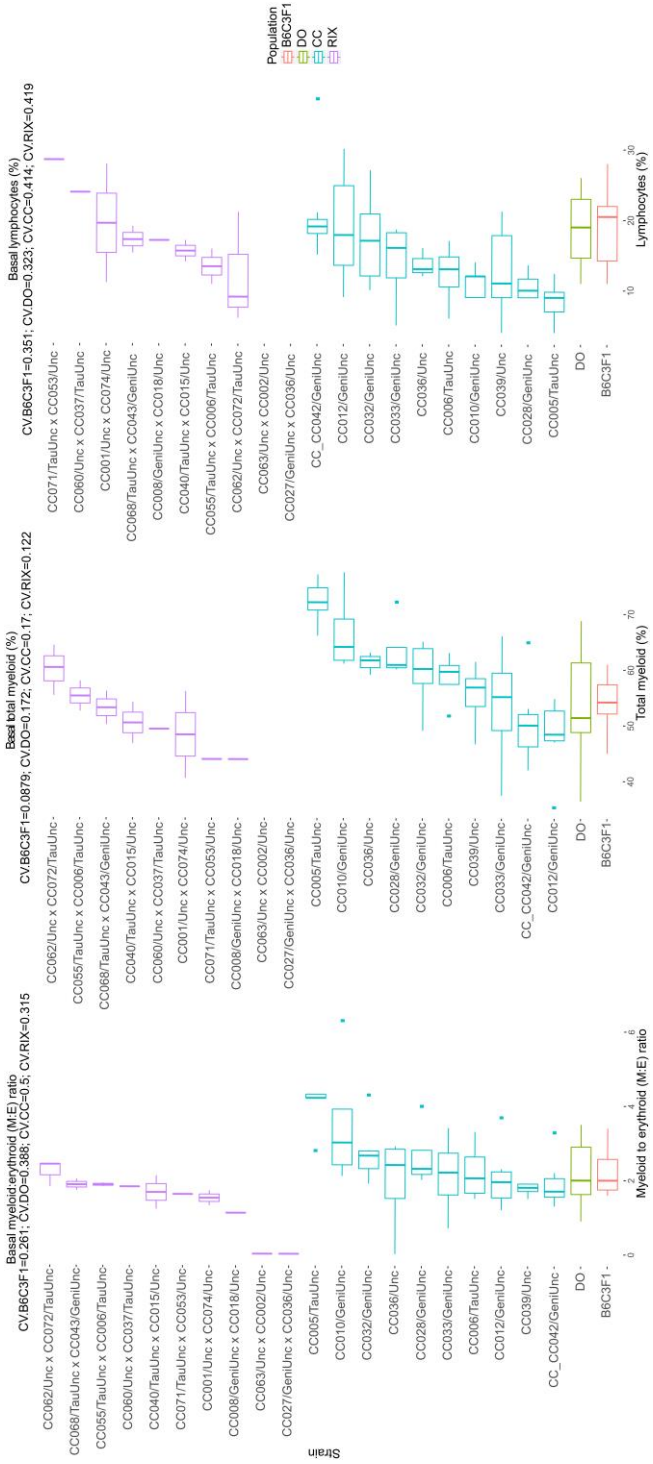

Figure 4.9. Box-plots showing total histopathological scores of CC, CC-RIX, and DO populations, and B6C3F1. '+' sign represents the mean and the box is 1st and 3rd quartile ranges. The whiskers represents 5-95 percentile.

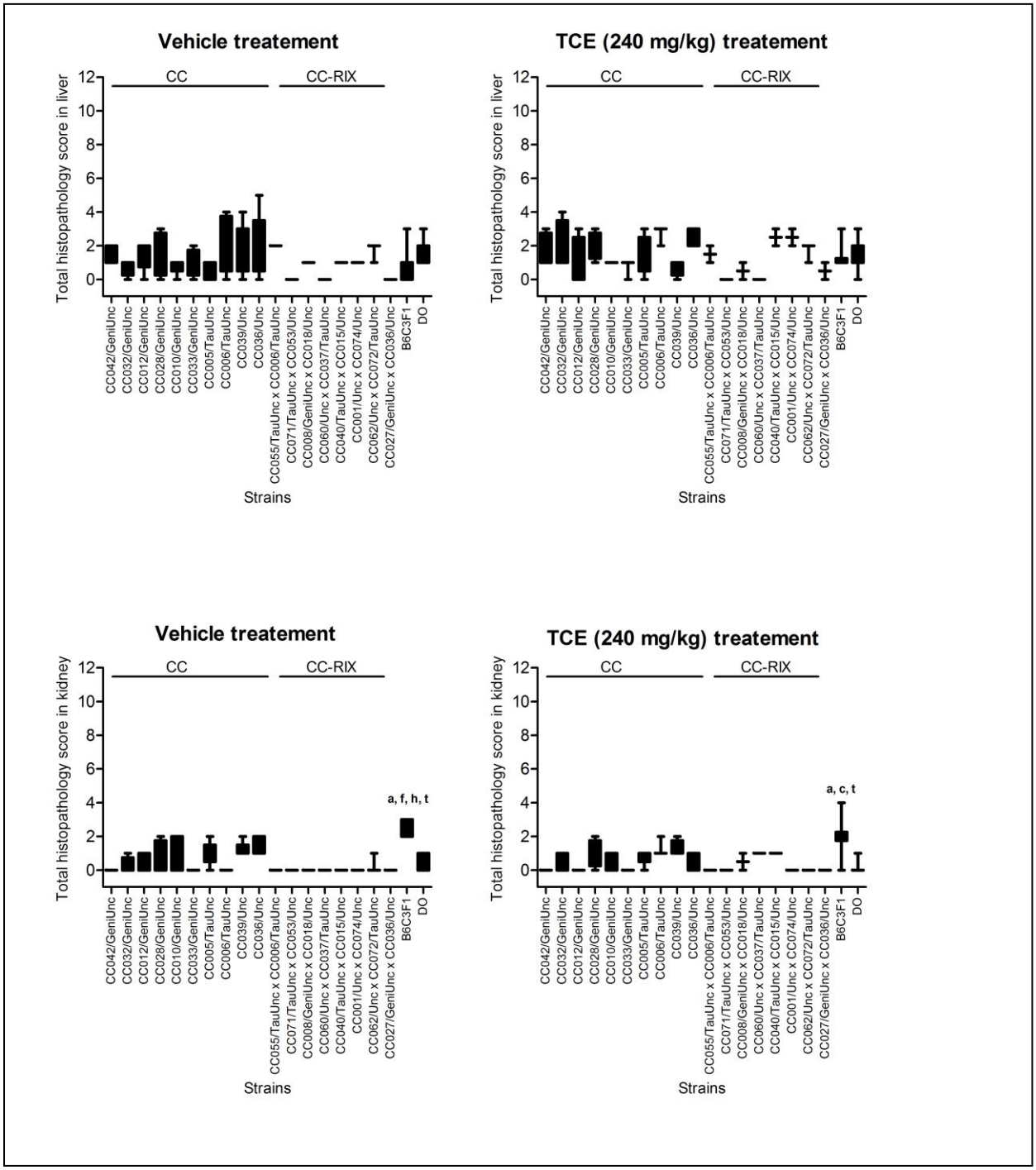

Figure 4.10. Ten percent change in the slope estimate per mg/kg per day dose of endpoints that demonstrated significant inter-strain differences across populations. Error bars represents 95% percent confidence interval.

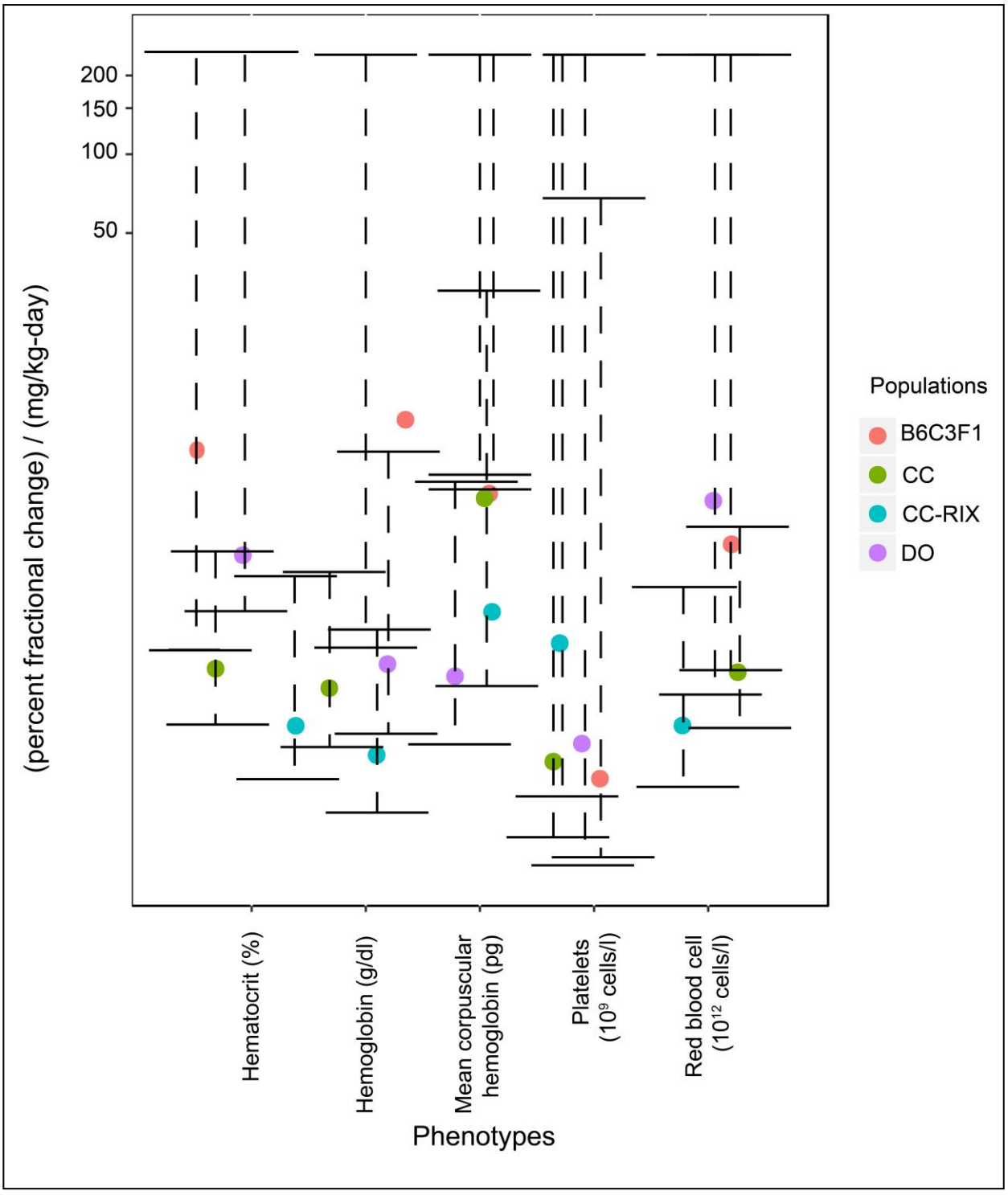

Supplemental Table 4.1. Histopathological scoring of liver and kidney among CC, CC-RIX, and DO populations, and B6C3F1 treated with vehicle or TCE (240 mg/kg).

Strain	TCE dose (mg/kg)	Chronic Progressive nephropathy	Tubular epithelial vacuolation	Tubular epithelial karyomegaly	Total kidney score	Centrilobular hypertrophy and karyomegaly	Focal Inflammation	Apoptosis /Necrosis	Total liver score
B6C3F1	0	0	2	0	2	1	0	0	1
B6C3F1	0	0	2	0	2	1	0	0	1
B6C3F1	0	0	2	0	2	1	0	0	1
B6C3F1	0	0	2	0	2	1	0	0	1
B6C3F1	0	0	2	0	2	1	2	0	3
B6C3F1	0	0	2	0	2	0	0	0	0
B6C3F1	0	0	3	0	3	0	0	0	0
B6C3F1	0	0	3	0	3	0	0	0	0
B6C3F1	0	0	2	0	2	0	0	0	0
B6C3F1	0	0	3	0	3	1	0	0	1
CC_CC042/ GeniUnc	0	0	0	0	0	1	0	0	1
CC_CC042/ GeniUnc	0	0	0	0	0	1	0	0	1
CC_CC042/ GeniUnc	0	0	0	0	0	1	0	0	1
CC_CC042/ GeniUnc	0	0	0	0	0	2	0	0	2
CC_CC042/ GeniUnc	0	0	0	0	0	2	0	0	2
CC_CC042/ GeniUnc	0	0	0	0	0	1	0	0	1
CC_CC042/ GeniUnc	0	0	0	0	0	2	0	0	2
CC032/Geni Unc	0	0	0	0	0	0	0	0	0
CC032/Geni Unc	0	0	0	0	0	1	0	0	1
CC032/Geni Unc	0	0	0	0	0	1	0	0	1
CC032/Geni Unc	0	1	0	0	1	0	0	1	1
CC012/Geni Unc	0	1	0	0	1	1	1	0	2
CC012/Geni Unc	0	1	0	0	1	0	0	0	0
CC012/Geni Unc	0	1	0	0	1	0	1	0	1
CC012/Geni Unc	0	0	0	0	0	0	0	2	2
CC012/Geni Unc	0	1	0	0	1	0	1	1	2
CC012/Geni Unc	0	0	0	0	0	0	1	1	2
CC028/Geni Unc	0	0	0	0	0	0	0	0	0
CC028/Geni Unc	0	2	0	0	2	1	1	0	2
CC028/Geni Unc	0	0	0	0	0	1	0	0	1

CC028/Geni Unc	0	1	0	0	1	2	1	0	3
CC010/Geni Unc	0	2	0	0	2	0	0	0	0
CC010/Geni Unc	0	0	0	0	0	1	0	0	1
CC010/Geni Unc	0	0	0	0	0	1	0	0	1
CC010/Geni Unc	0	1	0	1	2	1	0	0	1
CC010/Geni Unc	0	1	0	0	1	1	0	0	1
CC033/Geni Unc	0	0	0	0	0	0	1	0	1
CC033/Geni Unc	0	0	0	0	0	0	0	0	0
CC033/Geni Unc	0	0	0	0	0	0	2	0	2
CC033/Geni Unc	0	0	0	0	0	1	0	0	1
CC005/TauUnc	0	1	0	0	1	0	1	0	1
CC005/TauUnc	0	0	0	0	0	1	0	0	1
CC005/TauUnc	0	1	0	0	1	0	0	0	0
CC005/TauUnc	0	1	0	0	1	1	0	0	1
CC005/TauUnc	0	2	0	0	2	0	0	0	0
CC006/TauUnc	0	0	0	0	0	2	0	0	2
CC006/TauUnc	0	0	0	0	0	0	0	0	0
CC006/TauUnc	0	0	0	0	0	2	1	0	3
CC006/TauUnc	0	0	0	0	0	2	2	0	4
CC039/Unc	0	1	0	0	1	1	0	1	2
CC039/Unc	0	1	0	0	1	1	0	0	1
CC039/Unc	0	1	0	0	1	1	3	0	4
CC039/Unc	0	1	0	0	1	0	0	0	0
CC039/Unc	0	1	0	1	2	1	0	0	1
CC036/Unc	0	1	1	0	2	1	1	0	2
CC036/Unc	0	1	0	0	1	0	0	0	0
CC036/Unc	0	1	0	1	2	2	2	1	5
CC036/Unc	0	1	0	0	1	0	1	0	1
CC036/Unc	0	0	1	0	1	1	0	0	1
DO	0	0	0	0	0	2	0	0	2
DO	0	0	1	0	1	1	0	0	1
DO	0	1	0	0	1	2	0	0	2
DO	0	0	0	0	0	1	0	0	1
DO	0	0	0	0	0	1	1	1	3
DO	0	0	0	0	0	0	1	0	1
DO	0	0	0	0	0	2	0	0	2
DO	0	0	0	1	1	0	1	0	1

DO	0	0	0	0	0	1	0	0	1
DO	0	0	0	0	0	1	0	0	1
CC055/TauUnc x CC006/TauUnc	0	0	0	0	0	1	1	0	2
CC071/TauUnc x CC053/Unc	0	0	0	0	0	0	0	0	0
CC008/GeniUnc x CC018/Unc	0	0	0	0	0	1	0	0	1
CC060/Unc x CC037/TauUnc	0	0	0	0	0	0	0	0	0
CC040/TauUnc x CC015/Unc	0	0	0	0	0	1	0	0	1
CC040/TauUnc x CC015/Unc	0	0	0	0	0	1	0	0	1
CC001/Unc x CC074/Unc	0	0	0	0	0	1	0	0	1
CC001/Unc x CC074/Unc	0	0	0	0	0	1	0	0	1
CC062/Unc x CC072/TauUnc	0	0	0	0	0	1	0	0	1
CC062/Unc x CC072/TauUnc	0	0	0	0	0	2	0	0	2
CC062/Unc x CC072/TauUnc	0	1	0	0	1	2	0	0	2
CC027/GeniUnc x CC036/Unc	0	0	0	0	0	0	0	0	0
B6C3F1	240	0	1	0	1	2	1	0	3
B6C3F1	240	0	2	0	2	1	0	0	1
B6C3F1	240	0	0	0	0	1	0	0	1
B6C3F1	240	0	2	0	2	1	0	0	1
B6C3F1	240	0	2	0	2	1	0	0	1
B6C3F1	240	1	2	1	4	1	1	0	2
B6C3F1	240	0	2	0	2	1	0	0	1
B6C3F1	240	0	2	1	3	1	0	0	1
B6C3F1	240	0	2	0	2	1	0	0	1
B6C3F1	240	0	2	0	2	1	0	0	1
CC042/GeniUnc	240	0	0	0	0	1	0	0	1
CC042/GeniUnc	240	0	0	0	0	1	0	0	1
CC042/GeniUnc	240	0	0	0	0	0	1	2	3
CC042/GeniUnc	240	0	0	0	0	2	0	0	2

CC032/GeniUnc	240	1	0	0	1	1	0	0	1
CC032/GeniUnc	240	0	0	0	0	1	0	0	1
CC032/GeniUnc	240	0	0	0	0	2	2	0	4
CC032/GeniUnc	240	1	0	0	1	1	1	0	2
CC012/GeniUnc	240	0	0	0	0	0	0	0	0
CC012/GeniUnc	240	0	0	0	0	0	0	0	0
CC012/GeniUnc	240	0	0	0	0	1	0	0	1
CC012/GeniUnc	240	0	0	0	0	2	1	0	3
CC028/GeniUnc	240	1	0	0	1	2	1	0	3
CC028/GeniUnc	240	1	0	0	1	1	0	0	1
CC028/GeniUnc	240	2	0	0	2	2	0	0	2
CC028/GeniUnc	240	0	0	0	0	2	0	0	2
CC010/GeniUnc	240	0	0	0	0	1	0	0	1
CC010/GeniUnc	240	1	0	0	1	1	0	0	1
CC010/GeniUnc	240	1	0	0	1	1	0	0	1
CC010/GeniUnc	240	0	0	0	0	1	0	0	1
CC010/GeniUnc	240	0	0	0	0	1	0	0	1
CC033/GeniUnc	240	0	0	0	0	1	0	0	1
CC033/GeniUnc	240	0	0	0	0	1	0	0	1
CC033/GeniUnc	240	0	0	0	0	0	0	0	0
CC005/TauUnc	240	1	0	0	1	1	2	0	3
CC005/TauUnc	240	1	0	0	1	1	0	0	1
CC005/TauUnc	240	0	0	0	0	0	0	0	0
CC005/TauUnc	240	1	0	0	1	1	0	0	1
CC005/TauUnc	240	1	0	0	1	2	0	0	2
CC006/TauUnc	240	1	0	0	1	1	1	0	2
CC006/TauUnc	240	0	0	1	1	2	1	0	3
CC006/TauUnc	240	0	0	2	2	2	1	0	3
CC039/Unc	240	1	0	0	1	1	0	0	1
CC039/Unc	240	1	0	0	1	1	0	0	1
CC039/Unc	240	1	1	0	2	0	0	0	0
CC039/Unc	240	0	1	0	1	1	0	0	1
CC036/Unc	240	1	0	0	1	2	1	0	3
CC036/Unc	240	0	0	0	0	2	0	0	2
CC036/Unc	240	1	0	0	1	2	0	0	2

CC036/Unc	240	1	0	0	1	2	1	0	3
CC036/Unc	240	0	0	0	0	1	1	0	2
DO	240	0	0	0	0	1	1	0	2
DO	240	0	0	0	0	1	0	0	1
DO	240	0	0	0	0	1	0	0	1
DO	240	0	0	0	0	1	1	0	2
DO	240	0	0	0	0	1	0	0	1
DO	240	0	0	0	0	0	1	0	1
DO	240	1	0	0	1	1	0	0	1
DO	240	0	0	0	0	2	1	0	3
DO	240	0	0	0	0	0	0	0	0
CC055/TauUnc x CC006/TauUnc	240	0	0	0	0	1	0	0	1
CC055/TauUnc x CC006/TauUnc	240	0	0	0	0	2	0	0	2
CC071/TauUnc x CC053/Unc	240	0	0	0	0	0	0	0	0
CC071/TauUnc x CC053/Unc	240	0	0	0	0	0	0	0	0
CC008/GeniUnc x CC018/Unc	240	0	0	0	0	1	0	0	1
CC008/GeniUnc x CC018/Unc	240	1	0	0	1	0	0	0	0
CC060/Unc x CC037/TauUnc	240	1	0	0	1	0	0	0	0
CC040/TauUnc x CC015/Unc	240	1	0	0	1	1	0	1	2
CC040/TauUnc x CC015/Unc	240	1	0	0	1	2	1	0	3
CC001/Unc x CC074/Unc	240	0	0	0	0	2	1	0	3
CC001/Unc x CC074/Unc	240	0	0	0	0	2	0	0	2
CC062/Unc x CC072/TauUnc	240	0	0	0	0	1	0	0	1
CC062/Unc x CC072/TauUnc	240	0	0	0	0	2	0	0	2
CC062/Unc x CC072/TauUnc	240	0	0	0	0	2	0	0	2
CC027/GeniUnc x CC036/Unc	240	0	0	0	0	0	0	0	0

CC027/Geni Unc x CC036/Unc	240	0	0	0	0	1	0	0	1

CHAPTER 5: DISCUSSION

I. Conclusions

Hazard identification and dose response assessments are key steps in chemical risk assessment that aim to identify and characterize potential adverse effects with exposure to stressors. Due to technological and scientific advances, the approaches employed in chemical assessments have evolved over time. For example, *in vitro, in silico* and tissue chip models are often envisioned to replace or reduce animal based-testing (Esch, King, & Shuler, 2011; National Research Council, 2007). The U.S. Environmental Agency's Toxicity Forecaster (ToxCast™) program implements high- throughput screening approaches that identifies bioactivity profiles with exposures to rank chemicals for further testing (Benigni, 2013; Dix et al., 2007). The Toxicology Testing in the 21st Century (Tox21) collaboration aims to establish a database providing bioactivity information on more than 10,000 compounds for prioritizing chemicals for hazard identification (Tice, Austin, Kavlock, & Bucher, 2013). Tissue chips are biomechanical devices comprising of living cells within silicon engraved systems that are perceived to be physiologically closer to *in vivo* models compared to classical cell based- models. Tissue chips are currently being tested for their utility in hazard identification in both industry and academia (Willyard, 2017). Quantitative structure-activity relationships (QSAR) are based on computational models that predict potential bioactivity of an analyte based on available data on structurally-similar chemicals (Zhang et al., 2013). Although the above described approaches have vastly helped in providing experimental or predicted data to understand chemical-target interactions and

aid with the regulatory decision making processes, they fail to address population variability in such interactions that lead to differences in degree of adverse reactions as seen in humans.

Addressing population variability in toxic responses is a persistent challenge in chemical risk assessments (Zeise et al., 2013). Population-based *in vitro* models are emerging resources that have been recently implemented in biomedical research and toxicological studies (Harrill & McAllister, 2017; Siva, 2008). The Lock et al. 2012 study also showed the utility of population–based models to conduct high throughput screening of chemicals to evaluate inter-individual differences in dose-response assessment and its relevance in addressing the issue of subpopulations. The 1000 Genomes Project is a collaborative effort that aimed to catalogue genetic variations that occur at relatively low frequencies in coding regions of genes. This resource has been previously used to characterize inter-individual differences in hazard and to conduct population level dose-response assessments. For instance, the (Abdo, Xia, et al., 2015) study demonstrated the feasibility to conduct high throughput screening of cytotoxic responses to 179 chemicals in immortalized lymphoblastoid cell lines from 1000 donors. Further, the use of *in vitro* population models enabled high precision genome wide association mapping to identify genetic loci associated with toxicity outcomes thereby providing information on novel mechanisms driving variability in adverse effects (Abdo, Wetmore, et al., 2015). Although the use of population-based *in vitro* models offer several advantages than traditional cell-based approaches, rodent models are still considered a gold standard for toxicity testing.

Population-based mouse models are often implemented in research with a focus on understanding genotype-phenotype associations. Several studies have demonstrated the utility of population-based mouse models in systems genetics, addressing variability in toxicokinetic and toxicodynamic responses, and identifying susceptible strains that accurately mimic adverse

responses as seen in humans (Cichocki et al., 2017; French et al., 2015; Rasmussen et al., 2014). Despite available information on population-based rodent models, their utility in addressing variability and uncertainty in hazard identification and dose-response assessments have not been extensively explored. This dissertation focused on the role of population-based rodent models in toxicity testing using trichloroethylene as a case study toxicant.

II. Summary of Findings

In Specific Aim 1, we observed that the CC model demonstrates large diversity in TCE toxicokinetic and toxicodynamic responses compared to classical inbred lines but comparable to humans. One interesting finding from this study was that levels of hepatic TCA significantly correlated with hepatic gene expression of *Acox1* but did not correlate with protein expression or activity levels of known TCE metabolizing enzymes demonstrating that TCA is a complex trait involving multiple pathways of formation, transformation, and elimination. This evidence also suggests the simple hypothesis that gene environment interactions may also apply for toxicokinetic responses. The mosaic representation of the founder alleles in the CC model facilitated genetic mapping with improved precision in identifying novel markers driving variability in TCE metabolism and toxicodynamics.

In Specific Aim 2, we identified genetic background as profoundly affecting gene expression compared to dose or interaction effects. We also observed that expression of genes significantly influenced by TCE were also influenced by TCA suggesting that PPARα signaling plays a major role in liver transcriptional responses. Pathway enrichment analysis revealed several pathways significantly perturbed within the CC population with 10-fold differences in their median PoDs. Also, appreciable differences within the CC population in median PoDs of aggregated

pathways enabled identification of potential susceptible and resistant strains for pre-chronic and chronic studies. Expression-quantitative trait loci (eQTL) analysis identified a linkage between liver expression of *Fitm2* and TCA levels. Collectively, these data demonstrate the potential of the CC model for conducting systems genetics. Another interesting finding that CC population enabled estimating variability in transcriptional PoDs and demonstrates reasonable correlation with PoDs of apical endpoints from previous pre-chronic and chronic studies.

In Specific Aim 3, we tested the feasibility of incorporating different population-based rodent models in a standard 90-day oral toxicity study to directly compare variability in TCE toxicokinetic and toxicodynamic responses in population-based experiments with variability in the B6C3F1 strain. We identified CC and CC-RIX as demonstrating large variability in liver and kidney TCA levels in comparison to B6C3F1. We also observed that basal variability in several physiological, hematological, and hematopoietic endpoints were highly variable within the CC and CC-RIX populations. Dose-response assessments revealed that 10-fold differences in PoDs of few endpoints between strains within CC and CC-RIX populations. In addition, qualitative differences in dose response relationships were also marked among several strains within the CC and CC-RIX populations. Interestingly, the variability within the DO population was comparable to intra-strain variability of the B6C3F1. Results from this study identifies strains from CC and CC-RIX as diverse responders to TCE and which could be used to replace B6C3F1 in chronic studies. In summary, the use of CC model and other population-based mouse models have provided experimental data to address significant gaps of knowledge relevant to human variability in risk assessment.

III. Significance

One of the critical challenges in risk assessment is addressing variability and uncertainty in hazard identification and dose-response assessments. Several outcomes from of this dissertation shed light on using population-based models to address these concerns. Firstly, differences in mechanisms of toxicity within a population may lead to challenges in identifying the appropriate strain or model to conduct toxicity testing. Evidence from our studies show large diversity in responses for several toxicokinetic and toxicodynamic endpoints suggesting the possibility of susceptible individuals that maybe incorporated in chronic studies as an alternative to B6C3F1. Secondly, uncertainty in differences in toxicokinetic and toxicodynamic responses are historically addressed using uncertainty factors. A safety factor of 10 accounting for 3.3 fold-differences in toxicokinetic and toxicodynamic responses within a population is often used as a default in the absence of population-based data. This dissertation demonstrates that greater than 10-fold variability exists in TCE toxicokinetic and toxicodynamic responses in both single- and repeated-dose studies suggesting that default assumptions maybe underestimating risk leading to inaccurate toxicity values. Thirdly, safety assessments have always been conducted with the assumption that susceptible individuals do exist in a population. However, often due to lack of data in these assessments it is difficult to directly compare individual- versus population - dose response relationships to ensure that the susceptible individuals are indeed protected from risk. Data from this dissertation identified genes associated with TCE toxicokinetics and toxicodynamics that are either highly variable or consistent in their responses among individuals in the CC population. This information is useful in interpreting biological endpoints that maybe strongly dependent on genetic background.

Efforts to integrate mechanistic and genetic data to address inter-individual variability in toxic responses are often limited due to cross-disciplinary research challenges. Population-based rodent models facilitate systems genetic tools to identify genetic variants driving variability in an endpoint. Further, use of gene expression data permits identification of all local and distal genetic interactions contributing to the variability of an endpoint. In this study, the CC model enabled identification of a link between expressions of *Fitm2* that is driven by PPARα and TCA levels in the liver.

Hazard identification: Historically, single strains of rodents have often been used to assess hazard with exposures. Evidences from pharmacogenomics have shown vast differences in drug metabolizing capacity among individuals carrying genetic variants (W. E. Evans & Relling, 2004). So it can be perceived that for any given toxicity endpoint there would exist susceptible and resistant strains in a population. Further, due to the diverse responses in a population certain strains may better reproduce the clinical manifestations as seen in susceptible groups or individuals in the human population. This dissertation provides experimental data that shows large variability in TCE oxidative metabolism and toxicodynamic responses in both single- and repeated-dose studies suggesting the existence of susceptible and resistant strains to toxicity upon chronic exposures. As this dissertation focused on a single case study toxicant, selection of good or appropriate individuals for hazard identification maybe challenging for other chemicals. However, based on available toxicity data or structure-activity relationships chemicals can be broadly categorized based on their mechanisms of toxicity. For example, activation of PPARα-signaling in mice may contribute to hepatocarcinogenesis via non-genotoxic mechanisms. Thus, selection of strains with diverse levels of PPARα activators as metabolites or PPARα-responsive gene expression may represent a panel of genetically-diverse mice that serves as good models to enhance hazard

identification of potential PPARα agonists. Similarly, strains with diverse toxicokinetic activities can be selected to improve hazard identification of chemicals where adverse reactions are metabolism dependent.

Dose-response assessments: Dose-response assessment is an essential component in the chemical risk assessment process and is conducted to derive PoDs. Sufficient data from this dissertation highlights the critical need to characterize individual- versus population-level differences in dose-response relationships. As toxic outcomes arise from chemical-host interactions genetic differences between hosts pose a challenge to characterize chemical-driven responses that are strongly dependent on dose, genetic background, or their combinatory effects.

One significant finding from this dissertation is the strong influence of genetic background on toxicokinetic and toxicodynamic responses. As traditional dose-response assessments are often conducted in single strains, PoDs derived from these models may not be protective towards susceptible individuals or groups. Also, the effect of genetic background on all the routinely evaluated toxicity endpoints remains vastly unknown to make informed decision on the strain of choice for a given endpoint. Further, dose-response assessments from both single- and repeated-dose studies in single strain rodent models have demonstrated not only quantitative differences but also qualitative differences in the derived PoDs. Consequently, there is uncertainty in the choice of single-strain model-based PoD for regulatory risk assessment. Population-based models will better characterize variability across strains in a population thereby address uncertainty in dose-response assessments.

Population-based 90-day oral toxicity study: The two-year cancer bioassay is considered as the gold standard for carcinogenicity. 90-day toxicity studies often provide preliminary toxicity

data on a test chemical to justify conducting chronic studies. As a single strain of rodents are often implemented in pre-chronic studies it is unrealistic that such models would represent susceptible individuals for all the chemicals and toxicity endpoints that requires investigation. Incorporation of population-based approaches in toxicity testing of chemicals would increase the likelihood of identifying susceptible strains that may be used for chronic studies. Further, population models would also help to characterize the role of genetic background in dose-response assessments. One major concern with population approaches is that sample size of the study designs may need to be increased to achieve adequate statistical power. However, Specific Aim 3 of this dissertation shows that population-based repeated toxicity studies can still be conducted without increasing the sample size of the studies. Such an approach helps address variability in chemical risk assessments.

IV. Limitations

Although population models offer several advantages in addressing significant gaps in risk assessments, there are also limitations associated with using these models. First, population Although this dissertation highlights the significance of using population-based rodent approaches to address significant gaps in risk assessments, there are several considerations and limitations that need to be considered with these models. It is perceived that population-based rodent models facilitate systems genetic analysis, an approach to understand the flow of biological information controlling a trait or adverse outcome. Evidence from this dissertation demonstrate limitations in identifying genetic regions driving transcriptional changes contributing to adverse reaction. For instance, we identified a local genetic region associated with gene expression of *Fitm2* that is associated with hepatic TCA levels. However, no association between distal genetic loci and gene expression profiles were found to draw conclusions on other genes and possibly gene-environment

interactions associated with TCA levels. These data suggest that depending on the complexity that underlie the phenotype or outcome of interest, systems genetic approaches maybe less effective in dissecting mechanistic associations in the flow of biological information.

As the case study toxicant used in this dissertation is TCE, implications of using population-based rodent models from this dissertation should be carefully interpreted. Evidence from previous studies in classical inbred strains demonstrated large inter-strain differences in oxidative metabolism and toxicodynamics that were found to be much more pronounced in the population models. Further, these effects were then associated with several genetic loci that led to the identification of novel mechanisms of toxicity. However, not all inter-individual differences observed in an endpoint may be driven by genetics. Non-genetic factors such as environment, epigenetics, age, sex, and pre-existing conditions may also have a role in inter-individual differences in therapeutic or adverse outcomes.

Next, statistical testing used in population models would be different in comparison to classical models. Pair-wise testing may be inappropriate as population models are similar to epidemiological studies. Thus, other statistical approaches such as random effect models or Bayesian approaches may be better suited for population models. In order to maintain existing sample sizes in traditional toxicity testing another trade off in population models would be to replace more biological replicates of one strain per dose group with few biological replicates of different strains per dose group.

Lastly, population-based studies are often expensive and tedious. In order to conduct genetic mapping experiments with high precision a large panel of strains is often required to characterize variability in toxicodynamic and toxicokinetic responses. Further, certain polygenic

endpoints maybe highly complex so that even a large genetically-diverse population may fail to identify all molecular interactions contributing to inter-individual differences observed in the population. In the context of toxicity screening, knowledge on background lesions, survivability, and other pre-disposed health conditions in the strains within these models are yet to be fully characterized and curated. This information is useful for selecting strains for chronic studies. Reproducibility of the findings from non-reproducible population models is a significant concern that needs to be addressed in safety assessments. In summary, these limitations should be taken into consideration while designing and conducting population-based rodent studies.

V. Future Studies

Exposure Assessments: Exposure assessment is a major step in chemical risk assessments. This step aims in measuring the amount and duration of exposure to an agent. Exposure assessments are often conducted to calculate internal dose – the amount of chemical that is biologically available within the body. Previous studies in mouse diversity panels have demonstrated large differences in tissue-specific internal doses of TCE, and PBPK models have shown comparable estimates in variability between humans and mice (Bradford et al., 2011; Chiu et al., 2014a; Yoo, Bradford, Kosyk, Uehara, et al., 2015). One future direction would be to extent current PBPK models to include data from population-based mouse models. Such an approach can inform whether models such as CC are good surrogates for human population toxicokinetic variability.

Two year cancer bioassay: The two-year cancer bioassay has been traditionally used to assess carcinogenic potential of chemicals. One approach to incorporate population-based rodent models in toxicity testing would be to select strains within the CC and CC-RIX populations from the pre-

chronic study that are high and low responders to TCE exposures to conduct a chronic study. Another important study to further address uncertainty in assessments would be to conduct a single exposure toxicokinetic study using strains with diverse responses within the CC population. Comprehensive metabolite profiling of both oxidative and glutathione dependent metabolites can be incorporated into existing PBPK models to better assess inter-species differences in TCE metabolism. This approach would help test whether there is variability in the mechanisms of toxicity are driven by differences in genetic background.

REFERENCES

Abdo, N., Wetmore, B. A., Chappell, G. A., Shea, D., Wright, F. A., & Rusyn, I. (2015). In vitro screening for population variability in toxicity of pesticide-containing mixtures. *Environ Int, 85*, 147-155. doi:10.1016/j.envint.2015.09.012

Abdo, N., Xia, M., Brown, C. C., Kosyk, O., Huang, R., Sakamuru, S., . . . Wright, F. A. (2015). Population-based in vitro hazard and concentration-response assessment of chemicals: the 1000 genomes high-throughput screening study. *Environ Health Perspect, 123*(5), 458-466. doi:10.1289/ehp.1408775

Adami, H. O., Berry, S. C., Breckenridge, C. B., Smith, L. L., Swenberg, J. A., Trichopoulos, D., . . . Pastoor, T. P. (2011). Toxicology and epidemiology: improving the science with a framework for combining toxicological and epidemiological evidence to establish causal inference. *Toxicological sciences, 122*(2), 223-234. doi:10.1093/toxsci/kfr113

Anders, S., Pyl, P. T., & Huber, W. (2015). HTSeq--a Python framework to work with high-throughput sequencing data. *Bioinformatics, 31*(2), 166-169. doi:10.1093/bioinformatics/btu638

Andersen, M. E., Clewell, H. J., 3rd, Bermudez, E., Willson, G. A., & Thomas, R. S. (2008). Genomic signatures and dose-dependent transitions in nasal epithelial responses to inhaled formaldehyde in the rat. *Toxicological sciences, 105*(2), 368-383. doi:10.1093/toxsci/kfn097

Andersen, M. E., & Krewski, D. (2009). Toxicity testing in the 21st century: bringing the vision to life. *Toxicological sciences, 107*(2), 324-330.

Atienzar, F. A., Blomme, E. A., Chen, M., Hewitt, P., Kenna, J. G., Labbe, G., . . . Dambach, D. M. (2016). Key Challenges and Opportunities Associated with the Use of In Vitro Models to Detect Human DILI: Integrated Risk Assessment and Mitigation Plans. *Biomed Res Int, 2016*, 9737920. doi:10.1155/2016/9737920

Aylor, D. L., Valdar, W., Foulds-Mathes, W., Buus, R. J., Verdugo, R. A., Baric, R. S., . . . Churchill, G. A. (2011). Genetic analysis of complex traits in the emerging Collaborative Cross. *Genome Res, 21*(8), 1213-1222. doi:10.1101/gr.111310.110

Barkan, I. D. (1985). Industry invites regulation: the passage of the Pure Food and Drug Act of 1906. *Am J Public Health, 75*(1), 18-26.

Bassig, B. A., Zhang, L., Vermeulen, R., Tang, X., Li, G., Hu, W., . . . Lan, Q. (2016). Comparison of hematological alterations and markers of B-cell activation in workers exposed to benzene, formaldehyde and trichloroethylene. *Carcinogenesis, 37*(7), 692-700. doi:10.1093/carcin/bgw053

Benigni, R. (2013). Evaluation of the toxicity forecasting capability of EPA's ToxCast Phase I data: can ToxCast in vitro assays predict carcinogenicity? *J Environ Sci Health C Environ Carcinog Ecotoxicol Rev, 31*(3), 201-212. doi:10.1080/10590501.2013.824188

Bercu, J. P., Jolly, R. A., Flagella, K. M., Baker, T. K., Romero, P., & Stevens, J. L. (2010). Toxicogenomics and cancer risk assessment: a framework for key event analysis and dose-response assessment for nongenotoxic carcinogens. *Regul Toxicol Pharmacol, 58*(3), 369-381. doi:10.1016/j.yrtph.2010.08.002

Berger, J., & Moller, D. E. (2002). The mechanisms of action of PPARs. *Annu Rev Med, 53*, 409-435. doi:10.1146/annurev.med.53.082901.104018

Bhattacharya, S., Zhang, Q., Carmichael, P. L., Boekelheide, K., & Andersen, M. E. (2011). Toxicity Testing in the 21(st) Century: Defining New Risk Assessment Approaches Based on Perturbation of Intracellular Toxicity Pathways. *PLoS One, 6*(6). doi:ARTN e20887

Bogue, M. A., Churchill, G. A., & Chesler, E. J. (2015). Collaborative Cross and Diversity Outbred data resources in the Mouse Phenome Database. *Mamm Genome, 26*(9-10), 511-520. doi:10.1007/s00335-015-9595-6

Bolger, A. M., Lohse, M., & Usadel, B. (2014). Trimmomatic: a flexible trimmer for Illumina sequence data. *Bioinformatics, 30*(15), 2114-2120. doi:10.1093/bioinformatics/btu170

Boverhof, D. R., Chamberlain, M. P., Elcombe, C. R., Gonzalez, F. J., Heflich, R. H., Hernandez, L. G., . . . Gollapudi, B. B. (2011). Transgenic animal models in toxicology: historical perspectives and future outlook. *Toxicological sciences, 121*(2), 207-233. doi:10.1093/toxsci/kfr075

Bradford, B. U., Lock, E. F., Kosyk, O., Kim, S., Uehara, T., Harbourt, D., . . . Rusyn, I. (2011). Interstrain differences in the liver effects of trichloroethylene in a multistrain panel of inbred mice. *Toxicological sciences, 120*(1), 206-217. doi:10.1093/toxsci/kfq362

Bronley-DeLancey, A., McMillan, D. C., McMillan, J. M., Jollow, D. J., Mohr, L. C., & Hoel, D. G. (2006). Application of cryopreserved human hepatocytes in trichloroethylene risk assessment: relative disposition of chloral hydrate to trichloroacetate and trichloroethanol. *Environ Health Perspect., 114*(8), 1237-1242.

Bucher, J. R. (2002). The National Toxicology Program rodent bioassay: designs, interpretations, and scientific contributions. *Ann N Y Acad Sci, 982*, 198-207.

Bull, R. J., Orner, G. A., Cheng, R. S., Stillwell, L., Stauber, A. J., Sasser, L. B., . . . Thrall, B. D. (2002). Contribution of dichloroacetate and trichloroacetate to liver tumor induction in mice by trichloroethylene. *Toxicology and applied pharmacology, 182*(1), 55-65.

Bull, R. J., Sanchez, I. M., Nelson, M. A., Larson, J. L., & Lansing, A. J. (1990). Liver tumor induction in B6C3F1 mice by dichloroacetate and trichloroacetate. *Toxicology, 63*(3), 341-359.

Burczynski, M. E., McMillian, M., Ciervo, J., Li, L., Parker, J. B., Dunn, R. T., 2nd, . . . Johnson, M. D. (2000). Toxicogenomics-based discrimination of toxic mechanism in HepG2 human hepatoma cells. *Toxicol Sci, 58*(2), 399-415.

Bystrykh, L., Weersing, E., Dontje, B., Sutton, S., Pletcher, M. T., Wiltshire, T., . . . de Haan, G. (2005). Uncovering regulatory pathways that affect hematopoietic stem cell function using 'genetical genomics'. *Nat Genet, 37*(3), 225-232.

Chandra, V., Huang, P. X., Hamuro, Y., Raghuram, S., Wang, Y. J., Burris, T. P., & Rastinejad, F. (2008). Structure of the intact PPAR-gamma-RXR-alpha nuclear receptor complex on DNA. *Nature, 456*(7220), 350-U333. doi:10.1038/nature07413

Chang, L. W., Daniel, F. B., & DeAngelo, A. B. (1992). Analysis of DNA strand breaks induced in rodent liver in vivo, hepatocytes in primary culture, and a human cell line by chlorinated acetic acids and chlorinated acetaldehydes. *Environ Mol Mutagen, 20*(4), 277-288.

Chesler, E. J., Wang, J., Lu, L., Qu, Y., Manly, K. F., & Williams, R. W. (2003). Genetic correlates of gene expression in recombinant inbred strains: a relational model system to explore neurobehavioral phenotypes. *Neuroinformatics., 1*(4), 343-357.

Chhabra, R. S., Huff, J. E., Schwetz, B. S., & Selkirk, J. (1990). An overview of prechronic and chronic toxicity/carcinogenicity experimental study designs and criteria used by the National Toxicology Program. *Environ Health Perspect, 86*, 313-321.

Chiu, W. A., Campbell, J. L., Clewell, H. J., Zhou, Y. H., Wright, F. A., Guyton, K. Z., & Rusyn, I. (2014a). Physiologically-Based Pharmacokinetic (PBPK) Modeling of Inter-strain Variability in Trichloroethylene Metabolism in the Mouse. *Environ Health Perspect, 122*(5), 456-463.

Chiu, W. A., Campbell, J. L., Jr., Clewell, H. J., 3rd, Zhou, Y. H., Wright, F. A., Guyton, K. Z., & Rusyn, I. (2014b). Physiologically based pharmacokinetic (PBPK) modeling of interstrain variability in trichloroethylene metabolism in the mouse. *Environ Health Perspect, 122*(5), 456-463. doi:10.1289/ehp.1307623

Chiu, W. A., & Ginsberg, G. L. (2011). Development and evaluation of a harmonized physiologically based pharmacokinetic (PBPK) model for perchloroethylene toxicokinetics in mice, rats, and humans. *Toxicology and applied pharmacology, 253*(3), 203-234. doi:10.1016/j.taap.2011.03.020

Chiu, W. A., Jinot, J., Scott, C. S., Makris, S. L., Cooper, G. S., Dzubow, R. C., . . . Caldwell, J. C. (2013). Human health effects of trichloroethylene: key findings and scientific issues. *Environ Health Perspect, 121*(3), 303-311. doi:10.1289/ehp.1205879

Chiu, W. A., Micallef, S., Monster, A. C., & Bois, F. Y. (2007). Toxicokinetics of inhaled trichloroethylene and tetrachloroethylene in humans at 1 ppm: empirical results and comparisons with previous studies. *Toxicological sciences, 95*(1), 23-36. doi:10.1093/toxsci/kfl129

Chiu, W. A., Okino, M. S., & Evans, M. V. (2009). Characterizing uncertainty and population variability in the toxicokinetics of trichloroethylene and metabolites in mice, rats, and humans using an updated database, physiologically based pharmacokinetic (PBPK) model, and Bayesian approach. *Toxicology and applied pharmacology, 241*(1), 36-60.

Chiu, W. A., & Rusyn, I. (2018). Advancing Chemical Risk Assessment Decision-Making with Population Variability Data: Challenges and Opportunities. *Mamm Genome*, in press.

Church, R. J., Gatti, D. M., Urban, T. J., Long, N., Yang, X., Shi, Q., . . . Harrill, A. H. (2015). Sensitivity to hepatotoxicity due to epigallocatechin gallate is affected by genetic background in diversity outbred mice. *Food and Chemical Toxicology, 76*, 19-26. doi:10.1016/j.fct.2014.11.008

Churchill, G. A., Airey, D. C., Allayee, H., Angel, J. M., Attie, A. D., Beatty, J., . . . Zou, F. (2004). The Collaborative Cross, a community resource for the genetic analysis of complex traits. *Nat Genet, 36*(11), 1133-1137.

Churchill, G. A., Gatti, D. M., Munger, S. C., & Svenson, K. L. (2012). The Diversity Outbred mouse population. *Mamm Genome, 23*(9-10), 713-718. doi:10.1007/s00335-012-9414-2

Cichocki, J. A., Furuya, S., Venkatratnam, A., McDonald, T. J., Knap, A. H., Wade, T., . . . Rusyn, I. (2017). Characterization of Variability in Toxicokinetics and Toxicodynamics of

Tetrachloroethylene Using the Collaborative Cross Mouse Population. *Environ Health Perspect, 125*(5), 057006. doi:10.1289/EHP788

Cichocki, J. A., Guyton, K. Z., Guha, N., Chiu, W. A., Rusyn, I., & Lash, L. H. (2016). Target Organ Metabolism, Toxicity, and Mechanisms of Trichloroethylene and Perchloroethylene: Key Similarities, Differences, and Data Gaps. *The Journal of pharmacology and experimental therapeutics, 359*(1), 110-123. doi:10.1124/jpet.116.232629

Corton, J. C. (2008). Evaluation of the role of peroxisome proliferator-activated receptor alpha (PPARalpha) in mouse liver tumor induction by trichloroethylene and metabolites. *Crit Rev Toxicol, 38*(10), 857-875. doi:10.1080/10408440802209796

Cote, I., Anastas, P. T., Birnbaum, L. S., Clark, R. M., Dix, D. J., Edwards, S. W., & Preuss, P. W. (2012). Advancing the next generation of health risk assessment. *Environ Health Perspect, 120*(11), 1499-1502. doi:10.1289/ehp.1104870

Cotter, L. H. (1950). Trichloroethylene poisoning. *Arch Ind Hyg Occup Med, 1*(3), 319-322.

Crowley, J. J., Zhabotynsky, V., Sun, W., Huang, S., Pakatci, I. K., Kim, Y., . . . Pardo-Manuel de Villena, F. (2015). Analyses of allele-specific gene expression in highly divergent mouse crosses identifies pervasive allelic imbalance. *Nat Genet, 47*(4), 353-360. doi:10.1038/ng.3222

Cummings, B. S., & Lash, L. H. (2000). Metabolism and toxicity of trichloroethylene and S-(1,2-dichlorovinyl)-L-cysteine in freshly isolated human proximal tubular cells. *Toxicological sciences, 53*(2), 458-466.

Dalen, P., Dahl, M. L., Bernal Ruiz, M. L., Nordin, J., & Bertilsson, L. (1998). 10-Hydroxylation of nortriptyline in white persons with 0, 1, 2, 3, and 13 functional CYP2D6 genes. *Clin Pharmacol Ther, 63*(4), 444-452. doi:10.1016/S0009-9236(98)90040-6

Dekant, W., Vamvakas, S., Berthold, K., Schmidt, S., Wild, D., & Henschler, D. (1986). Bacterial beta-lyase mediated cleavage and mutagenicity of cysteine conjugates derived from the nephrocarcinogenic alkenes trichloroethylene, tetrachloroethylene and hexachlorobutadiene. *Chem Biol Interact, 60*(1), 31-45.

Dennis, G., Jr., Sherman, B. T., Hosack, D. A., Yang, J., Gao, W., Lane, H. C., & Lempicki, R. A. (2003). DAVID: Database for Annotation, Visualization, and Integrated Discovery. *Genome Biol, 4*(5), P3.

Dix, D. J., Houck, K. A., Martin, M. T., Richard, A. M., Setzer, R. W., & Kavlock, R. J. (2007). The ToxCast program for prioritizing toxicity testing of environmental chemicals. *Toxicological sciences, 95*(1), 5-12. doi:10.1093/toxsci/kfl103

Doerge, R. W. (2002). Mapping and analysis of quantitative trait loci in experimental populations. *Nature Reviews Genetics, 3*(1), 43-52. doi:10.1038/nrg703

Domino, M. M., Pepich, B. V., Munch, D. J., Fair, P. S., & Xie, Y. (2003). *Method 552.3: Determination of haloacetic acids and dalapon in drinking water by liquid-liquid microextraction, derivatization, and gas chromatography with electron capture detection*. Retrieved from Cincinnati, OH:

Donehower, L. A. (1996). The p53-deficient mouse: a model for basic and applied cancer studies. *Semin Cancer Biol, 7*(5), 269-278. doi:10.1006/scbi.1996.0035

Dorne, J. L., Walton, K., & Renwick, A. G. (2003). Polymorphic CYP2C19 and N-acetylation: human variability in kinetics and pathway-related uncertainty factors. *Food and Chemical Toxicology, 41*(2), 225-245.

Dorne, J. L., Walton, K., & Renwick, A. G. (2005). Human variability in xenobiotic metabolism and pathway-related uncertainty factors for chemical risk assessment: a review. *Food and Chemical Toxicology, 43*(2), 203-216. doi:10.1016/j.fct.2004.05.011

Dorner, M., Horwitz, J. A., Robbins, J. B., Barry, W. T., Feng, Q., Mu, K., . . . Ploss, A. (2011). A genetically humanized mouse model for hepatitis C virus infection. *Nature, 474*(7350), 208-211. doi:10.1038/nature10168

Dourson, M. L., Felter, S. P., & Robinson, D. (1996). Evolution of science-based uncertainty factors in noncancer risk assessment. *Regulatory Toxicology & Pharmacology, 24*(2 Pt 1), 108-120.

Duerr, R. H., Taylor, K. D., Brant, S. R., Rioux, J. D., Silverberg, M. S., Daly, M. J., . . . Cho, J. H. (2006). A genome-wide association study identifies IL23R as an inflammatory bowel disease gene. *Science, 314*(5804), 1461-1463.

Durrant, C., Tayem, H., Yalcin, B., Cleak, J., Goodstadt, L., de Villena, F. P. M., . . . Iraqi, F. A. (2011). Collaborative Cross mice and their power to map host susceptibility to Aspergillus fumigatus infection. *Genome Res, 21*(8), 1239-1248. doi:10.1101/gr.118786.110

Eduati, F., Mangravite, L. M., Wang, T., Tang, H., Bare, J. C., Huang, R., . . . Saez-Rodriguez, J. (2015). Prediction of human population responses to toxic compounds by a collaborative competition. *Nat Biotechnol, 33*(9), 933-940. doi:10.1038/nbt.3299

Ertle, T., Henschler, D., Muller, G., & Spassowski, M. (1972). Metabolism of trichloroethylene in man. I. The significance of trichloroethanol in long-term exposure conditions. *Arch Toxikol, 29*(3), 171-188.

Esch, M. B., King, T. L., & Shuler, M. L. (2011). The Role of Body-on-a-Chip Devices in Drug and Toxicity Studies. *Annual Review of Biomedical Engineering, Vol 13, 13*, 55-72. doi:10.1146/annurev-bioeng-071910-124629

Evans, M. V., Chiu, W. A., Okino, M. S., & Caldwell, J. C. (2009). Development of an updated PBPK model for trichloroethylene and metabolites in mice, and its application to discern the role of oxidative metabolism in TCE-induced hepatomegaly. *Toxicology and applied pharmacology, 236*(3), 329-340.

Evans, W. E., & Relling, M. V. (2004). Moving towards individualized medicine with pharmacogenomics. *Nature, 429*(6990), 464-468. doi:10.1038/nature02626

Fang, Z. Z., Krausz, K. W., Tanaka, N., Li, F., Qu, A., Idle, J. R., & Gonzalez, F. J. (2013). Metabolomics reveals trichloroacetate as a major contributor to trichloroethylene-induced metabolic alterations in mouse urine and serum. *Archives of Toxicology, 87*(11), 1975-1987. doi:10.1007/s00204-013-1053-1

Farmahin, R., Williams, A., Kuo, B., Chepelev, N. L., Thomas, R. S., Barton-Maclaren, T. S., . . . Yauk, C. L. (2017). Recommended approaches in the application of toxicogenomics to derive points of departure for chemical risk assessment. *Archives of Toxicology, 91*(5), 2045-2065. doi:10.1007/s00204-016-1886-5

Ferris, M. T., Aylor, D. L., Bottomly, D., Whitmore, A. C., Aicher, L. D., Bell, T. A., . . . Heise, M. T. (2013). Modeling host genetic regulation of influenza pathogenesis in the collaborative cross. *PLoS Pathog, 9*(2), e1003196. doi:10.1371/journal.ppat.1003196

Festing, M. F. (1986). The case for isogenic strains in toxicological screening. *Arch Toxicol.Suppl, 9*, 127-137.

Forkert, P. G., Lash, L. H., Nadeau, V., Tardif, R., & Simmonds, A. (2002). Metabolism and toxicity of trichloroethylene in epididymis and testis. *Toxicology and applied pharmacology, 182*(3), 244-254.

Fostel, J. M. (2008). Towards standards for data exchange and integration and their impact on a public database such as CEBS (Chemical Effects in Biological Systems). *Toxicology and applied pharmacology, 233*(1), 54-62. doi:10.1016/j.taap.2008.06.015

French, J. E., Gatti, D. M., Morgan, D. L., Kissling, G. E., Shockley, K. R., Knudsen, G. A., . . . Churchill, G. A. (2015). Diversity Outbred Mice Identify Population-Based Exposure Thresholds and Genetic Factors that Influence Benzene-Induced Genotoxicity. *Environ Health Perspect, 123*(3), 237-245. doi:10.1289/ehp.1408202

Ganter, B., Tugendreich, S., Pearson, C. I., Ayanoglu, E., Baumhueter, S., Bostian, K. A., . . . Jarnagin, K. (2005). Development of a large-scale chemogenomics database to improve drug candidate selection and to understand mechanisms of chemical toxicity and action. *J Biotechnol., 119*(3), 219-244.

Gatti, D., Maki, A., Chesler, E. J., Kirova, R., Kosyk, O., Lu, L., . . . Rusyn, I. (2007). Genome-level analysis of genetic regulation of liver gene expression networks. *Hepatology, 46*(2), 548-557. doi:10.1002/hep.21682

Gatti, D. M., Harrill, A. H., Wright, F. A., Threadgill, D. W., & Rusyn, I. (2009). Replication and narrowing of gene expression quantitative trait loci using inbred mice. *Mamm Genome, 20*(7), 437-446. doi:10.1007/s00335-009-9199-0

Gatti, D. M., Svenson, K. L., Shabalin, A., Wu, L. Y., Valdar, W., Simecek, P., . . . Churchill, G. A. (2014). Quantitative trait locus mapping methods for diversity outbred mice. *G3 (Bethesda), 4*(9), 1623-1633. doi:10.1534/g3.114.013748

Geter, D. R., Bhat, V. S., Gollapudi, B. B., Sura, R., & Hester, S. D. (2014). Dose-response modeling of early molecular and cellular key events in the CAR-mediated hepatocarcinogenesis pathway. *Toxicol Sci, 138*(2), 425-445. doi:10.1093/toxsci/kfu014

Giller, S., Le Curieux, F., Gauthier, L., Erb, F., & Marzin, D. (1995). Genotoxicity assay of chloral hydrate and chloropicrine. *Mutat Res, 348*(4), 147-152.

Graham, J. B., Thomas, S., Swarts, J., McMillan, A. A., Ferris, M. T., Suthar, M. S., . . . Lund, J. M. (2015). Genetic diversity in the collaborative cross model recapitulates human West Nile virus disease outcomes. *MBio, 6*(3), e00493-00415. doi:10.1128/mBio.00493-15

Green, R., Wilkins, C., Thomas, S., Sekine, A., Ireton, R. C., Ferris, M. T., . . . Gale, M. (2016a). Identifying protective host gene expression signatures within the spleen during West Nile virus infection in the collaborative cross model. *Genomics Data, 10*, 114-117. doi:10.1016/j.gdata.2016.10.006

Green, R., Wilkins, C., Thomas, S., Sekine, A., Ireton, R. C., Ferris, M. T., . . . Gale, M. (2016b). Transcriptional profiles of WNV neurovirulence in a genetically diverse Collaborative Cross population. *Genomics Data, 10,* 137-140. doi:10.1016/j.gdata.2016.10.005

GTEx Consortium. (2013). The Genotype-Tissue Expression (GTEx) project. *Nat Genet, 45*(6), 580-585. doi:10.1038/ng.2653

GTEx Consortium. (2015). Human genomics. The Genotype-Tissue Expression (GTEx) pilot analysis: multitissue gene regulation in humans. *Science, 348*(6235), 648-660. doi:10.1126/science.1262110

Guha, N., Loomis, D., Grosse, Y., Lauby-Secretan, B., El Ghissassi, F., Bouvard, V., . . . International Agency for Research on Cancer Monograph Working Group. (2012). Carcinogenicity of trichloroethylene, tetrachloroethylene, some other chlorinated solvents, and their metabolites. *Lancet Oncol, 13*(12), 1192-1193.

Han, W. K., Bailly, V., Abichandani, R., Thadhani, R., & Bonventre, J. V. (2002). Kidney Injury Molecule-1 (KIM-1): a novel biomarker for human renal proximal tubule injury. *Kidney Int, 62*(1), 237-244. doi:10.1046/j.1523-1755.2002.00433.x

Harrill, A. H., & McAllister, K. A. (2017). New Rodent Population Models May Inform Human Health Risk Assessment and Identification of Genetic Susceptibility to Environmental Exposures. *Environ Health Perspect, 125*(8), 086002. doi:10.1289/EHP1274

Harrill, A. H., Ross, P. K., Gatti, D. M., Threadgill, D. W., & Rusyn, I. (2009). Population-based discovery of toxicogenomics biomarkers for hepatotoxicity using a laboratory strain diversity panel. *Toxicological sciences, 110*(1), 235-243. doi:10.1093/toxsci/kfp096

Harrill, A. H., & Rusyn, I. (2008). Systems biology and functional genomics approaches for the identification of cellular responses to drug toxicity. *Expert Opin Drug Metab Toxicol, 4*(11), 1379-1389. doi:10.1517/17425255.4.11.1379

Harrill, A. H., Watkins, P. B., Su, S., Ross, P. K., Harbourt, D. E., Stylianou, I. M., . . . Threadgill, D. W. (2009). Mouse population-guided resequencing reveals that variants in CD44 contribute to acetaminophen-induced liver injury in humans. *Genome Res, 19*(9), 1507-1515. doi:10.1101/gr.090241.108

Hattis, D., Erdreich, L., & Ballew, M. (1987). Human variability in susceptibility to toxic chemicals--a preliminary analysis of pharmacokinetic data from normal volunteers. *Risk Anal, 7*(4), 415-426.

Heijne, W. H., Stierum, R. H., Slijper, M., van Bladeren, P. J., & van Ommen, B. (2003). Toxicogenomics of bromobenzene hepatotoxicity: a combined transcriptomics and proteomics approach. *Biochem Pharmacol, 65*(5), 857-875.

IARC. (2014). IARC Monographs on the Evaluation of Carcinogenic Risks to Humans (Vol. 106): Trichloroethylene, Tetrachloroethylene and Some Other Chlorinated Agents. *106*.

Igarashi, I., Makino, T., Suzuki, Y., Kai, K., Teranishi, M., Takasaki, W., & Furuhama, K. (2013). Background lesions during a 24-month observation period in connexin 32-deficient mice. *J Vet Med Sci, 75*(2), 207-210.

Ito, Y., Yamanoshita, O., Kurata, Y., Kamijima, M., Aoyama, T., & Nakajima, T. (2007). Induction of peroxisome proliferator-activated receptor alpha (PPARalpha)-related enzymes by di(2-ethylhexyl) phthalate (DEHP) treatment in mice and rats, but not marmosets. *Archives of Toxicology, 81*(3), 219-226.

Kaeppler, S. M. (1997). Quantitative trait locus mapping using sets of near-isogenic lines: relative power comparisons and technical considerations. *Theor Appl Genet, 95*, 384-392.

Kile, B. T., Mason-Garrison, C. L., & Justice, M. J. (2003). Sex and strain-related differences in the peripheral blood cell values of inbred mouse strains. *Mamm Genome, 14*(1), 81-85. doi:10.1007/s00335-002-2160-0

Kim, D., Langmead, B., & Salzberg, S. L. (2015). HISAT: a fast spliced aligner with low memory requirements. *Nat Methods, 12*(4), 357-360. doi:10.1038/nmeth.3317

Kim, R. B., O'Shea, D., & Wilkinson, G. R. (1994). Relationship in healthy subjects between CYP2E1 genetic polymorphisms and the 6-hydroxylation of chlorzoxazone: a putative measure of CYP2E1 activity. *Pharmacogenetics, 4*(3), 162-165.

Kim, S., Collins, L. B., Boysen, G., Swenberg, J. A., Gold, A., Ball, L. M., . . . Rusyn, I. (2009). Liquid chromatography electrospray ionization tandem mass spectrometry analysis method for simultaneous detection of trichloroacetic acid, dichloroacetic acid, S-(1,2-dichlorovinyl)glutathione and S-(1,2-dichlorovinyl)-L-cysteine. *Toxicology, 262*(3), 230-238. doi:10.1016/j.tox.2009.06.013

King-Herbert, A., & Thayer, K. (2006). NTP workshop: animal models for the NTP rodent cancer bioassay: stocks and strains--should we switch? *Toxicol Pathol, 34*(6), 802-805. doi:10.1080/01926230600935938

Klaunig, J. E., Ruch, R. J., & Lin, E. L. (1989). Effects of trichloroethylene and its metabolites on rodent hepatocyte intercellular communication. *Toxicology and applied pharmacology, 99*(3), 454-465.

Knight, A. W., Little, S., Houck, K., Dix, D., Judson, R., Richard, A., . . . Walmsley, R. M. (2009). Evaluation of high-throughput genotoxicity assays used in profiling the US EPA ToxCast (TM) chemicals. *Regulatory Toxicology and Pharmacology, 55*(2), 188-199. doi:10.1016/j.yrtph.2009.07.004

Koturbash, I., Scherhag, A., Sorrentino, J., Sexton, K., Bodnar, W., Swenberg, J. A., . . . Pogribny, I. P. (2011). Epigenetic mechanisms of mouse interstrain variability in genotoxicity of the environmental toxicant 1,3-butadiene. *Toxicological sciences, 122*(2), 448-456. doi:10.1093/toxsci/kfr133

Kovacs, A., Ben-Jacob, N., Tayem, H., Halperin, E., Iraqi, F. A., & Gophna, U. (2011). Genotype Is a Stronger Determinant than Sex of the Mouse Gut Microbiota. *Microbial Ecology, 61*(2), 423-428. doi:10.1007/s00248-010-9787-2

Krueger, S. K., & Williams, D. E. (2005). Mammalian flavin-containing monooxygenases: structure/function, genetic polymorphisms and role in drug metabolism. *Pharmacol Ther, 106*(3), 357-387.

Kwara, A., Lartey, M., Boamah, I., Rezk, N. L., Oliver-Commey, J., Kenu, E., . . . Court, M. H. (2009). Interindividual variability in pharmacokinetics of generic nucleoside reverse transcriptase inhibitors in TB/HIV-coinfected Ghanaian patients: UGT2B7*1c is associated with faster zidovudine clearance and glucuronidation. *J Clin Pharmacol, 49*(9), 1079-1090. doi:10.1177/0091270009338482

Lan, Q., Zhang, L. P., Tang, X. J., Shen, M., Smith, M. T., Qiu, C. Y., . . . Huang, H. L. (2010). Occupational exposure to trichloroethylene is associated with a decline in lymphocyte subsets and soluble CD27 and CD30 markers. *Carcinogenesis, 31*(9), 1592-1596. doi:10.1093/carcin/bgq121

Lanfear, D. E., & McLeod, H. L. (2007). Pharmacogenetics: using DNA to optimize drug therapy. *Am Fam.Physician, 76*(8), 1179-1182.

Lappalainen, T., Sammeth, M., Friedlander, M. R., t Hoen, P. A., Monlong, J., Rivas, M. A., . . . Geuvadis, C. (2013). Transcriptome and genome sequencing uncovers functional variation in humans. *Nature, 501*(7468), 506-511. doi:10.1038/nature12531

Lash, L. H., Chiu, W. A., Guyton, K. Z., & Rusyn, I. (2014). Trichloroethylene biotransformation and its role in mutagenicity, carcinogenicity and target organ toxicity. *Mutat Res Rev Mutat Res, 762*, 22-36. doi:10.1016/j.mrrev.2014.04.003

Lash, L. H., Fisher, J. W., Lipscomb, J. C., & Parker, J. C. (2000). Metabolism of trichloroethylene. *Environ Health Perspect, 108 Suppl 2*, 177-200.

Lash, L. H., Putt, D. A., & Parker, J. C. (2006). Metabolism and tissue distribution of orally administered trichloroethylene in male and female rats: identification of glutathione- and cytochrome P-450-derived metabolites in liver, kidney, blood, and urine. *J Toxicol Environ Health A, 69*(13), 1285-1309.

Leeuwen, C. J. v., & Hermens, J. L. M. (1995). *Risk assessment of chemicals : an introduction*. Dordrecht ; Boston: Kluwer Academic Publishers.

Lehman, A. F., OG (1954). 100-fold margin of safety *Quarterly Bulletin - Association of Food & Drug Officials of the United States, 18*, 33-35.

Li, R., Zhao, Z., Sun, M., Luo, J., & Xiao, Y. (2016). ALDH2 gene polymorphism in different types of cancers and its clinical significance. *Life Sci, 147*, 59-66. doi:10.1016/j.lfs.2016.01.028

Liu, C. X., Musco, S., Lisitsina, N. M., Yaklichkin, S. Y., & Lisitsyn, N. A. (2000). Genomic organization of a new candidate tumor suppressor gene, LRP1B. *Genomics, 69*(2), 271-274. doi:10.1006/geno.2000.6331

Lock, E. F., Abdo, N., Huang, R., Xia, M., Kosyk, O., O'Shea, S. H., . . . Rusyn, I. (2012). Quantitative high-throughput screening for chemical toxicity in a population-based in vitro model. *Toxicological sciences, 126*(2), 578-588. doi:10.1093/toxsci/kfs023

Love, M. I., Huber, W., & Anders, S. (2014). Moderated estimation of fold change and dispersion for RNA-seq data with DESeq2. *Genome Biol, 15*(12), 550. doi:10.1186/s13059-014-0550-8

Luo, Y. S., Furuya, S., Chiu, W., & Rusyn, I. (2018). Characterization of inter-tissue and inter-strain variability of TCE glutathione conjugation metabolites DCVG, DCVC, and NAcDCVC in the mouse. *J Toxicol Environ Health A, 81*(1-3), 37-52. doi:10.1080/15287394.2017.1408512

Maloney, E. K., & Waxman, D. J. (1999). Trans-activation of PPARalpha and PPARgamma by structurally diverse environmental chemicals. *Toxicology and applied pharmacology, 161*(2), 209-218.

McGregor, D. B., Heseltine, E., & Moller, H. (1995). Dry cleaning, some solvents used in dry cleaning and other industrial chemicals. IARC meeting, Lyon, 7-14 February 1995. *Scand J Work Environ Health, 21*(4), 310-312.

Meek, M. E. (1987). Handbook of Carcinogen Testing - Milman,Ha, Weisburger,Ek. *Canadian Journal of Public Health-Revue Canadienne De Sante Publique, 78*(1), 66-66.

Mosedale, M., Kim, Y., Brock, W. J., Roth, S. E., Wiltshire, T., Eaddy, J. S., . . . Watkins, P. B. (2017). Candidate Risk Factors and Mechanisms for Tolvaptan-Induced Liver Injury Are Identified Using a Collaborative Cross Approach. *Toxicological sciences, 156*(2), 438-454. doi:10.1093/toxsci/kfw269

Muller, G., Spassovski, M., & Henschler, D. (1974). Metabolism of trichloroethylene in man. II. Pharmacokinetics of metabolites. *Archives of Toxicology, 32*(4), 283-295.

Muller, G., & Spassows.M. (1973). Pharmacokinetics of Trichloroethylene Metabolites in Man. *Naunyn-Schmiedebergs Archives of Pharmacology*, R48-R48.

Muller, G., Spassowski, M., & Henschler, D. (1975). Metabolism of trichloroethylene in man. III. Interaction of trichloroethylene and ethanol. *Archives of Toxicology, 33*(3), 173-189.

National Research Council. (1994). *Science and judgment in risk assessment*. Washington, D.C.: National Academy Press.

National Research Council. (2007). *Toxicity testing in the 21st century: A vision and a strategy*. Washington, DC: The National Academies Press.

National Research Council. (2009). *Science and Decisions: Advancing Risk Assessment*. Washington, DC: National Academies Press.

National Toxicology Program. (1988). Toxicology and Carcinogenesis Studies of Trichloroethylene (CAS No. 79-01-6) in Four Strains of Rats (ACI, August, Marshall, Osborne-Mendel) (Gavage Studies). *Natl Toxicol Program Tech Rep Ser, 273*, 1-299.

National Toxicology Program. (1990). Carcinogenesis Studies of Trichloroethylene (Without Epichlorohydrin) (CAS No. 79-01-6) in F344/N Rats and B6C3F1 Mice (Gavage Studies). *Natl Toxicol Program Tech Rep Ser, 243*, 1-174.

Odum, J., Foster, J. R., & Green, T. (1992). A mechanism for the development of Clara cell lesions in the mouse lung after exposure to trichloroethylene. *Chem Biol Interact, 83*(2), 135-153.

OECD. (1996). *OECD Guideline for Testing of Chemicals, No 423: Acute Oral Toxicity-Acute Toxic Class Method*. Paris: Organisation for Economic Co-operation and Development.

Pastino, G. M., Yap, W. Y., & Carroquino, M. (2000). Human variability and susceptibility to trichloroethylene. *Environ Health Perspect, 108 Suppl 2*, 201-214.

Prout, M. S., Provan, W. M., & Green, T. (1985). Species differences in response to trichloroethylene. I. Pharmacokinetics in rats and mice. *Toxicology and applied pharmacology, 79*(3), 389-400.

Rakhshandehroo, M., Knoch, B., Muller, M., & Kersten, S. (2010). Peroxisome proliferator-activated receptor alpha target genes. *PPAR Res, 2010*. doi:10.1155/2010/612089

Ramdhan, D. H., Kamijima, M., Yamada, N., Ito, Y., Yanagiba, Y., Nakamura, D., . . . Nakajima, T. (2008). Molecular mechanism of trichloroethylene-induced hepatotoxicity mediated by CYP2E1. *Toxicology and applied pharmacology, 231*(3), 300-307.

Rasmussen, A. L., Okumura, A., Ferris, M. T., Green, R., Feldmann, F., Kelly, S. M., . . . Katze, M. G. (2014). Host genetic diversity enables Ebola hemorrhagic fever pathogenesis and resistance. *Science, 346*(6212), 987-991. doi:10.1126/science.1259595

Reif, D. M., Martin, M. T., Tan, S. W., Houck, K. A., Judson, R. S., Richard, A. M., . . . Kavlock, R. J. (2010). Endocrine profiling and prioritization of environmental chemicals using ToxCast data. *Environ Health Perspect, 118*(12), 1714-1720. doi:10.1289/ehp.1002180

Richardson, G. M. (1996). Deterministic versus probabilistic risk assessment: Strengths and weaknesses in a regulatory context. *Human and Ecological Risk Assessment, 2*(1), 44-54. doi:Doi 10.1080/10807039.1996.10387459

Roberts, R. B., & Threadgill, D. W. (2005). The Mouse in Biomedical Research. *Mouse in Animal Genetics and Breeding Research*, 319-340. doi:Doi 10.1142/9781860947162_0015

Robinson, J. F., van Beelen, V. A., Verhoef, A., Renkens, M. F., Luijten, M., van Herwijnen, M. H., . . . Piersma, A. H. (2010). Embryotoxicant-specific transcriptomic responses in rat postimplantation whole-embryo culture. *Toxicol Sci, 118*(2), 675-685. doi:10.1093/toxsci/kfq292

Rogala, A. R., Morgan, A. P., Christensen, A. M., Gooch, T. J., Bell, T. A., Miller, D. R., . . . de Villena, F. P. M. (2014). The Collaborative Cross as a Resource for Modeling Human Disease: CC011/Unc, a New Mouse Model for Spontaneous Colitis. *Mammalian Genome, 25*(3-4), 95-108. doi:10.1007/s00335-013-9499-2

Rusyn, I., Chiu, W. A., Lash, L. H., Kromhout, H., Hansen, J., & Guyton, K. Z. (2014). Trichloroethylene: Mechanistic, epidemiologic and other supporting evidence of carcinogenic hazard. *Pharmacol Ther, 141*(1), 55-68. doi:10.1016/j.pharmthera.2013.08.004

Rusyn, I., Gatti, D. M., Wiltshire, T., Kleeberger, S. R., & Threadgill, D. W. (2010). Toxicogenetics: population-based testing of drug and chemical safety in mouse models. *Pharmacogenomics, 11*(8), 1127-1136. doi:10.2217/pgs.10.100

Sauer, U. G., Deferme, L., Gribaldo, L., Hackermuller, J., Tralau, T., van Ravenzwaay, B., . . . Gant, T. W. (2017). The challenge of the application of 'omics technologies in chemicals risk assessment: Background and outlook. *Regul Toxicol Pharmacol*. doi:10.1016/j.yrtph.2017.09.020

Schadt, E. E., Molony, C., Chudin, E., Hao, K., Yang, X., Lum, P. Y., . . . Ulrich, R. (2008). Mapping the genetic architecture of gene expression in human liver. *PLoS Biol, 6*(5), e107. doi:10.1371/journal.pbio.0060107

Schadt, E. E., Monks, S. A., Drake, T. A., Lusis, A. J., Che, N., Colinayo, V., . . . Friend, S. H. (2003). Genetics of gene expression surveyed in maize, mouse and man. *Nature, 422*(6929), 297-302.

Sipes, N. S., Martin, M. T., Reif, D. M., Kleinstreuer, N. C., Judson, R. S., Singh, A. V., . . . Knudsen, T. B. (2011). Predictive models of prenatal developmental toxicity from ToxCast high-throughput screening data. *Toxicological sciences, 124*(1), 109-127. doi:10.1093/toxsci/kfr220

Siva, N. (2008). 1000 Genomes project. *Nat Biotechnol, 26*(3), 256. doi:10.1038/nbt0308-256b

Smallwood, T. L., Gatti, D. M., Quizon, P., Weinstock, G. M., Jung, K. C., Zhao, L. Y., . . . Bennett, B. J. (2014). High-Resolution Genetic Mapping in the Diversity Outbred Mouse

Population Identifies Apobec1 as a Candidate Gene for Atherosclerosis. *G3-Genes Genomes Genetics, 4*(12), 2353-2363. doi:10.1534/g3.114.014704/-/DC1

The International HapMap Consortium. (2003). The International HapMap Project. *Nature, 426*(6968), 789-796.

Thomas, R. S., Allen, B. C., Nong, A., Yang, L., Bermudez, E., Clewell, H. J., 3rd, & Andersen, M. E. (2007a). A method to integrate benchmark dose estimates with genomic data to assess the functional effects of chemical exposure. *Toxicol Sci, 98*(1), 240-248. doi:10.1093/toxsci/kfm092

Thomas, R. S., Allen, B. C., Nong, A., Yang, L., Bermudez, E., Clewell, H. J., III, & Andersen, M. E. (2007b). A method to integrate benchmark dose estimates with genomic data to assess the functional effects of chemical exposure. *Toxicological sciences, 98*(1), 240-248.

Thomas, R. S., Clewell, H. J., Allen, B. C., Wesselkamper, S. C., Wang, N. C., Lambert, J. C., . . . Andersen, M. E. (2011). Application of transcriptional benchmark dose values in quantitative cancer and noncancer risk assessment. *Toxicological sciences, 120*(1), 194-205.

Thomas, R. S., Clewell, H. J., Allen, B. C., Yang, L. L., Healy, E., & Andersen, M. E. (2012). Integrating pathway-based transcriptomic data into quantitative chemical risk assessment: A five chemical case study. *Mutation Research-Genetic Toxicology and Environmental Mutagenesis, 746*(2), 135-143. doi:10.1016/j.mrgentox.2012.01.007

Thomas, R. S., Philbert, M. A., Auerbach, S. S., Wetmore, B. A., Devito, M. J., Cote, I., . . . Nong, A. (2013a). Incorporating new technologies into toxicity testing and risk assessment: moving from 21st century vision to a data-driven framework. *Toxicological sciences, 136*(1), 4-18. doi:10.1093/toxsci/kft178

Thomas, R. S., Philbert, M. A., Auerbach, S. S., Wetmore, B. A., Devito, M. J., Cote, I., . . . Nong, A. (2013b). Incorporating New Technologies Into Toxicity Testing and Risk Assessment: Moving From 21st Century Vision to a Data-Driven Framework. *Toxicological Sciences, 136*(1), 4-18. doi:10.1093/toxsci/kft178

Thomas, R. S., Wesselkamper, S. C., Wang, N. C., Zhao, Q. J., Petersen, D. D., Lambert, J. C., . . . Andersen, M. E. (2013). Temporal concordance between apical and transcriptional points of departure for chemical risk assessment. *Toxicological sciences, 134*(1), 180-194. doi:10.1093/toxsci/kft094

Threadgill, D. W., & Churchill, G. A. (2012). Ten years of the Collaborative Cross. *Genetics, 190*(2), 291-294. doi:10.1534/genetics.111.138032

Threadgill, D. W., Hunter, K. W., & Williams, R. W. (2002). Genetic dissection of complex and quantitative traits: from fantasy to reality via a community effort. *Mammalian Genome, 13*(4), 175-178.

Threadgill, D. W., Miller, D. R., Churchill, G. A., & de Villena, F. P. M. (2011). The Collaborative Cross: A Recombinant Inbred Mouse Population for the Systems Genetic Era. *Ilar Journal, 52*(1), 24-31.

Tice, R. R., Austin, C. P., Kavlock, R. J., & Bucher, J. R. (2013). Improving the human hazard characterization of chemicals: a Tox21 update. *Environ Health Perspect, 121*(7), 756-765. doi:10.1289/ehp.1205784

U.S. EPA. (2011a). *Toxicological Review of Tetrachloroethylene (CAS No. 127-18-4): In Support of Summary Information on the Integrated Risk Information System (IRIS)*. (EPA/635/R-08/011A). Washington, DC: U.S. Environmental Protection Agency.

U.S. EPA. (2011b). Toxicological Review of Trichloroethylene (CAS No. 79-01-6): In Support of Summary Information on the Integrated Risk Information System (IRIS).

Uehara, T., Ono, A., Maruyama, T., Kato, I., Yamada, H., Ohno, Y., & Urushidani, T. (2010). The Japanese toxicogenomics project: application of toxicogenomics. *Mol Nutr Food Res, 54*(2), 218-227.

Vamvakas, S., Elfarra, A. A., Dekant, W., Henschler, D., & Anders, M. W. (1988). Mutagenicity of amino acid and glutathione S-conjugates in the Ames test. *Mutat Res, 206*(1), 83-90.

Venkatratnam, A., Furuya, S., Kosyk, O., Gold, A., Bodnar, W., Konganti, K., . . . Rusyn, I. (2017). Collaborative Cross Mouse Population Enables Refinements to Characterization of the Variability in Toxicokinetics of Trichloroethylene and Provides Genetic Evidence for the Role of PPAR Pathway in Its Oxidative Metabolism. *Toxicological sciences, 158*(1), 48-62. doi:10.1093/toxsci/kfx065

Venkatratnam, A., House, J. S., Konganti, K., McKenney, C., Threadgill, D. W., Chiu, W. A., . . . Rusyn, I. (2018). Population-based dose–response analysis of liver transcriptional response to trichloroethylene in mouse. *Mamm Genome*.

WHO, G. (1995). Application of Risk Analysis to Food Standards Issues *Geneva : World Health Organization*.

Willyard, C. (2017). Channeling chip power: Tissue chips are being put to the test by industry. *Nat Med, 23*(2), 138-140. doi:10.1038/nm0217-138

Xu, E. Y., Perlina, A., Vu, H., Troth, S. P., Brennan, R. J., Aslamkhan, A. G., & Xu, Q. (2008). Integrated pathway analysis of rat urine metabolic profiles and kidney transcriptomic profiles to elucidate the systems toxicology of model nephrotoxicants. *Chemical Research in Toxicology, 21*(8), 1548-1561. doi:10.1021/tx800061w

Xu, J., Thakkar, S., Gong, B., & Tong, W. (2016). The FDA's Experience with Emerging Genomics Technologies-Past, Present, and Future. *AAPS J, 18*(4), 814-818. doi:10.1208/s12248-016-9917-y

Yang, L., Allen, B. C., & Thomas, R. S. (2007). BMDExpress: a software tool for the benchmark dose analyses of genomic data. *BMC Genomics, 8*, 387. doi:10.1186/1471-2164-8-387

Yoo, H. S., Bradford, B. U., Kosyk, O., Shymonyak, S., Uehara, T., Collins, L. B., . . . Rusyn, I. (2015a). Comparative analysis of the relationship between trichloroethylene metabolism and tissue-specific toxicity among inbred mouse strains: liver effects. *J Toxicol Environ Health A, 78*(1), 15-31. doi:10.1080/15287394.2015.958417

Yoo, H. S., Bradford, B. U., Kosyk, O., Shymonyak, S., Uehara, T., Collins, L. B., . . . Rusyn, I. (2015b). Comparative Analysis of the Relationship Between Trichloroethylene Metabolism and Tissue-Specific Toxicity Among Inbred Mouse Strains: Liver Effects. *Journal of Toxicology and Environmental Health-Part a-Current Issues, 78*(1), 15-31. doi:Doi 10.1080/15287394.2015.958417

Yoo, H. S., Bradford, B. U., Kosyk, O., Uehara, T., Shymonyak, S., Collins, L. B., . . . Rusyn, I. (2015). Comparative analysis of the relationship between trichloroethylene metabolism and tissue-specific toxicity among inbred mouse strains: kidney effects. *J Toxicol Environ Health A, 78*(1), 32-49. doi:10.1080/15287394.2015.958418

Yoo, H. S., Cichocki, J. A., Kim, S., Venkatratnam, A., Iwata, Y., Kosyk, O., . . . Rusyn, I. (2015). The Contribution of Peroxisome Proliferator-Activated Receptor Alpha to the Relationship Between Toxicokinetics and Toxicodynamics of Trichloroethylene. *Toxicological sciences, 147*(2), 339-349. doi:10.1093/toxsci/kfv134

Zeise, L., Bois, F. Y., Chiu, W. A., Hattis, D., Rusyn, I., & Guyton, K. Z. (2013). Addressing human variability in next-generation human health risk assessments of environmental chemicals. *Environ Health Perspect, 121*(1), 23-31. doi:10.1289/ehp.1205687

Zhang, L., Sedykh, A., Tripathi, A., Zhu, H., Afantitis, A., Mouchlis, V. D., . . . Tropsha, A. (2013). Identification of putative estrogen receptor-mediated endocrine disrupting chemicals using QSAR- and structure-based virtual screening approaches. *Toxicology and applied pharmacology, 272*(1), 67-76. doi:10.1016/j.taap.2013.04.032

Zhou, Y. C., & Waxman, D. J. (1998). Activation of peroxisome proliferator-activated receptors by chlorinated hydrocarbons and endogenous steroids. *Environ Health Perspect., 106 Suppl 4*, 983-988.

Zhou, Y. H., Cichocki, J. A., Soldatow, V. Y., Scholl, E. H., Gallins, P. J., Jima, D., . . . Rusyn, I. (2017). Comparative Dose-Response Analysis of Liver and Kidney Transcriptomic Effects of Trichloroethylene and Tetrachloroethylene in B6C3F1 Mouse. *Toxicological sciences, 160*(1), 95-110. doi:10.1093/toxsci/kfx165